

TR 86-07

THE ADSORPTION OF CHELATING REAGENTS ON  
OXIDE MINERALS

A thesis submitted in partial fulfilment of the requirements for  
the degree of Doctor of Philosophy in the Department of Chemistry,  
Rhodes University, Grahamstown.

by

M.A.W. Bryson,  
Rhodes University,  
Grahamstown,  
South Africa

June, 1984



## ABSTRACT

This work constitutes a fundamental study of the interaction between chelating reagents and oxide minerals. The adsorption mechanisms have been elucidated for most of the systems generated by the oxides of copper(II) or iron(III) and chelating reagents octyl hydroxamate, N-phenylbenzohydroxamate, salicylaldoxime, 5-nitrosalicylaldoxime or 8-hydroxyquinoline.

The results of the preliminary work on one of the systems, viz. the oxide-hydroxamate system, indicated that the classical type adsorption process, in which the reagent forms a uniform layer of chelate over the oxide surface was not applicable. Rather, the adsorption occurred via the formation of a discrete metal-chelate precipitate at the oxide surface.

In order to better understand the adsorption process associated with copper (II) oxide, the oxide was recrystallized to produce a coarser material with a more uniform surface. This allowed the oxide surface to be viewed under the scanning electron microscope and also enabled the relative concentration of "surface" and "bulk" chelate to be assessed.

A detailed investigation of the effect of the system variables; pH, conditioning period, concentration,

temperature, surface area and dispersing reagent on the rate of precipitation of the copper chelate species of general form,  $\text{Cu}(\text{chel})_2$ , was made. In addition the chemical nature of the adsorbed species and the structural form of the precipitates were determined with the aid of infra-red spectroscopy and the scanning electron microscope. On the basis of these results a model has been formulated for the adsorption processes. In this model the adsorption is considered to occur in stages : 1. oxide dissolution, 2. metal complex formation, 3. metal chelate precipitation at the oxide surface and 4. "bulk" chelate formation by post-precipitation processes.

The precipitation process was examined in more detail by the study of the adsorption of chelate on copper metal. The results of this study showed that it was possible to relate the structural type of precipitate formed, ie. fibrous or platelike, to the degree of supersaturation of the metal complex in solution. Furthermore, it was found that the precipitate structure determined whether it remained attached to the surface or detached.

Contact angle measurements of air bubbles on copper metal conditioned with chelate were related to the adsorption results in an attempt to isolate the optimum conditions for flotation of oxide minerals.

To George and Enid.

CONTENTS

	<u>Page</u>
ABSTRACT	
TABLE OF CONTENTS	i
ACKNOWLEDGEMENTS	vi
A. INTRODUCTION	1
A.1. General	1
A.2. The use of chelating reagents as collectors in flotation	8
A.2.a. Sulphides	8
A.2.b. Oxides	9
A.3. The mechanism of adsorption of chelating reagents on oxide minerals.	20
A.3.a. Nagaraj's study of the copper(II) oxide- salicylaldoxime system	21
A.3.b. Cecile's study of the malachite-salicylaldoxime system	26
A.3.c. Fuerstenau's study of the haematite Fe <sub>2</sub> O <sub>3</sub> - octyl hydroxamate system	30
A.4. Metal complexation	33
A.4.a. "Hard" and "Soft" acids and bases	34
A.4.b. Chelation	35
A.4.c. Stereochemical	37
B. SCOPE OF THE PRESENT WORK	39
B.1. General	39
B.2. Preliminary work	39
B.2.a. Iron(III) oxide system	39
B.2.b. Copper(II) oxide system	40
B.2.c. Sulphidization system	41
B.3. Detailed work	42
B.3.a. Substrate choice	42
B.3.b. Reagent choice	43
B.3.c. Experimental approach	44
C. PRELIMINARY WORK	46
C.1. Experimental	46
C.1.a. Materials	46
C.1.b. Reagents	47
C.1.c. Analysis	47
C.1.c.i. Octyl hydroxamate	47
C.1.c.ii. Tris-N- phenylbenzohydroxamate iron(III)	48
C.1.c.iii. Bis-N- phenylbenzohydroxamate	48

	copper(II)	
	C.1.d. Adsorption studies	48
	C.1.d.i. Residual method	48
	C.1.d.ii. Direct method	49
	C.1.e. Infra-red studies	50
	C.2. The iron(III) oxide system	51
	C.2.a. Results	51
	C.2.a.i. Adsorption of octyl hydroxamate	51
	C.2.a.ii. Scanning electron microscope study	54
	C.2.a.iii. Formation of $\text{Fe}(\text{NPBA})_3$	57
	C.2.a.iv. Infra-red spectra	58
	C.2.b. Discussion	61
	C.3. Copper(II) oxide system	64
	C.3.a. Results	64
	C.3.a.i. Adsorption of octyl hydroxamate	64
	C.3.a.ii. Infra-red study	67
	C.3.a.iii. $\text{Cu}(\text{NPBA})_2$ formation	69
	C.3.b. Discussion	70
	C.4. Xanthate and sulphidization	71
	C.4.a. Sulphidization procedure	72
	C.4.b. Xanthate adsorption	72
	C.4.c. Reaction between sulphidized copper(II) oxide and xanthate	73
	D. DETAILED WORK	75
	D.1. EXPERIMENTAL	75
	D.1.a. Materials	75
	D.1.a.i. Re-crystallized copper(II) oxide	75
	D.1.a.ii. Copper metal	76
	D.1.b. Analysis	75
	D.1.b.i. Salicylaldoxime and 5-nitrosalicylaldoxime	76
	D.1.b. ii. $\text{Cu}(\text{SALO})_2$	76
	D.1.b.iii. $\text{Cu}(\text{Ox})_2$	77
	D.1.c. Infra-red studies	77
	D.1.d. Scanning electron microscope studies	78
	D.1.e. Adsorption isotherms	78
	D.1.e.i. Residual method	78
	D.1.e.ii. Extraction technique	79
	1) Apparatus	79
	2) Method	79
	3) Separation of bulk and surface chelate	80
	D.1.f. Precipitation studies	83
	D.2. SOLUBILITY OF RE-CRYSTALLIZED COPPER(II) OXIDE	84
	D.3. RESULTS AND DISCUSSION	87

D.3.a.	HYDROXAMIC ACIDS	87
D.3.a.i.	General features	87
D.3.a.ii.	N-phenylbenzohydroxamate	88
D.3.a.iii.	Metal-species distribution	89
D.3.a.iv.	Adsorption isotherms	92
	1) Time, surface area	92
	2) Temperature	94
	3) pH	95
	4) Dispersing reagents	95
D.3.a.v.	Infra-red spectroscopy	101
D.3.a.vi.	Scanning electron microscope study	101
	1) Precipitates	101
	2) Copper(II) oxide, surface area $2,18\text{m}^2/\text{g}$	102
	3) Copper(II) oxide, surface area $0,07\text{m}^2/\text{g}$	102
D.3.b.	HYDROXY OXIMES	108
D.3.b.i.	General features	108
	1) $\alpha$ -Acylloximes and related ligands	108
	2) Salicylaldoxime and substituted derivatives	109
D.3.b.ii.	Metal species distribution	111
	1) Salicylaldoxime	111
	2) Substituted SALO derivative	117
D.3.b.iii.	Adsorption isotherms	122
	1) Time, surface area	123
	2) pH, concentration	125
	3) Temperature	126
	4) Comparison between SALO and SNSALO	126
	5) Discussion	128
D.3.b.iv.	Scanning electron microscope study	131
	1) Nucleation	131
	2) Crystal growth	135
	a) Time	136
	b) Surface area	136
	c) Reagent types	136
D.3.b.v.	Infra-red study	141
D.3.c.	8-HYDROXYQUINOLINE	146
D.3.c.i.	General features	146
D.3.c.ii.	Metal-species distribution	147
D.3.c.iii.	Adsorption isotherms	150
	1) Time	150

	a) Copper(II) oxide surface area	151
	0,07m <sup>2</sup> /g	
	b) Copper(II) oxide sample, surface area	152
	0,17m <sup>2</sup> /g	
	2) pH	154
	3) Temperature	156
	4) Dispersing reagents	158
	5) Discussion	159
D.3.c.iv.	Infra-red spectroscopic study	159
	1) Copper oxinate precipitates	159
	2) Copper(II) oxide, surface area	162
	2,18m <sup>2</sup> /g - oxine system	
	3) Copper(II) oxide, surface area	162
	0,07m <sup>2</sup> /g - oxine system	
	4) Discussion	163
D.3.c.v.	Scanning electron microscope study	164
	1) Low surface area copper(II) oxide investigation	164
	2) High surface area copper(II) oxide investigation	164
	3) Discussion	169
E.	METAL CHELATE PRECIPITATION STUDIES	170
E.1.	Precipitation from well stirred solutions	171
E.1.a.	8-Hydroxyquinoline	171
E.1.a.i.	Polished copper metal	171
	1) Adsorption study	171
	2) Scanning electron microscope study	172
E.1.a.ii.	Etched copper metal	172
	1) Adsorption study	173
E.1.b.	Salicylaldoxime	177
E.1.c.	Conclusion	177
E.2.	Diffusion controlled growth of precipitate	178
F.	ATTEMPTS TO MEASURE SURFACE HYDROPHOBICITY	182
F.1.	Bubble pick-up method	182
F.2.	Single bubble stream flotation method	183
F.3.	Contact angle measurement on copper	183

G.	SUMMARY OF THE MODEL FOR THE ADSORPTION OF CHELATING REAGENTS ON OXIDE MINERALS	187
	G.1. Step 1. Oxide dissolution	187
	G.2. Step 2. Metal-chelate complexation	188
	G.3. Step 3. Precipitation	189
	G.4. Step 4. Post-precipitation processes	191
H.	ADSORPTION RESULTS IN RELATION TO THE FLOTATION PROCESS	193
I.	FUTURE WORK	196
J.	APPENDIX	197
K.	REFERENCES	200

Acknowledgements

The author wishes to express sincere thanks to :-

1. The Council for Mineral Technology for the award of a bursary which enabled this work to be conducted.
2. His supervisors Dr. P. Harris of MINTEK and Professors D. Eve and T. Letcher of Rhodes University. Their advice and encouragement throughout the project is appreciated.
3. Mr. R. Cross and colleagues of the S.E.M. unit for the production of the excellent quality micrographs.
4. Mr. B. Hird and Miss. M. Carle for their help in the preparation of the final draft.
5. The staff of the chemistry department.

## A. INTRODUCTION

### A.1. General

Mineral deposits of about 2% copper sulphide content have been treated very successfully for many years by an ore dressing scheme consisting of a flotation plant and a pyrometallurgical installation.<sup>1</sup> The flotation process produces a copper concentrate which can be smelted to give the metal. However, most of the rich copper deposits of traditional copper-producing areas are now being depleted and so attention is being focussed increasingly on the treatment of low grade sulphide ores and also on the recovery of other copper minerals.

The efficiency of a pyrometallurgical plant designed to treat sulphides is reduced by the presence in the feed of heavily oxidised sulphides and metal oxides.<sup>1</sup> For this reason if low grade deposits and/or copper oxide minerals are to be treated, then other mineral processing methods need to be adopted. One method relies on the efficient flotation of all types of copper minerals by the introduction of new types of collectors. The concentrate produced is chemically leached (using acid or complex forming reagents) to give a solution of metal ions, which is further treated to produce a pure solution. This is then sent to an electrowinning plant where the metal can be recovered. Precipitation and solvent extraction are two hydrometallurgical routes

which can be used to separate metal ions in solution. Another mineral processing technique in which leaching is either performed on the ore in situ or from stockpiled dumps is restricted to deposits which do not contain any acid consuming gangue minerals, such as carbonates or clays. Although direct leaching appears an attractive option, the practical problems involved usually favour the use of a step to reduce the amount of material treated, ie. flotation.

The selective separation of a specific mineral from a complex ore is achieved most efficiently by the froth flotation process.<sup>2</sup> In this process the ore is ground to a range of particle sizes which are fine enough to give the maximum release of the specific mineral from associated gangue material and small enough to allow the buoyancy of the bubbles to carry the particles to the surface, but not so fine as to produce a solid that will not have sufficient kinetic energy to collide with the bubbles.

Once the minerals have been released, it is possible, through the introduction of certain chemicals (eg. collectors, depressants, frothers), followed by the introduction of air, to concentrate specific minerals in a stable froth. This is achieved because the variations in surface properties, such as surface energy and surface excess charge between minerals, result in differences in "interfacial tensions" which in turn result in

differences in wettability. As a result, these particles, on colliding with air bubbles are attached to the bubbles and are carried to the surface forming a froth which is later skimmed off. Most natural minerals are hydrated to some degree and in order to float these minerals some adjustment of the "interfacial tension" is required. This can be done very specifically through the adsorption (or immobilization) on the mineral surface of organic reagents called collectors.

Although oxygenated solutions of alkyl xanthates have been used for many years in the selective flotation of sulphide minerals, there is still some uncertainty as to the adsorption mechanism. Some researchers consider that the adsorption occurs in two stages,<sup>2,3</sup> :

1. An initial adsorption of xanthate ion via an electrochemical reaction produces a monolayer xanthate surface coverage, and
2. Subsequent oxidation of the sulphides resulting in the formation of metal-xanthate reaction products by a chemical reaction.

Other researchers consider that xanthate adsorption on sulphides occurs only in the presence of oxygen.<sup>4</sup>

Controversy also exists over the relative role of the species dixanthogen in the enhancement of the floatability of sulphide minerals.<sup>5</sup>

It is well established that excessive oxidation of

sulphide minerals causes a deterioration of their floatability when xanthates are used as collectors.<sup>2</sup> Furthermore, metal oxide minerals are difficult to float using xanthate collectors despite the fact that the consumption of collector by these minerals is higher. The loss of floatability is believed to be caused by the detachment of unevenly distributed thick patches of metal xanthates. It is argued<sup>2</sup> that as a result of excessively strong chemisorption bonds developing between the metal ions and the xanthate ions, the lattice bonds within the oxidised layer surrounding the sulphide particles are disturbed to such an extent that adhesion of the covalently bonded metal xanthate to the underlying substrate representing the oxidized layer is minimal. However, when the collector addition is increased to such an extent that the multilayer patches of collector reaction products are no longer isolated but a continuous layer of these products envelopes each particle, the floatability of the particles improves. The reason for this is that the initial weak adhesion to the substrate is now strengthened by lateral bonds existing within the continuous layer surrounding the particle. The weak van der Waals bonds are sufficiently numerous to be capable of withstanding the disruptive forces acting on the particle-bubble aggregate.<sup>2</sup>

At present there are two methods used commercially to prepare oxidised sulphides and copper oxide minerals for

flotation.<sup>6</sup> The Zairean copper mines have used, with some success, a fatty acid collector that consisted of a 3:1 mixture of a palm oil and fuel oil.<sup>6</sup> However, this collector lacks selectivity and also is restricted to the treatment of ores which only contain siliceous gangue minerals. The other important flotation method requires the conversion of the oxidised surface layer to a sulphide through the introduction of sodium sulphide.<sup>7-16</sup> The sulphidized mineral is then floated in the normal way with xanthate acting as the collector. Unfortunately, this process is difficult to control since an excess of the hydrogensulphide ion ( $\text{HS}^-$ ) in solution can act as a depressant for sulphide minerals. Consequently, it is necessary to add the sodium sulphide in stages and then to aerate for a limited period. Some researchers maintain that the important role of the sulphidizing agent is to produce the necessary hydrophobic conditions for dixanthogen to be adsorbed on the mineral surface.<sup>13</sup>

Mineral processing chemists have been attracted to the possible use of chelating reagents as collectors ever since analytical chemists demonstrated that these reagents could complex selectively to specific metal ions.<sup>17-23,26-43</sup> Ideally, it was hoped that the addition of a chelating collector would result in a more efficient recovery of a higher grade metal concentrate. Unfortunately although laboratory tests have shown that

the technique has potential, they have yet to be adopted commercially. This is partly as a result of economic considerations but also because flotation plant results were not promising.

There have been a number of attempts to understand the mechanism of the adsorption of chelates on oxide type copper minerals.<sup>17-23, 32,34</sup> Cecile and co-workers<sup>17-20</sup> in France observed at low surface coverages of salicylaldoxime on malachite that the surface infra-red spectrum resembled a basic mono-salicylaldoximate copper complex which was transformed into a bis-salicylaldoximate copper complex with higher surface coverages. However, other researchers<sup>21-23</sup> recognized that the copper chelate was partitioned between the surface and the solution, ie. some copper chelate was attached to the surface of the mineral whereas other copper chelate was in a dispersed form in solution ("bulk"). They were able to show that, for their oxide sample, only a small proportion of the bis-salicylaldoximate copper(II) complex actually was attached to the surface, but that it was enough to impart floatability to the solid. It was proposed that the formation of a large amount of dispersed chelate was caused by the rapid release of copper ions into the solution which resulted in the precipitation of a large proportion of the bis complex, away from, rather than on the surface. Surface chelate detachment was not believed

to be important in generating bulk chelate. The present work deals with the results of a study of the adsorption of some chelating reagents on some metal oxides. Copper(II) oxide was chosen as the substrate for the most detailed study because it can be used as a model for other oxides of copper and also because it was possible to produce it in a pure, uniform, crystalline form. As a result the crystalline surfaces contained no macrofeatures which can be expected to alter significantly the adsorption properties. This work differs significantly from other work in the area, in that the copper(II) oxide was obtained in such a form. The adsorption of two N-O type chelating reagents, viz. 8-hydroxyquinoline, salicylaldoxime, and one O-O type chelating reagents, viz. hydroxamate, was investigated. These reagents were chosen because 1. their chemistry is well documented, 2. they form an insoluble precipitate with copper ions and 3. they are relatively stable to oxidation. The nitro substituted derivative of salicylaldoxime was also considered. Further, an attempt was made to understand the factors which influence the partitioning of copper chelate between the surface and the bulk solution. This included a novel approach in which copper metal was used as the substrate.

## A. 2. The use of chelating reagents as collectors in flotation

### A.2.a) Sulphides

The most important raw materials for the production of the non-ferrous metals such as copper, lead, zinc, nickel, cobalt, molybdenum, mercury and antimony are those which contain these metals as sulphides. In order to produce a metal concentrate with a sufficiently high metal sulphide content it is necessary to separate sulphide minerals selectively from unwanted gangue material. This has been achieved very successfully in flotation plants through the introduction of thio collectors. Some of these organic reagents are shown in Table 1.<sup>2</sup>

Table 1. Examples of Thio Compounds\*

Parent compound	Thio derivative, usually a metal (M <sup>+</sup> ) salt such as Na <sup>+</sup> or K <sup>+</sup>		Oxidation product of the thio derivative
1. Alcohols ROH	RSH	Mercaptans	RS-SR (Dialkyl disulfides)
2. Carbonic acid			
		O-alkyl monothiocarbonates	(Carbonate disulfide)
		O-alkyl dithiocarbonates	
		Alkyl xanthates	(Dialkyl dioxanthogens)
		Alkyl trithiocarbonates	
3. Carbamic acid			
		Dialkyl dithiocarbamates	(Thurium disulfides)
		Alkyl thionocarbamate esters (e.g., Dow Z-200, where R <sub>1</sub> = C <sub>3</sub> H <sub>7</sub> <sup>-</sup> , R <sub>2</sub> = C <sub>1</sub> H <sub>5</sub> <sup>-</sup> )	
4. Phosphoric acid			Tetraalkyl bis-dithiophosphates
		Monoalkyl dithiophosphates	(oxidation products analogous to dioxanthogens and disulfides)
		Dialkyl dithiophosphates (Aerofloats)	
5. Urea			
		Diphenyl thiourea (thiocarbamilide)	
		Mercaptobenzothiazole (Flotagen, Captax)	

\* R denotes a nonpolar group, usually a hydrocarbon group: alkyl, aryl, or cyclic.

The basic structure of these thio (sulphur containing group) collectors, consists of an active part and an inactive part. The active section comprises an acidic and basic sulphur group, which can co-ordinate to a metal ion to form a four-membered chelate ring.<sup>24</sup> Four-membered rings are normally highly strained but in this case electron delocalization within the rings exerts a counterbalancing effect. In other words, the chelate ring can be stabilized if the bond with the metal is largely covalent. This is the case for "soft" metals such as Cu(I) but not for the alkali metals. This aspect is discussed in more detail at a later stage. (See section A.4a).

An extensive research effort has been directed towards the understanding of xanthate - sulphide interactions. The mechanism is acknowledged to be very complex because both the reagent and the solid are capable of undergoing chemical reaction to produce a variety of species.<sup>2</sup> A detailed review of these studies is considered outside the scope of the present work.

#### A.2. b) Oxides.

The recovery of oxidised sulphides and oxide minerals through conventional flotation with thio collectors is well known to be an inefficient process.<sup>2</sup> Consequently, there have been many attempts to improve the process through the adoption of new reagents. Chelating type compounds have been particularly attractive since their

specificity for particular metal ions is well documented by analytical chemists. The first recorded use of such a reagent, borrowed from the analytical chemists, was by Vivian<sup>25</sup> in 1927. He used cupferron to improve the recovery of cassiterite. Other early attempts such as Holman's<sup>26</sup> use of dimethyl glyoxime on oxidised nickel ores and de Witt's<sup>27</sup> use of oximes for copper oxides confirmed the potential of this type of reagent.

Recently there have been three distinct research schools involved in the investigation of the possible application of chelating reagents to flotation. An Italian group under G. Rinelli and A.M. Marabini<sup>28-30</sup> have been particularly concerned with the problem of the processing of cassiterite ores ( $\text{SnO}_2$ ) and oxidised lead and zinc ores. Research in France<sup>17-20</sup> has been directed towards improvement in the recovery of oxidised copper and lead-zinc ores and, more recently, titaniferous material. The American effort has been directed towards increasing the efficiency of the recovery of chrysocolla<sup>31-34</sup> (a hydrated copper silicate) and haematite ( $\text{Fe}_2\text{O}_3$ ). The results of each research group will be considered separately.

The laboratory for Mineral Processing of C.N.R. in Rome, Italy has undertaken a wide-ranging research program with the aim of matching reagents to the particular metal ion in the mineral and not to the mineralogical form.

Initially, they were concerned with the problematic cassiterite flotation process.<sup>29,30</sup> It was shown that, once a certain amount of salicylaldehyde had been adsorbed by tin(IV) oxide, it could be separated selectively from a chloritic schist, provided that a small amount of fuel oil was added.<sup>29</sup> Examination of the oxide with the aid of infra-red spectroscopy revealed the presence of a surface Sn-salicylaldehyde compound.<sup>30</sup> They considered that fuel oil was physically attracted onto this initial metal-chelate layer so as to impart the extra hydrophobicity required for floatability. Marabini et al<sup>28</sup> have also been concerned with the recovery of zinc and lead oxide-sulphide ores (calamine) since Italy has good reserves of such ores but has only exploited them to a limited extent. They performed initial tests with a series of reagents that had appeared, from the analytical literature, to be specific for zinc and lead. 8-Hydroxyquinoline was eventually favoured over pyridine, anthranilic acid and quinaldinic acid. Good flotation of smithsonite occurred over a wide pH range from 2 to 11 provided, again, that fuel oil was added. Cerussite ( $\text{PbCO}_3$ ) on the other hand only responded well between pH 6 and 11 whereas the sulphides, sphalerite and galena floated well over the full pH range. Dolomitic gangue material was found to complicate the procedure since it also consumed oxine and thus showed a limited tendency to float, unlike the siliceous gangue which showed no floatability. The laboratory scale experiments on a real

ore showed such promise for good recovery of the zinc and lead that it was felt that the only feature preventing the use of oxine on a commercial scale was the price of the reagents.

The use of chelating reagents is now being studied in great detail by a number of French research institutions, in particular at the BRGM in Orleans. <sup>17-20</sup> They are concerned with the improvement of the recovery of oxidised minerals through the introduction of a collector which can adsorb selectively on all minerals containing a given element. Their basic premise was that a reagent which selectively complexes a metal ion in solution was likely to adsorb on minerals that contain that metal. The following mineral assemblages were considered.

1. Copper oxide type minerals such as malachite with dolomite or siliceous gangue.
2. Lead and zinc oxide type minerals such as cerussite and smithsonite with similar gangue.
3. Titanium and zirconium oxide types with ferric oxides.

Initially, they considered the copper and lead/zinc systems. From over 800 different types of chelating reagents they chose those which would allow the best separation of copper ions or lead/zinc ions from magnesium and calcium ions. The criteria used for selection were based on the study of the curves of the

variation of the conditional formation constant of the metal complex with pH. A reagent was considered selective for metal ion (1) over metal ion (2) if -:

$$\log K_1' - \log K_2' > 5$$
$$\text{and } \log K_1' > 12$$

where the conditional formation constant  $K' = \frac{(ML_z)}{(M^{Z+})(L^-)^z}$

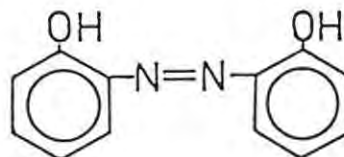
$(ML_z)$  = the total concentration of the metal complex.

$(M^{Z+})$  = the equilibrium concentration of metal ions either simple or hydroxylated.

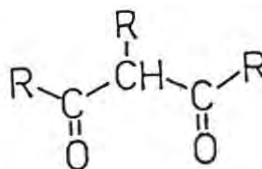
$(L^-)$  = the equilibrium concentration of ligand in neutral or acidic forms.

The suitable reagents were classified in the following family types:-

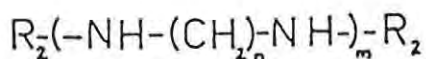
- hydroxyazoic



- beta-diketones



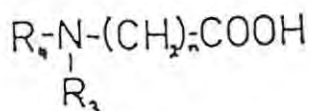
- polyalkylenediamines



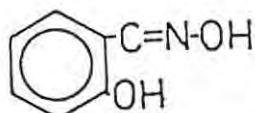
- pyridine derivs.



- amino acids

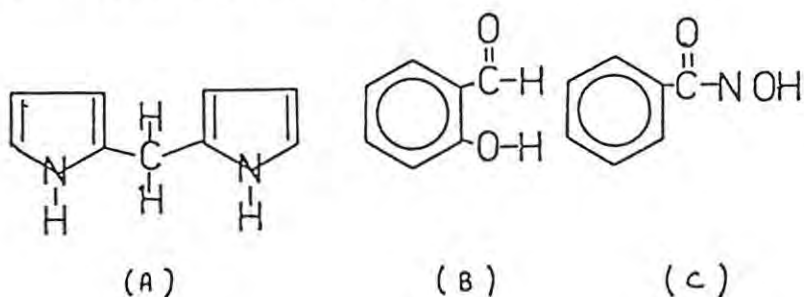


- oximes

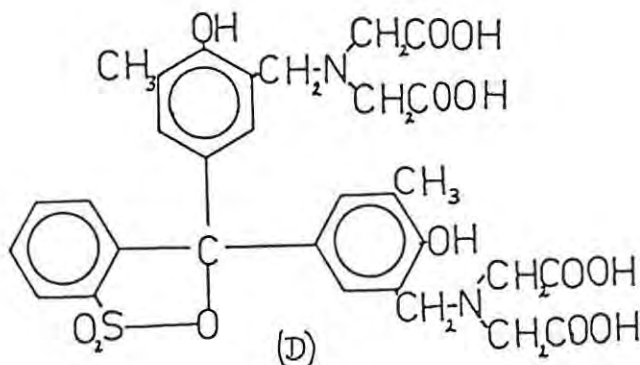


A number of commercially available reagents from these groups were tested as collectors. Hallimond cell tests confirmed that polyethylene amines and amino acids could not act as collectors since, although they formed stable chelates with the metal, the complexes they formed were water soluble. The diketones and oximes were shown to work well for the lead and copper minerals. However, the flotation order predicted from the stability constant data was not always observed in flotation. This was illustrated in the case where acetyl acetone was found to float cerussite ( $PbCO_3$ ) much better than malachite (a copper carbonate) despite the fact that copper forms a more stable bond to this ligand. In addition, hydroxyazoic was found to float cerussite and not malachite. This was believed to be caused by the dissolution of surface copper chelate in excess reagent. A fundamental study of the interaction between salicylaldoxime and copper(II) oxide was also attempted. A critical analysis of this work is included later. (see section A.3)

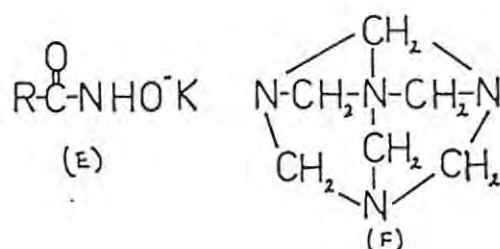
Recently these French researchers have concentrated on the recovery of titanium and zirconium oxides from ferric oxide. <sup>19</sup> They searched again for analytical reagents which would form more stable complexes with Ti(IV) and Zr(IV) than with Fe(III). The chosen reagents were tested for their collecting ability. The best reagent for the separation of rutile ( $TiO_2$ ) from haematite ( $Fe_2O_3$ ) was found to be diantipyrlmethane (A). Salicylaldehyde (B) and N-benzoylhydroxylamine (C) were effective only at low pH's.



The separation of zircon ( $ZrSiO_3$ ) was not very successful since in most cases haematite floated preferentially. Nevertheless, xylenol orange(D) at a pH 2 gave the best recovery of zircon.



M.C. Fuerstenau and co-workers, <sup>32</sup> in the U.S.A have confirmed that the formation of an insoluble copper chelate on the surface of chrysocolla (a hydrated copper silicate) was required for flotation. Potassium octyl hydroxamates (E) which was known to form an insoluble 1:1 copper chelate acted as an efficient collector at pH 6, whereas a compound which only formed soluble species, such as hexamethylene tetramine (F) did not.

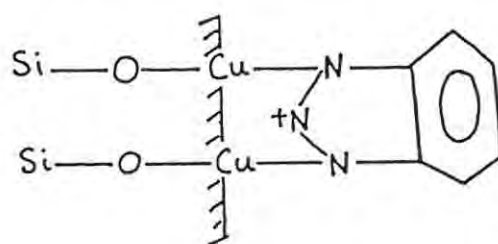


In fact they were able to identify cupric octyl hydroxamate on the surface with the aid of infra-red spectroscopy. It was believed that since the pH of maximum flotation coincided with the pH of maximum concentration of the species,  $\text{Cu}(\text{OH}^+)$ , that mineral dissolution and metal ion hydrolysis were intimately involved in the adsorption process.

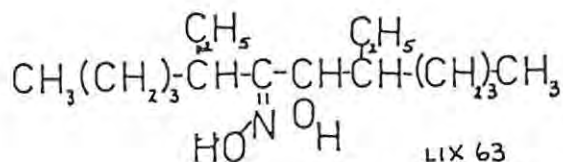
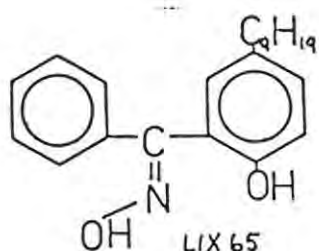
Recently Lenormand et al <sup>36</sup>, showed that hydroxamate flotation of malachite was effective between pH 6 and 10, a region in which  $\text{HCO}_3^-$  and  $\text{CuOH}^+$  ions were the predominant potential determining ions for malachite. They considered from adsorption and infra-red data that

octyl hydroxamate adsorbed through the displacement of surface  $\text{HCO}_3^-$  and  $\text{OH}^-$  ions.

Benzotriazole has also been used successfully to recover chrysocolla <sup>33</sup>, although it was found necessary to introduce a hydrocarbon to the flotation vessel. From infra-red spectroscopic data and zeta potential studies it has been concluded that the surface species bridged two surface copper atoms as shown below.



One of the biggest drawbacks to the use of new chelating reagents in the flotation process has been the cost of these materials. However, since solvent extraction plants have been commissioned, a new group of products has been marketed. Nagaraj <sup>21-23</sup> at Colombia University, New York, has investigated the potential use in flotation of one group of solvent extractants, viz. the LIX type of reagent. These reagents contain an oximic group and an hydroxy group.

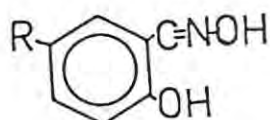


The LIX reagents were demonstrated to be excellent collectors for cuprite and chrysocolla. Flotation response of both minerals as a function of pH had maxima around pH 5 and pH 10. These maxima were observed to correspond to the minima in copper leached from the mineral. They reasoned that two adsorption processes occurred. In the first process the LIX adsorbed on the mineral and formed the surface chelate responsible for the mineral's floatability. This chelate could detach from the surface to form bulk copper chelate which they showed independently had no collecting property. In the second process copper ions were released from the mineral in such a manner that chelation occurred away from the surface and thus also generated bulk copper chelate. The rapid release of copper ions at acidic pH's would favour bulk chelate formation which explained the lack of flotation at low pH. It was concluded that the efficiency of the collector was dependent upon the partitioning of the chelate between the surface and the bulk and they therefore decided to investigate the system more fully. Their results from the study of the copper(II) oxide-salicylaldoxime system are evaluated later. (see section A.3).

The selective flotation of haematite through octyl hydroxamate addition has attracted interest in the U.S.A. 34,35 It was found that the maximum flotation was

favoured by conditions such as a high pH, high temperatures and long conditioning periods.<sup>34</sup> This was considered to indicate that the adsorption of hydroxamate by haematite was controlled by the formation of surface iron hydroxy complexes. Recently a more fundamental study has been made of the adsorption process<sup>35</sup>, and these results will be critically discussed later (see section A.3).

There have been a number of independent studies on the potential of other chelating reagents as collectors for oxide type minerals.<sup>37-39</sup> Polish workers have investigated the potential of 5-alkylsalicylaldoximes as collectors in the flotation of sphalerite from dolomite.<sup>37</sup>



R=H, Me, Pr, Bu, Pent.

They found that the adsorption density of these reagents on the surface of the minerals decreased in the order :- smithsonite, sphalerite and dolomite. An increase in the length of the alkyl chain also increased the extent of adsorption. However, the best reagent with regards to selectivity towards flotation proved to be the propyl derivative.

Atademir et al<sup>38</sup>, have attempted to separate scheelite ( $\text{CaWO}_4$ ) from calcite using 4-tertiary butyl catechol (4TBC). They chose this reagent because it was known to

complex with the tungstate ion. However, they found that although this reagent did adsorb and thus induced floatability, it was useless as a collector because 4TBC was found to be more strongly adsorbed by calcite than by scheelite. No attempt was made to identify the nature of the surface species.

A Japanese group <sup>39</sup>, has recommended the use of salicylaldoxime (rather than 8-hydroxyquinoline or  $\alpha$  benzoin oxime) as a promoter of xanthate adsorption for the flotation of chrysocolla. The pH region for optimum flotation was found to be closely related to that for the formation of the bis-salicylaldoximate copper(II) complex.

Numerous other types of chelating reagents have been tested for the flotation of cassiterite and also for certain rare earth element containing minerals. They include pelargonic hydroxamate <sup>40-42</sup> (basic constituent of the Soviet reagent, IM50), alkyl phosphonic acid <sup>43</sup>, alkyl (or aryl) arsonic acids, <sup>43</sup> and sulphonated fatty acid. <sup>43</sup>

### A.3. The mechanism of adsorption of chelating reagents on oxide minerals.

Although there have been a number of studies concerned with the use of chelating reagents in the flotation process, there has been relatively little research into the mechanism of interaction of these reagents with oxide

minerals. The important published work in this area will be reviewed and critically assessed.

A.3.a) Nagaraj's study of the copper(II) oxide-salicylaldoxime system.

Nagaraj<sup>21-23</sup> has contributed significantly to the understanding of the relationship between chelate adsorption by oxide minerals and their subsequent flotation. His approach differed from that of previous researchers in that he did not simply measure the concentration adsorbed by the residual method. Rather, he considered the adsorption in terms of the formation of a precipitate of  $\text{Cu}(\text{SALO})_2$ , where SALO is salicylaldoxime, at the oxide surface (surface chelate) and in a dispersed form in the solution (bulk chelate). He measured the concentration of surface and bulk chelate directly by extracting the precipitate into an organic solvent.

Nagaraj related the relative concentration of bulk and surface chelate to the flotation response curve as shown in fig.1.

His results showed that, although the concentration of surface chelate was significantly smaller than the concentration of bulk chelate, the maximum flotation of the oxide occurred under conditions which gave the

maximum surface chelate. He considered that the partitioning of SALO was determined by the solubility of both the mineral and the copper chelate.

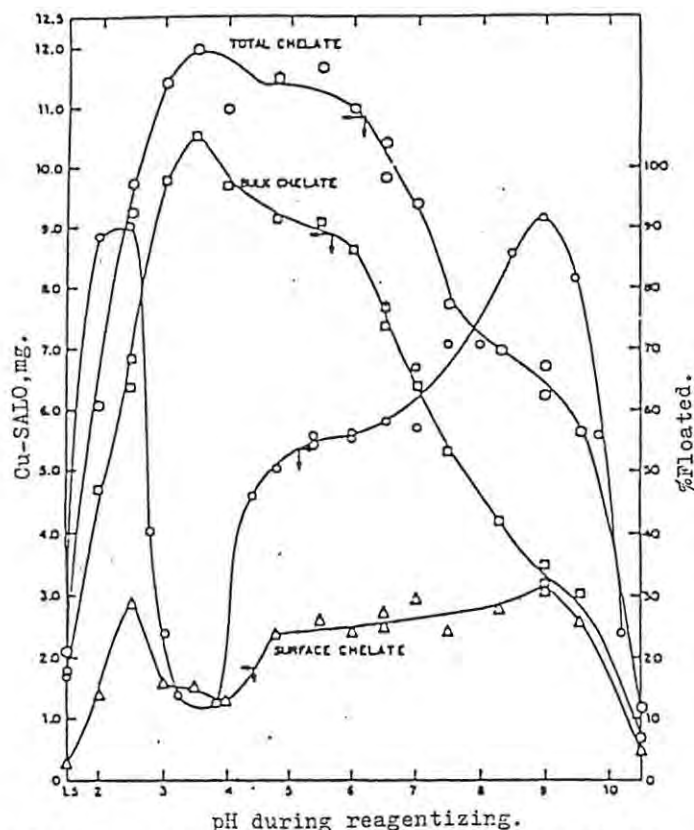


Fig.1 Nagaraj's data for the partitioning of SALO and flotation of CuO with SALO as a function of pH.

He postulated that at a precipitation edge (between pH 1,5 and 3,0 and also between pH 9,0 and 10,5), the rates of precipitation of chelate were expected to be slow unless a nucleating centre, such as the mineral surface, existed to favour chelate formation (or precipitation). If, on the other hand, the conditions were favourable for bulk chelation; eg. availability of sufficient copper ions or a favourable pH for quantitative copper chelate formation, then the partitioning of SALO favoured the formation of a large concentration of bulk chelate.

A criticism of Nagaraj's results (and most other similar studies) is the lack of control exercised in the flotation experiments. The bubble size, a variable that has a significant effect on flotation, was not controlled in his method. Consequently, it is considered that the variations in flotation response of the oxide were not always directly connected to changes in the concentration of surface chelate. A possible example of the influence of bubble size on the flotation rate was noted in some of Nagaraj's supplementary experiments. He found that the rate of flotation of the oxide was significantly reduced if the oxide was separated from the solution which contained the residual reagent and the bulk chelate.

Nagaraj also assessed the influence of the conditioning period on the flotation of copper(II) oxide. His results for experiments conducted at pH 4,0 and pH 9,0 are reproduced in fig. 2 and 3.

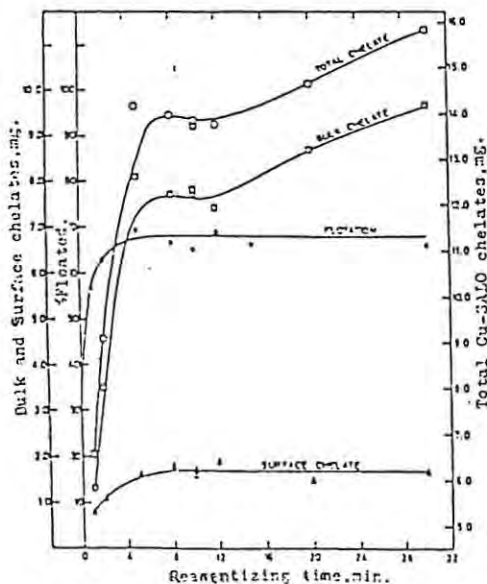


Fig.2. Nagaraj's data for the flotation of CuO with SALO at pH 4.

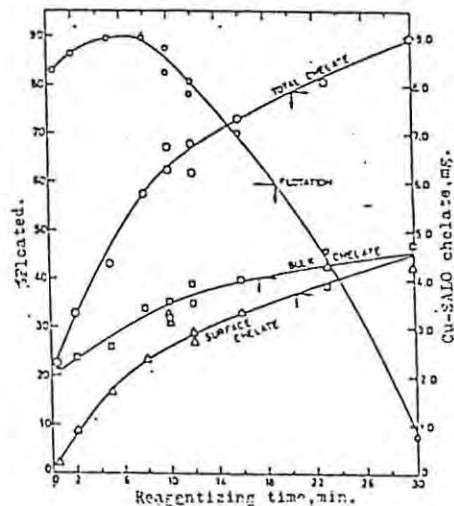


Fig.3. Nagaraj's data for the flotation of CuO with SALO at pH 9.

He found that at pH 4,0 the concentration of surface chelate remained constant with time, whereas the concentration of bulk chelate increased with time until the reagent was exhausted. The fact that the surface chelate remained constant was interpreted to indicate that it showed little tendency to detach. He did not attempt to explain the bulk chelate trend. His results at pH 9,0 showed that the concentration of surface chelate continued to increase up to 30 minutes conditioning but the flotation response started to decrease after only 10 minutes. The concentration of bulk chelate only increased slightly.

Nagaraj considered a number of reasons for the above anomalies. For instance, he proposed that excess of the ligand anion or the complex,  $\text{Cu}(\text{SALO})_2$ , might co-adsorb on the precipitate and thus prevent the mineral's flotation. However, he did not consider in much detail the possibility that the results of his separation of "bulk" and "surface" chelate (in essence a compromise procedure) could be in error. There could be two major sources of error. Firstly, there could be problems caused by the flocculation of the precipitate. The flocculated material could have settled at an equivalent rate to the copper(II) oxide. This type of problem was only acknowledged by

Nagaraj to exist in the experiment in which high concentrations of SALD were used at acidic pH values but he ignored it under all other conditions. Secondly, some of the chelate recorded as surface chelate could have been only weakly attached and as such could be detached in the turbulence of the flotation vessel. The attachment of the chelate to the surface is dependent on the physical state of the copper(II) oxide surface. Nagaraj's oxide was prepared by the oxidation of a copper(I) oxide sample to a copper(II) oxide and this could have resulted in weak bonds between the surface and inner layers of the solid. This type of problem was evident from the results of Nagaraj's attempt to reduce the amount of fine material by washing the solid in an ultrasonic bath. The effect of this treatment on the pore volume, surface area and solubility of the oxide is shown in table 2.

Table 2.  
Nagaraj's data from an attempt to reduce the amount of fine material in his oxide sample.

	Pore volume (cc/g)	Surface area (m <sup>2</sup> /g)	solubility (ppm)
Undeslimed	0,1	0,55	10
Deslimed	0,2	1,09	2,5

The results showed that the washing process did reduce the amount of fines as reflected in the lower oxide solubility but it also increased the pore volume and

therefore the surface area. The evidence suggests that the oxide surface was unstable and tended to detach in a way that increased the pore volume.

Nagaraj also investigated the adsorption of SALD on the undeslimed and deslimed samples (see table 2). He found that the concentration of surface chelate formed at acidic pH values was more or less the same for both samples. On the contrary, the concentration formed at pH 9.0 was substantially greater for the deslimed solid. This result was in agreement with the high surface area but not with the reduced solubility. It is considered that Nagaraj introduced additional complications such as differences between inner pore surface and outer surface by his choice of substrate. The present author therefore considered it vital to synthesise a more uniform, crystalline copper(II) oxide surface on which to study the adsorption of chelating type reagents on oxide minerals.

A. 3.b) Cecile's study of the malachite-salicylaldoxime system.

The aim of this work was to determine the nature of the species present on the surface of malachite,  $(\text{Cu}_2(\text{CO}_3)(\text{OH})_2)$ , when it was reacted with salicylaldoxime (SALO) at a specific pH. <sup>18-20</sup> In the first place Cecile derived the adsorption isotherm shown below by the residual method, ie. he determined the adsorption density from the

differences between the reagent concentration before and after mineral addition. His isotherm is reproduced in fig. 4.

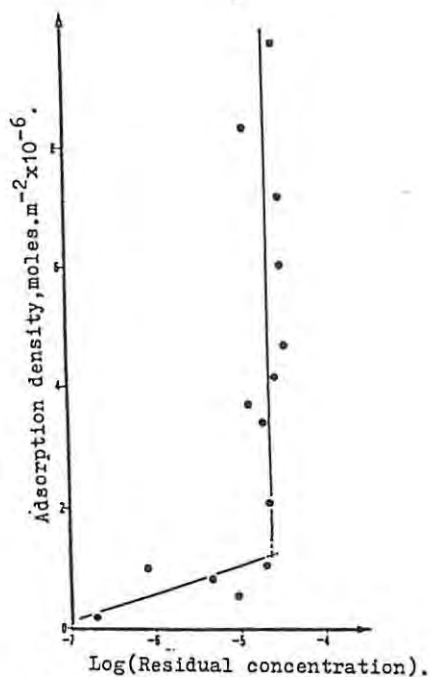


Fig.4. Cecile's data for the variation in adsorption density of SALO on malachite (pH ambient, time 600secs).

Cecile found that after a poorly defined plateau, the adsorption density increased sharply. This was probably caused by the onset of the precipitation of  $\text{Cu}(\text{SALO})_2$ .

Cecile next attempted, with the aid of infra-red spectroscopy, to determine the surface species involved. He measured the infra-red spectra of the following compounds in order to compare these spectra with the surface spectrum of the SALO coated malachite.

1. Salicylaldoxime,  $\text{H}_2\text{L}$
2. Bis-salicylaldoximato copper(II),  $\text{Cu}(\text{HL})_2$

3. Basic-mono-salicylaloximato copper(II),  
Cu(HL)OH or CuL

The surface spectrum at high concentrations of SALO was found to resemble the bis complex, whereas at low SALO concentrations the spectrum was found to resemble the mono basic complex. The change in the intensity of the N-O stretching vibrations at  $1190\text{ cm}^{-1}$  and deformation vibrations for aromatic or aliphatic C-H at  $1220\text{ cm}^{-1}$  and  $1295\text{ cm}^{-1}$  was shown to correspond to the sharp increase in adsorption density. These results are illustrated in fig. 5.

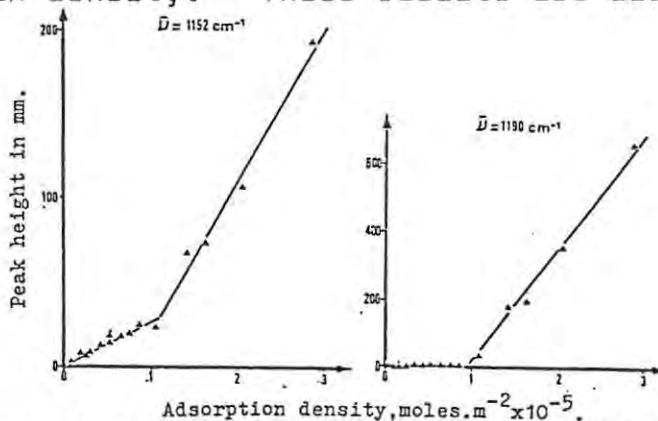
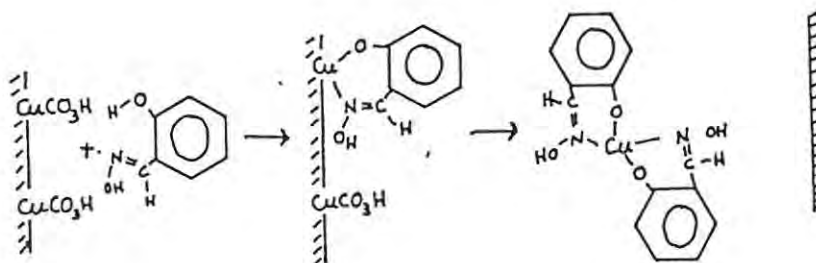


Fig.5. Cecile's data on the variation in peak height as a function of SALO adsorption density.

Cecile therefore concluded that the first step in the adsorption of SALO on malachite was a two-dimensional ordering of the complexing agent. The next stage corresponded to a three-dimensional organization of several layers of complexes resulting from the removal of copper ions from the surface. His proposed scheme is represented below.



Recently Cecile, in conjunction with a number of European research institutions, <sup>19</sup> has re-investigated the nature of the surface species. They have applied Fourier transform interferometry, which has enabled them to extend the wavelength range studied and also to detect minor absorption peaks. Their results confirmed the existence of absorption peaks similar to the bis and basic mono-salicylaldoximate complexes. However, they also identified numerous peaks which they could not attribute to any known compound. It must be concluded that the nature of surface species is more complex than it had been previously assumed.

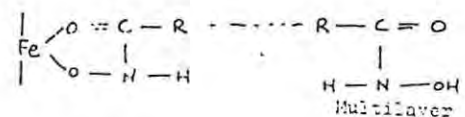
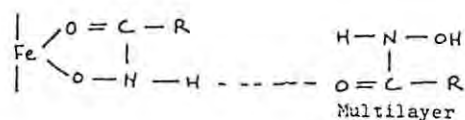
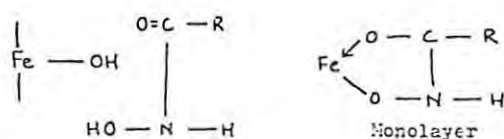
Cecile and co-workers <sup>19</sup>, have also attempted to use ESCA to study the nature of the surface species on SALO coated malachite. ESCA (electron spectroscopy for chemical analysis) is an analytical technique which allows the identification of the surface atoms. It can also be used by comparing surface spectra and reference compounds spectra to determine the type of surface species present. Unfortunately Cecile's results were not very conclusive because: 1. the spectra of the basic mono and bis SALO copper complexes were very similar, 2. the peaks of malachite tended to interfere, and 3. the surface coating was not uniform. They were unable to confirm their adsorption mechanism which they had proposed previously on the basis of infra-red data.

Cecile has concentrated on the characterization of the

surface species present on SALD coated malachite. However, the present author considers that Cecile and his co-workers have neglected to consider in any detail the mechanism for the conversion of the surface species from a two-dimensional to a three-dimensional ordering. It is considered that it is the degree of adherence of these multilayers of copper chelate to the malachite that dictates the efficiency of the recovery of the oxide. Furthermore, study of the precipitation of metal chelates on surfaces would be an important contribution to the understanding of oxide-chelate interactions.

A.3.c) Fuerstenau's study of the haematite ( $Fe_2O_3$ ) - octyl hydroxamate system.

D.W. Fuerstenau et al have studied the interaction of octyl hydroxamate on synthetic haematite through adsorption studies, electrophoretic measurements and infra-red spectroscopy.<sup>35</sup> He proposed an adsorption mechanism in which hydroxamic acid molecules reacted with Fe-OH sites to produce a monolayer coverage of an iron hydroxamate complex. Physisorption of further hydroxamate through either H-bonding or hydrophobic bonding through the alkyl groups led to multilayer build up.



Hydroxamic acid molecules rather than the hydroxamate anion were believed to be involved since the maximum adsorption occurred at a pH which corresponded to the point of zero charge of the haematite, viz. pH 8,5. Fuerstenau considered that the adsorption of ions was unlikely since if this was the case, a greater sensitivity of the adsorption to pH would be expected.

The adsorption isotherm at 20°C shown in fig. 6 clearly indicated a plateau at an adsorption density value of about  $6,7-7,5 \times 10^{-10}$  moles.  $\text{cm}^{-2}$  which Fuerstenau thought was probably caused by the formation of a monolayer.

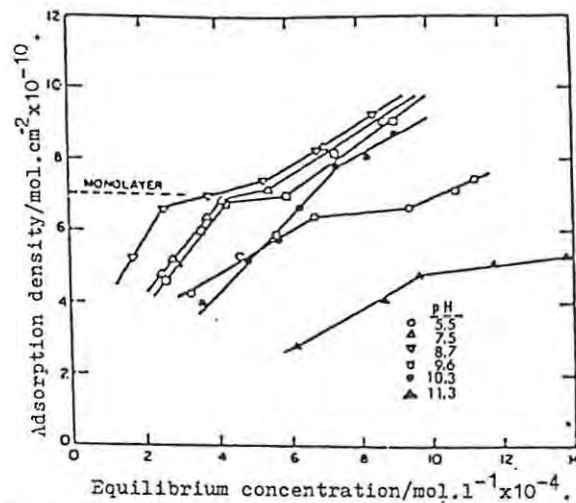
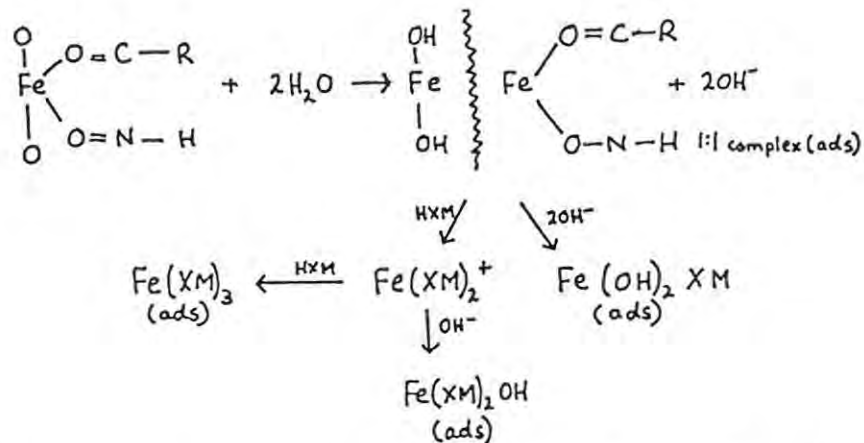


Fig.6. Fuerstenau's adsorption isotherm of octyl hydroxamate on  $\text{Fe}_2\text{O}_3$ .

Interestingly, he found that an increase in temperature resulted in a significant increase in the adsorption of hydroxamate such that, the adsorption density at 60°C corresponded to many layers. He attempted to explain this fact by proposing that at higher temperatures the

surface chelate formed, might have had a greater tendency to displace iron from the surface sites and interact then with hydroxamic molecules in the vicinity of the surface to form 1:2 and 1:3 complexes. The following scheme was visualized.



Infra-red spectroscopic investigation of haematite conditioned with hydroxamate confirmed the presence of hydroxamate complex at the surface. Fuerstenau considered that it was possible to distinguish between the infra-red absorption bands of ferric hydroxamate and the physically adsorbed hydroxamate.

The present author considers that Fuerstenau did not investigate in sufficient depth the possibility that hydroxamate adsorbs as  $\text{Fe}(\text{XM})_3$ , although it is acknowledged that he did allude to its possible presence. It is considered essential that the relative role of adsorption of hydroxamate by displacement of surface groups, the precipitation of iron hydroxamate and iron hydroxy hydroxamate complexes and the physisorption of

hydroxamate be determined. The iron(III) oxide-octyl hydroxamate system was re-investigated with this aim in mind.

#### A.4. Metal complexation.

The tendency for a metal ion and a ligand to associate together to form a metal complex is expressed as a stability constant,  $\beta$ , as defined below.

$$\beta = \frac{(ML_y)^{(x-y)+}}{(M^{x+})(L^-)^y}$$

where  $(M^{x+})$  corresponds to the concentration of the free metal ion at equilibrium,  $(L^-)$  corresponds to the concentration of ligand anion at equilibrium and  $(ML_y)^{(x-y)+}$  corresponds to the concentration of the metal complex at equilibrium.

Stability constants of many reactions have been extensively reported and compiled.<sup>44,45</sup> There are three factors that are directly responsible for the great range in the values of these constants.<sup>24,46,47</sup>

1. The bonding properties of the ligands which can be expressed in term of the concept of "hard" and "soft" acids and bases.
2. The ability of many ligands to co-ordinate to a metal ion through more than one centre, producing five or six membered rings.

3. The preferred stereochemical arrangement of bonds about metal ions.

A.4.a) "Hard" and "Soft" acids and bases.

A ligand is described as a "soft" base if the donor atom is of high polarizability and it possesses empty, low lying molecular orbitals. Such a donor atom is usually of low electronegativity and is easily oxidised. Conversely, in a "hard" base the donor atom is of low polarizability, hard to oxidize, has a high electronegativity and its empty molecular orbitals are of high energy. Similarly, a metal ion is classified as a "soft" acid if it is of low charge, large size, and has several easily excited outer electrons. Conversely, a metal ion is a "hard" acid if it is of high positive charge, small size and lacks easily excited outer electrons. The classification of metals and ligands as "soft" or "hard" is given in tables 3 and 4. <sup>46</sup>

Table 3. Ligands as Hard or Soft Bases

Hard									
H <sub>2</sub> O	OH <sup>-</sup>	RCO <sub>2</sub> <sup>-</sup>	PO <sub>4</sub> <sup>3-</sup>	SO <sub>4</sub> <sup>2-</sup>	CO <sub>3</sub> <sup>2-</sup>	NO <sub>2</sub> <sup>-</sup>	ROH	RO <sup>-</sup>	R <sub>2</sub> O
F <sup>-</sup>	Cl <sup>-</sup>								
Intermediate									
NH <sub>3</sub>	RNH <sub>2</sub>	N <sub>2</sub> H <sub>4</sub>							
Br <sup>-</sup>	N <sub>3</sub> <sup>-</sup>	NO <sub>2</sub> <sup>-</sup>	SO <sub>3</sub> <sup>2-</sup>	pyridine	aniline				
Soft									
R <sub>2</sub> S	RSH	/RS <sup>-</sup>	SCN <sup>-</sup>	S <sub>2</sub> O <sub>4</sub> <sup>2-</sup>					
R <sub>2</sub> P	(RO) <sub>2</sub> P								
I <sup>-</sup>	CN <sup>-</sup>								

Table 4. Metal Ions as Hard or Soft Acids

Hard											
H <sup>+</sup>											
Li <sup>+</sup>	Be <sup>2+</sup>										
Na <sup>+</sup>	Mg <sup>2+</sup>	Al <sup>3+</sup>	Si <sup>4+</sup>								
K <sup>+</sup>	Ca <sup>2+</sup>	Sc <sup>3+</sup>	Ti <sup>4+</sup>	VO <sup>2+</sup>	Cr <sup>3+</sup>	Mn <sup>3+</sup>	Fe <sup>3+</sup>	Cu <sup>2+</sup>	Ga <sup>3+</sup>	As <sup>3+</sup>	
Rb <sup>+</sup>	Sr <sup>2+</sup>	Y <sup>3+</sup>	Zr <sup>4+</sup>		MoO <sup>4+</sup>				In <sup>3+</sup>		
Cs <sup>+</sup>	Ba <sup>2+</sup>	La <sup>3+</sup>	Hf <sup>4+</sup>								
			Th <sup>4+</sup>								
			U <sup>4+</sup>	UO <sub>2</sub> <sup>2+</sup> and the rare earth ions							
Intermediate											
				Fe <sup>2+</sup>	Co <sup>2+</sup>	Ni <sup>2+</sup>	Cu <sup>1+</sup>	Zn <sup>2+</sup>			
				Ru <sup>2+</sup>	Rh <sup>3+</sup>				Sn <sup>2+</sup>	Si <sup>2+</sup>	
				Os <sup>2+</sup>	Ir <sup>3+</sup>				Pb <sup>2+</sup>	Bi <sup>3+</sup>	
Soft											
					Cu <sup>+</sup>						
					Pd <sup>2+</sup>	Ag <sup>+</sup>	Cd <sup>2+</sup>				Tc <sup>4+</sup>
					Pt <sup>2+</sup> , Pt <sup>4+</sup>	Au <sup>+</sup>	Hg <sup>2+</sup> , Hg <sup>1+</sup>	Tl <sup>+</sup> , Tl <sup>3+</sup>			

It has been generalized that metal complexes are usually more stable if they are formed between "compatible" metal and ligand types. The bonding between a "hard" metal and "hard" ligand gives the maximum electrostatic interaction with the resultant high stability. This electrostatic bonding model explains the increase in stability of metal hydroxides with an increase in charge to radius ratio. It is also useful in the explanation of the general increase in stability of high spin complexes of the divalent ions of the first row transition metal ions.

The radii of these ions vary in the order  $Mn^{2+} > Fe^{3+} > Co^{2+} > Ni^{2+} < Cu^{2+} < Zn^{2+}$  which correlates well with their natural order of stability (Irving-Williams order). A highly deformed cation ("soft") such as  $Cu^+$ ,  $Ag^+$  and  $Au^+$  forms stronger complexes with  $CN^-$ ,  $I^-$  and  $HS^-$  than with  $OH^-$ ,  $F^-$ , and  $H_2O$ . These transition elements in their low oxidation states have high d electron densities which can be transferred to a ligand via  $\pi$  bonding. This transfer increases the covalent nature of the bond.

#### A.4.b) Chelation.

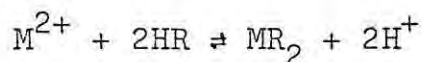
Many molecules or ions contain more than one donor atom and it may be sterically possible for them to co-ordinate one metal at two positions in its co-ordination shell. This multidentate type bonding imparts extra thermodynamic stability to metal complexes which is

usually termed the "chelate effect". This effect is considered to be related to an increase in entropy. This entropy change could be caused by a number of factors, such as changes in translational entropy (change in the number of species), changes in rotational entropy of the ligand through loss of internal rotation with ring closure, changes in solvation entropy of the metal ions and the ligand and an entropy change arising from the ligand assuming the necessary conformation to co-ordinate to the metal ion. <sup>26</sup>

In general, it has been observed that ligands which do not contain double bonds form very stable products containing 5-membered rings. Ligands that contain double bonds, such as acetyl acetone, form very stable metal complexes containing 6-membered rings.

Metal chelates can be formed through the co-ordination of two groups (bidentate) or many groups (multidentate). Bidentate ligands can be subdivided into those with two basic groups, two acidic groups and one acidic and one basic group. The most important chelating ligand containing two basic groups are those which have two nitrogen groups, such as ethylenediamine and 1,10 phenanthroline. They form very stable, water soluble metal complexes. Simple inorganic acids, such as  $\text{CO}_3^{2-}$ ,  $\text{SO}_4^{2-}$ , and  $\text{PO}_4^{2-}$ , and organic dibasic acids, such as oxalic, or malonic, chelate to metal ions through two acidic functional groups. The metal complexes produced by

the reaction of a metal ion and a molecule which carries an acidic and a basic functional group are designated as "inner" complexes. For example, a divalent metal ion,  $M^{2+}$ , with a co-ordination number of 4, reacts with a monobasic acid, HR as follows :-



The uncharged metal chelate often resembles an organic compound in its physical properties. In fact they are often soluble in organic solvents. This group of chelates is the subject of the present study, since they form insoluble metal chelate precipitates which, it is suspected, can adsorb on the mineral surface. Examples of chelates with an acidic and basic functional group are 8-hydroxyquinoline and salicylaloxime.

#### A.4.c) Stereochemical.

The stability of a metal complex is enhanced if the stereochemistry of the ligand allows the metal ion to adopt its natural coordination structure. This is illustrated in the case of the metal coordination of the straight chained, triethylene tetramine,  $H_2N CH_2 CH_2 NH CH_2 CH_2 NH CH_2 CH_2 NH_2$ , and the branched chained version,  $N(CH_2 CH_2 NH_2)_3$ .<sup>47</sup> The former group easily forms a square planar structure with the metal, whereas the latter is prevented stereochemically from doing so and thus loses some stability. Strained bonds are often formed when a chelating reagent contains a substituent

that interfered with its coordination. For example -2-methyl-8-hydroxyquinoline has a lower stability than 8-hydroxyquinoline or 4-methyl-8-hydroxyquinoline because of the interference of the methyl group. In addition, the inclusion of a bulky alkyl group in N-substituted ethylenediamine decreases the stability of the copper complex as the size of the substituent increases from  $\text{CH}_3$  to  $n\text{-C}_3\text{H}_7$ .

## B. SCOPE OF THE PRESENT WORK

### B.1. General

Copper oxide minerals create unique problems in a flotation circuit, because they appear to require an excessive adsorption of the traditional collectors to become readily floatable. This can be overcome to some extent, by firstly sulphidizing the oxide surface by the addition of sodium sulphide, and then adding the collector. This process has not proved generally acceptable since it is difficult to operate successfully. Consequently chelating type reagents have been tested and shown to enhance copper oxide mineral recovery. The aim of the present study was to attempt to understand in a fundamental way the mechanism of adsorption of chelating reagents on oxide minerals. Preliminary experiments on iron(III) oxide and copper(II) oxide were conducted in an attempt to formulate a general mechanism for the adsorption process.

### B.2. Preliminary Work

#### B.2.a) Iron(III) oxide system

In order to establish techniques of study of adsorption on oxide minerals an attempt was made to repeat some of Fuerstenau's <sup>35</sup> work on the haematite ( $\text{Fe}_2\text{O}_3$ ) - octyl hydroxamate system. The iron(III) oxide available was found to have a much smaller relative surface area (i.e. larger particle size) than that used by Fuerstenau. On

the basis of these results it was suspected that the adsorption did not occur by a simple displacement of surface ions but rather by the formation of a metal-chelate precipitate,  $\text{Fe}(\text{XM})_3$ , where  $\text{XM} =$  hydroxamate. Further studies with this type of ligand were made with the iron(III) oxide N-phenylbenzohydroxamate system. This was chosen because it has the advantage of high absorptivity, which made it possible to measure the concentration of the precipitate adsorbed spectrophotometrically. Studies were also made with recrystallized iron(III) oxide which had a lower relative surface area and a larger particle size. The larger particle size facilitated electron microscope examination of the surface. This work was not developed in greater detail because the copper(II) oxide system was considered more important.

#### B.2.b) Copper(II) oxide system

The scope of the preliminary study was extended to include the adsorption of octyl hydroxamate on copper(II) oxide. Firstly, the concentration of reagent adsorbed was determined by the residual method. On the basis of these results it was suspected again that the adsorption might involve metal-chelate precipitation. In order to assess the relative concentration of the precipitate,  $\text{Cu}(\text{XM})_2$ , where  $\text{XM} =$  hydroxamate, formed under different conditions it was necessary again to use the reagent, N-phenylbenzohydroxamate. This was partly because of the

need to analyse for the copper complex and also because the precipitate of the octyl derivative was insoluble in organic solvents. The precipitate could therefore not be extracted from the oxide surface to allow the concentration to be measured. The overall results suggested that the precipitation step was very important in the absorption process. It was therefore decided to investigate the copper(II) oxide system in more detail.

B.2.c) Sulphidization process

In a preliminary investigation it was considered of interest to study briefly the effect of the sulphidization process on the adsorption of reagents on copper(II) oxide. The investigation was concerned with the effect of sodium sulphide addition on the physical appearance of the oxide surface and on the adsorption characteristics of the xanthate ion. The results proved interesting in that the adsorbed material was not a uniform, smooth layer but rather a group of isolated patches of crystallites. It was considered outside the scope of this study to develop this research direction in great detail because of the complications introduced by the possibility of oxidation of the sulphide.

### B.3. Detailed Work

#### B.3. a) Substrate choice

Instead of naturally occurring tenorite or commercially available copper(II) oxide it was decided to study a re-crystallized sample for the following reasons:

- 1) In the preliminary work it was shown that the formation of copper-chelate precipitate was an important feature of the adsorption process. It was considered necessary to be able to distinguish between precipitate attached to the oxide surface (called surface chelate) and precipitate dispersed in the solution (called bulk chelate). This can be achieved by the exploitation of the difference in the specific gravities and therefore the settling rates of the oxide and the precipitate. However, for this method to work reasonably well, the copper(II) oxide particles were required to be sufficiently large so as to settle very rapidly. Reagent grade copper(II) oxide as supplied by most chemical supply houses has a very small particle size (surface area  $1,00 \text{ m}^2/\text{g}$ ). The crystal size was therefore increased by the re-crystallization of the oxide,
- 2) the new oxide surface was smooth and uniform which made it easy to distinguish the surface chelate with the aid of the scanning electron microscope, and
- 3) it was considered important to produce a material which was free of any obvious surface imperfections such as pore spaces, cracks, indentations etc. These sites

were considered to be possibly different to the bulk of the solid and so capable of having an influence on the adsorption process. Furthermore, it was considered that the access of solutions to and from pore spaces, for instance, would be substantially different from the more exposed areas of the surface.

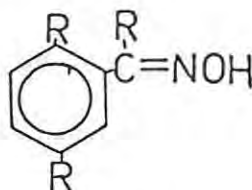
#### B.3.b) Reagent Choice

The following features influenced the choice of chelating reagent for the adsorption studies.

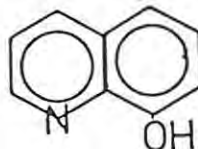
- 1) The reagents contained groups such as nitrogen and oxygen (i.e. "hard" bases) which strongly complexed copper(II) ions. The literature values for the formation constants of the copper complexes were consulted in this choice.
- 2) The reagents contained an acidic and a basic group, eg. O-O and N-O types, which complexed to copper(II) ions to form a water insoluble precipitate.
- 3) The copper complex was soluble in a common, water immiscible organic solvent, such as dichloromethane. The solvent could therefore be used to extract the copper(II) complex from the oxide surface and also from the bulk solution.
- 4) The reagent contained a chromophore with a high extinction co-efficient and high wavelength of absorption. This allowed the easy measurement of low concentrations of the copper(II) complex by spectrophotometric means.

Three types were eventually chosen:

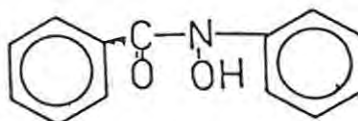
- 1) Salicylaldehyde and substituted derivatives



- 2) 8-Hydroxyquinoline



- 3) N-phenylbenzohydroxamate



### B.3.c) Experimental Approach

The approach can be subdivided into three main sections:

- 1) The determination of the concentration of metal-chelate precipitate present on the copper(II) oxide surface and in a dispersed form in the bulk solution. The influence of variables such as conditioning period, surface area, pH, temperature and dispersing agents (eg. gum arabic) on the formation of the precipitate was assessed.
- 2) The scanning electron microscope was used to distinguish the presence of the surface chelate and also to ascertain the distribution and structural nature of the growth.
- 3) The chemical nature of the surface species was studied with the aid of infra-red spectroscopy.
- 4) Supplementary experiments were performed in an attempt

to understand more about the factors which control metal-chelate precipitation. In this regard a copper metal substrate was found more suitable than the copper(II) oxide particles.

## C. PRELIMINARY WORK

The aim in this section was to formulate a general mechanistic framework for the adsorption process. This would enable more detailed experiments to be designed to test the model. These will be discussed in section D.

### C.1 Experimental

#### C.1.a) Materials

Commercially available iron and copper oxides were used for the adsorption experiments. The surface area was determined by the standard Krypton B.E.T. method at the Council for Mineral Technology, Randburg, South Africa.

i) Iron(III) oxide (Merck chemicals, pro analysis), surface area  $1,80 \text{ m}^2/\text{g}$ .

ii) Copper(II) oxide (B.D.H., reagent grade), surface area  $1,00 \text{ m}^2/\text{g}$ .

iii) Recrystallized iron(III) oxide. A 1:1 mixture of sodium tetraborate and 100% pure iron(III) oxide was heated in a platinum vessel at  $1200^\circ\text{C}$  for one hour. The melt was cooled at a rate determined by the crystal size required. The re-crystallized iron(III) oxide was removed from the crucibles with a hot dilute mixture of nitric and hydrochloric acids. All fines were removed by washing the solid in an ultrasonic bath.

### C.1.b) Reagents

N-phenylbenzohydroxamate (NPBA) was purchased from Merck chemicals. Potassium octyl hydroxamate - one mole of potassium hydroxide (56 g) in 140 ml of methyl alcohol was combined with 0,6 mole of hydroxylamine hydrochloride (42 g) in 240 ml of methyl alcohol. The solution was cooled to 10°C and filtered. Methyl octanoate (0,33 mole, 53 g) was periodically added to the filtrate at 40°C. The mixture was cooled to 0°C and filtered to collect the hydroxamate. Purification was achieved by re-crystallization from hot alcohol solution.

### C.1.c) Analysis

#### C.1.c.i) Octyl Hydroxamate

A standard calibration curve for hydroxamate was determined as follows: 5 ml of hydroxamate solution of known concentration was added to a fixed volume of iron(III) perchlorate (10 ml) and the absorbance at 521 nm (NPBA = 512 nm) measured spectrophotometrically. The solutions obeyed Beer's law up to an absorbance of 0,8. The iron(III) perchlorate solution was prepared as follows: A mixture of 5 ml 70% perchloric acid and 1,16 g iron(III) chloride was evaporated to dryness. The residue was extracted with 10 ml water and this was added to a 500 ml volumetric flask. Ethanol and 70% perchloric acid were added alternately until 25 ml perchloric acid had been added. The solution was cooled and made up to volume.

C.1.c.ii) Tris-N-phenylbenzohydroxamate iron(III)

A precipitate  $\text{Fe}(\text{NPBA})_3$  was generated by adding an alcoholic solution of the reagent to a dilute aqueous solution of ammonium ferric sulphate. A stock solution of known concentration was prepared by dissolving a known amount of  $\text{Fe}(\text{NPBA})_3$  in dichloromethane. Aliquots of the stock solution were further diluted and the absorbance at wavelength 435 nm measured. The extinction co-efficient of  $4314 \text{ l}^{-1}\text{cm.mol}^{-1}$  was determined.

C.1.c.iii) Bis-N-phenylbenzohydroxamate copper(II)

A calibration curve for this complex in dichloromethane was determined in a similar manner to that for the iron analogue. An extinction co-efficient of  $18800 \text{ l}^{-1}\text{cm.mol}^{-1}$  was calculated for the peak at 262 nm.

C.1.d) Adsorption Studies

C.1.d.i) Residual Method

A known mass of oxide (0,2 g) and a known amount of hydroxamate solution (13 g, at a set PH) were weighed into test tubes. The tubes were sealed and then placed in a mixing device that rotated the tube at an approximate 40 revs per minute. The apparatus is illustrated in fig. 7. This device kept the solid in a constant, gentle motion. The temperature was controlled by placing the device in a water bath controlled at a constant temperature. After the period of adsorption (48 hrs for iron(III) oxide) the tubes were centrifuged

until all the solid had settled. 5 mls of the liquid was then removed and analysed for hydroxamate. The adsorption density was calculated by subtracting the residual number of moles from the original number of moles.

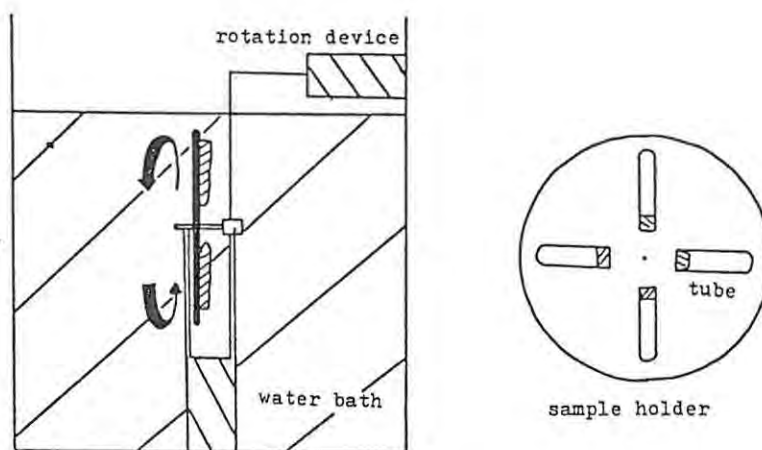


Fig 7. Mixing device for preliminary adsorption experiments.

C.1.d.ii) Direct Method

Iron(III) oxide (2,0 gm) or copper(II) oxide was added to the solution of NPBA at pH 5,0 ( $1 \times 10^{-3}$  mol.l<sup>-1</sup>, 100 ml). After 20 hours of conditioning the solid was centrifuged down and the residual concentration of hydroxamate analysed. The solid was dried at 110<sup>o</sup>C and then washed repeatedly with dichloromethane until the solution extracts became clear. The combined dichloromethane solution was then made up to a known volume and then measured spectrophotometrically at 435 nm or 262 nm. The amount of Fe(NPBA)<sub>3</sub> or Cu(NPBA)<sub>2</sub> was then calculated using the extinction co-efficients for these complexes.

C.1.e) Infra-red studies

Infra-red spectra were recorded on a Perkin Elmer 180 spectrophotometer using the pressed halide (KBr) disc method.

C.2 The Iron(III) oxide ( $Fe_2O_3$ ) system

C.2.a) Results

C.2.a.i) Adsorption of octyl hydroxamate.

The concentration of octyl hydroxamate adsorbed by iron(III) oxide from aqueous solutions controlled at pH 7,55 and at pH 9,50 at 20°C for 48 hrs was measured. The hydroxamate adsorption density was calculated by dividing the concentration adsorbed by the available surface area of oxide. The adsorption densities are given in fig. 8 together with the results on the same system as derived by Fuerstenau.<sup>35</sup>

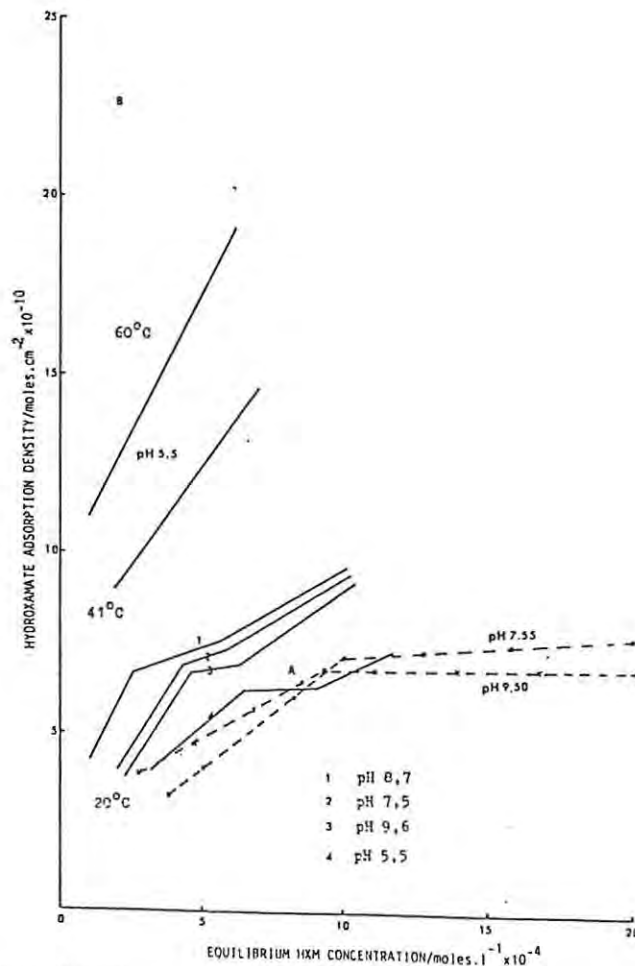
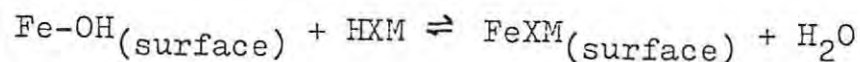


Fig. 8. Adsorption density of octyl hydroxamate on  $Fe_2O_3$  after 48hrs conditioning.

— refers to Fuerstenau's data.  
--- refers to new data.

The adsorption density of octyl hydroxamate on iron(III) oxide (surface area  $2,18 \text{ m}^2/\text{g}$ ) increased linearly with increased equilibrium hydroxamate concentration, up to a point where the adsorption density reached a value of approximately  $7 \times 10^{-10} \text{ moles. cm}^{-2}$  and the equilibrium hydroxamate concentration was  $9 \times 10^{-4} \text{ mol.l}^{-1}$ . Similarly, the adsorption density for N-phenylbenzohydroxamate under equivalent conditions also reached a plateau at approximately the same value, viz,  $7,7 \times 10^{-10} \text{ moles.cm}^{-2}$  (see point A, fig. 8). On the other hand Fuerstenau found that in his system ( $\text{Fe}_2 \text{O}_3$ , surface area  $7,90 \text{ m}^2/\text{g}$ ) that the adsorption density (for experiments conducted at similar pH values) also reached a plateau at approximately the same value but in his case the equilibrium hydroxamate concentration was lower at  $4 \times 10^{-4} \text{ mol.l}^{-1}$ . Fuerstenau calculated on the basis of the area of the polar head of the hydroxamate molecule (25A) that the plateau could co-incide with the monolayer of hydroxamate on iron(III) oxide. The following equilibrium was envisaged;



The fact that the equilibrium concentration at which the plateau was reached in the present work did not co-incide with the value found by Fuerstenau from experiments performed at similar pH values, suggests that such a simple equilibrium probably does not exist. This is reinforced by the observation that the hydroxamate did

not desorb from the oxide when the hydroxamate solution was removed. In addition Fuerstenau noted that the adsorption density increased significantly with an increase in the equilibrium hydroxamate concentration after the plateau had been reached. He ascribed this additional uptake to physisorption of hydroxamate on the initial monolayer. In the present work it was found that a further hydroxamate concentration increase resulted in only a slight addition to the adsorption density at pH 7,55 and no addition at pH 9,50.

Fuerstenau found that when the adsorption experiments were performed at higher temperatures and at pH 5,5 then the hydroxamate adsorption density was well above monolayer coverage (see fig. 8). In fact he showed that the adsorption density rose to  $20 \times 10^{-10}$  moles.cm<sup>-2</sup> for experiments at 60°C. This would give a theoretical three layers of hydroxamate on the oxide. The influence of temperature on the adsorption of octyl hydroxamate was not studied in the present work. However, it was shown that the hydroxamate adsorption density on iron(III) oxide treated with N-phenylbenzohydroxamate (NPBA) at 65°C for 24 hours was significantly greater than monolayer coverage (point B, fig. 8).

The results of these experiments indicated that the adsorption process was probably more complex than was originally suggested. The system needed further

investigation and in this regard it was decided to attempt to determine the physical appearance of the adsorbed species on the oxide surface.

2.a.ii) Scanning electron microscope study.

Iron(III) oxide was re-crystallized in order to produce a particle surface on which it would be possible to recognise adsorbed species easily under the scanning electron microscope. The original material was too fine for this type of study. Although NPBA was used for this section, it was considered that the octyl derivative would show the same type of result since the adsorption data had indicated that they behave similarly.

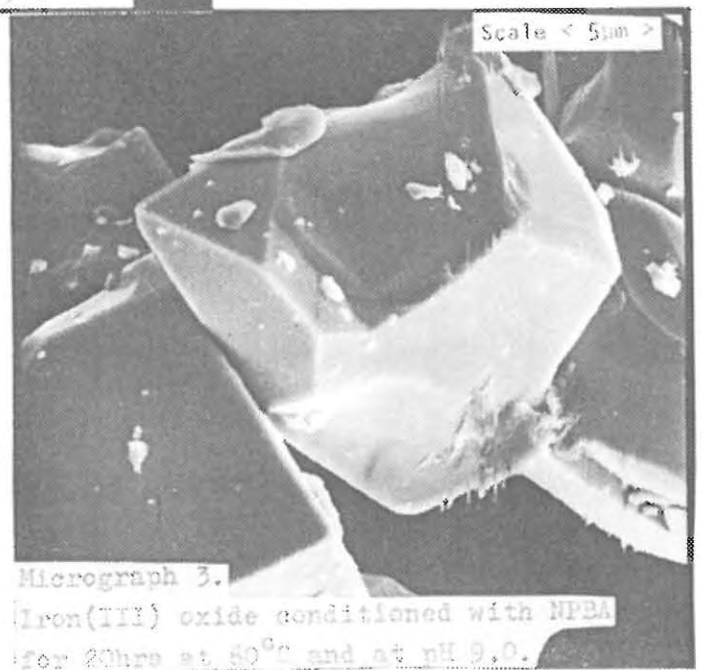
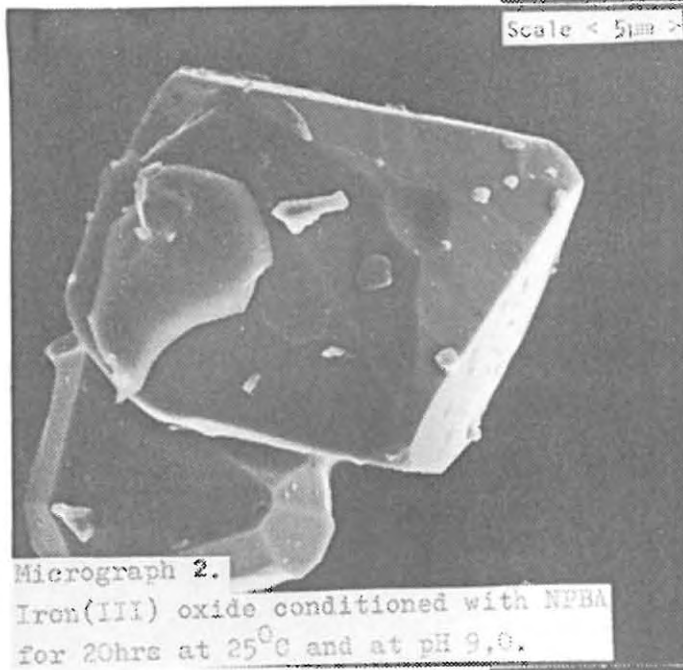
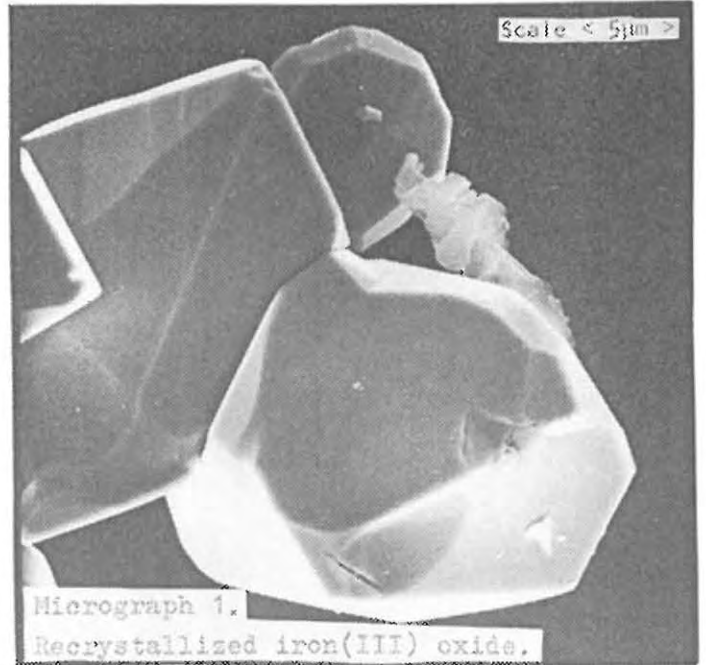
Micrograph 1: This shows the solid after conditioning in aqueous solution without reagent at pH 9,0 for 24 hours at 25°C. The surface was smooth and was almost completely free of any visible surface imperfections.

Micrograph 2: This shows iron(III) oxide treated with NPBA ( $1 \times 10^{-3} \text{ mol.l}^{-1}$ ) at pH 9,0 at 25°C for 24 hours. By analogy to the adsorption results for similar conditions it was expected that the hydroxamate adsorption density was close to a monolayer coverage. There is evidence for the formation of a new solid phase on the surface of the oxide. The new feature occurred as isolated patches, randomly distributed across the oxide surface.

Micrograph 3: Iron(III) oxide was treated under the same conditions as the previous sample, except the

temperature was increased to 65°C. The hydroxamate adsorption density was expected to be greater than monolayer coverage by analogy to the previous adsorption data. A similar growth on the oxide crystal surface was again visible under the S.E.M. In addition, the surface coverage of the growth was approximately the same as in the sample treated at 25°C.

This study has shown that some of the adsorbed hydroxamate occurred as isolated patches of a new solid phase on the oxide surface. These patches were apparent even at levels which would only have given a theoretical monolayer coverage. In order to account for the accumulations of hydroxamate at selected sites and still have a total theoretical monolayer coverage, it is necessary to propose that other areas of the surface would be unaffected by the reagent. This suggests that there is no uniform layer of hydroxamate across the oxide surface. It was suspected that the surface growth could be tris-N-phenylbenzohydroxamate iron(III), because this complex is known to be insoluble in aqueous solution. It was therefore considered important to assess the role of this complex in the adsorption process.



2.a.iii) Formation of Fe(NPBA)<sub>3</sub>.

It is considered that a precipitate of Fe(NPBA)<sub>3</sub> could form either on the oxide surface or in a dispersed form in the bulk solution. In this section no attempt was made to distinguish between the two forms of precipitate. The concentration of Fe(NPBA)<sub>3</sub> formed could be determined because this species was very soluble in an organic solvent. It could therefore be extracted from the oxide surface and the concentration measured by spectrophotometric means. The concentration of Fe(NPBA)<sub>3</sub> formed (which can be converted to a hydroxamate adsorption density) is given in table 5. Also included in this table is the hydroxamate adsorption density for equivalent experiments as determined by the residual method.

Table 5.

The variation with temperature of the concentration of the precipitate, Fe(NPBA)<sub>3</sub>, formed from N-phenylbenzohydroxamate solutions ( $1 \times 10^{-3} \text{ mol.l}^{-1}$  100ml) and iron(III) oxide (surface area  $1,80 \text{ m}^2/\text{g}$ ) 1,0g) after 24hrs at pH 5,5.

Temp. °C	Fe(NPBA) <sub>3</sub> moles. $10^{-5}$ (by extraction)	Adsorption density (HXM) calc. ex. Fe(NPBA) <sub>3</sub> .	Adsorption density (HXM) calc. by resid. meth.	Hydroxamate unaccounted for.
		moles. $\text{cm}^{-2} \times 10^{-10}$		
25	0,36	3,00	7,72	4,72
65	0,86	7,17	22,82	15,65

The results confirm that Fe(NPBA)<sub>3</sub> was formed on iron (III) oxide treated with the reagent at 25°C and at

65°C. However, the comparison between the hydroxamate adsorption density as calculated on the basis of the concentration of the precipitate and the adsorption density as determined experimentally by the residual method indicated that there was a fair proportion of hydroxamate adsorbed that was not accounted for as  $\text{Fe}(\text{NPBA})_3$ . An attempt was therefore made to determine the chemical identity of the hydroxamate on the oxide surface with the aid of infra-red spectroscopy.

2.a.iv). Infra-red spectra.

The infra-red results must be considered in terms of the experimental problems associated with the measurement of spectra of solids dispersed in potassium bromide discs. Most authors study the infra-red absorption spectra of compounds adsorbed on solids with a very much higher surface area than they used for the derivation of the adsorption data. This is because the higher the surface area of the solid the greater the amount of adsorbed reagent in the disc and therefore the greater the sensitivity. At high relative concentrations of iron(III) oxide transmission of radiation is restricted to such a level that a spectrum is no longer obtainable. In this study the same samples were used for both the adsorption and infra-red studies. It was considered that the use of a higher surface area oxide could change the type of surface species formed. Unfortunately with this material the baseline absorbance due to the scatter caused by

the presence of the iron (III) oxide in the disc changed rapidly. This caused slight wavelength shifts and it also introduced uncertainty into the exact intensity of the peaks. The problem became significant when in order to detect the very low intensities of the adsorbed peaks it was necessary to use the maximum scale expansion (x20) and noise damping facilities available on the instrument. The baseline slope was now such that it was only possible to measure the spectrum over a restricted range before the baseline setting needed adjustment. However, since the baseline varied in a constant way it was possible to detect peaks of the adsorbed reagent.

The spectra of the following are illustrated in figure 9 and in tabulated form in table 6.

- a)  $\text{Fe}(\text{NPBA})_3$ . This solid was prepared by the addition of a NPBA solution to a solution of ammonium iron (III) sulphate.
- b)  $\text{Fe}_2\text{O}_3$  was conditioned in a  $1 \times 10^{-3} \text{ mol.l}^{-1}$  NPBA solution for 24 hrs. at pH 5,5 and at  $25^\circ\text{C}$ . The solid was centrifuged down and then washed twice with de-ionised water and then air dried.
- c) The same conditions as for (b), except in this case the solution temperature was  $65^\circ\text{C}$ .
- d) The  $\text{Fe}_2\text{O}_3$  from (c) was extracted (ie. washed) repeatedly with dichloromethane. An ultrasonic bath was used to assist in the re-dispersion of the solid.

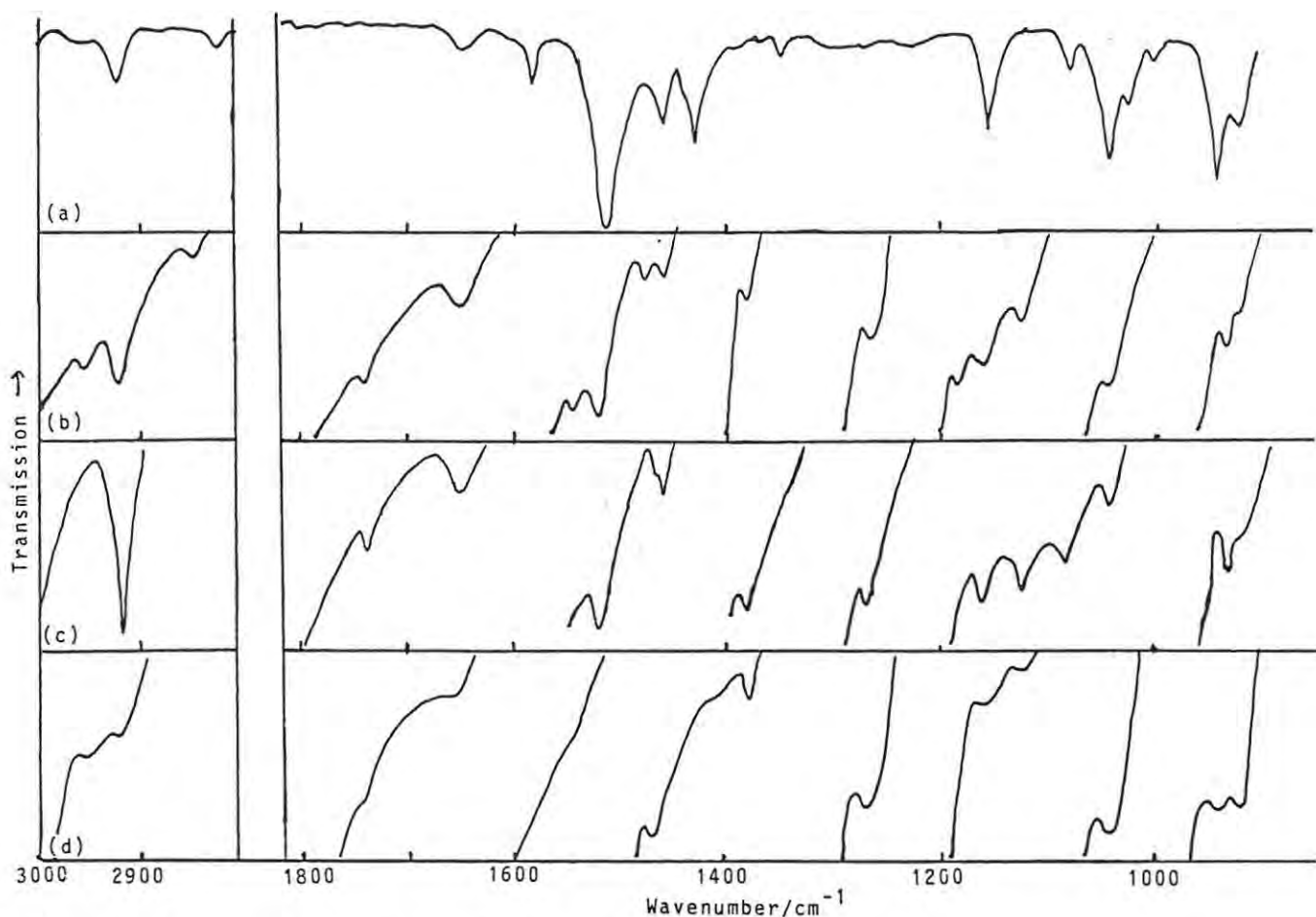


Fig. 9. Infra-red spectra of iron (III) oxide treated with *N*-phenylbenzohydroxamate. (a)  $\text{Fe}(\text{NPBA})_3$ , (b)  $\text{Fe}_2\text{O}_3$ -adsorbed NPBA/25°C, (c)  $\text{Fe}_2\text{O}_3$ -adsorbed NPBA/65°C, (d)  $\text{Fe}_2\text{O}_3$ -adsorbed NPBA/65°C  $\text{CH}_2\text{Cl}_2$  extracted.

Table 6.

Infra-red spectroscopic data of  $\text{Fe}_2\text{O}_3$  conditioned with *N*-phenylbenzohydroxamate (KBr disc). Wavenumber/ $\text{cm}^{-1}$

NPBA (K salt)	$\text{Fe}(\text{NPBA})_3$	$\text{Fe}_2\text{O}_3$ -adsorbed NPBA (25°C)	$\text{Fe}_2\text{O}_3$ -adsorbed NPBA (65°C)	$\text{Fe}_2\text{O}_3$ -adsorbed NPBA (65°C) $\text{CH}_2\text{Cl}_2$ ext.
3350(s)				
3050(s)	3050(w)			
		2955	2950	2960
2930(w)	2920(w)	2920	2915	2920
2860(w)		2850		2850
		1740	1735	1740
1655(s)	1645(w)	1665	1650	1655
1615(s)	1585(s)			
1595(vs)		1538		
1555(vs)				
1490(s)	1518(vs)	1518	1520	
		1478		
1465(w)	1460(s)	1465	1460	1470
1440(s)	1432(s)			
1395(s)				
1320(w)	1355(w)	1380	1380	1380
1260(w)				
		1265	1270	1270
		1185		
1160(s)	1155(w)	1155	1155	1160
		1120	1118	1125
1070(s)	1075(w)			
1035(w)			1080	
1015(w)	1040(s)	1045	1040	
	1020(s)			
	1000(w)			
	940(s)			
920(s)	918(s)	930	932	940

The results indicate that some hydroxamate species adsorbed on iron(III) oxide. There were a large number of similarities between the absorption peaks of the iron(III) oxide and  $\text{Fe}(\text{NPBA})_3$ . Some weak peaks associated with the complex were not detected and some additional peaks such as those at  $1740 \text{ cm}^{-1}$ ,  $1380 \text{ cm}^{-1}$  and  $1118 \text{ cm}^{-1}$  occurred with the iron(III) oxide. The oxide sample that was treated to remove all the  $\text{Fe}(\text{NPBA})_3$  still showed a number of peaks associated with hydroxamate. Interestingly, the main peaks for  $\text{Fe}(\text{NPBA})_3$ , viz.  $1518 \text{ cm}^{-1}$

had disappeared which confirmed that the extraction procedure had been successful. The surface spectrum of the washed oxide sample did not resemble the spectrum for the simple salt of the reagent either. This salt has the most prominent peaks at  $1595 \text{ cm}^{-1}$  and  $1555 \text{ cm}^{-1}$ . It was therefore concluded that the material which remained behind on the oxide surface was some other form of iron hydroxamate complex.

#### C.2.b) Discussion.

The results have shown that the concept of a uniform monolayer of hydroxamate adsorbed on iron(III) oxide was not applicable. Rather, the adsorption occurred as isolated patches of an iron hydroxamate precipitate. It was possible to show that some of this precipitate was the tris-N-phenylbenzohydroxamate iron(III) complex. However, a large proportion of the hydroxamate adsorbed

was not accounted for by this complex. At higher conditioning temperatures the amount of hydroxamate unaccounted for was particularly large. There are a number of possible reasons for the failure to account for the hydroxamate.

1) The formation of a very finely dispersed precipitate. Hydroxamate in this form would not be accounted for by the extraction method. This possibility was considered unlikely because there was no visual evidence for its formation.

2) The extraction procedure of the  $\text{Fe}(\text{NPBA})_3$  precipitate was inefficient. This reason was unlikely because the precipitate was very soluble in dichloromethane. Furthermore, this would not explain the increased loss at the higher conditioning temperature.

3) The hydroxamate physisorbed onto the precipitate. The fact that the concentration of hydroxamate unaccounted for increased with higher conditioning temperature effectively excludes this possibility because physisorption is usually reduced under these conditions.

4) The hydroxamate chemisorbs onto the oxide surface in a monodentate form. Fuerstenau has calculated that there is one iron atom for every area of approximately  $10^{-1} \text{ nm}^2$  of the iron(III) oxide surface. If a hydroxamate molecule could co-ordinate to every available iron atom then a hydroxamate adsorption density of  $31,9 \times 10^{-10} \text{ moles. cm}^{-2}$  would result. On the other hand Fuerstenau pointed

out that the size of the polar head of hydroxamate dictates that if the reagent chelates to one iron atom then approximately three iron atoms could be effectively covered by the adsorbing hydroxamate molecule. It would therefore be necessary for the hydroxamate to bond to the iron atom monodentately to allow access to all the available surface iron sites. It was hoped that it would be possible to distinguish between monodentate and bidentate bound hydroxamate on the iron surface with the aid of infra-red spectroscopy. The infra-red spectra of the oxide surface after the  $\text{Fe}(\text{NPBA})_3$  had been removed was similar to the original except for the absence of a few key peaks. Unfortunately without standard spectra of hydroxamate molecules in both co-ordination modes it was not possible to conclude whether monodentate co-ordination was a factor.

5) The hydroxamate forms a chemisorbed layer by the displacement of the surface hydroxyl groups. This possibility is not favoured because the SEM study showed that the adsorbed species occurred as a distinct surface feature, even at levels corresponding to monolayer coverage. This suggested that other parts of the surface would be unaffected by the reagent.

6) Iron hydroxy hydroxamate complex formation. It is possible that a precipitate of an iron hydroxy complex such as  $\text{Fe}(\text{OH})(\text{HXM})_2$  or  $\text{Fe}(\text{OH})_2\text{HXM}$  (where HXM = hydroxamate) or some iron hydroxy polymer, could form on the oxide surface. These complexes are unlikely to be

soluble in an organic solvent and therefore are unlikely to be extracted. Unfortunately, the importance of these species is difficult to assess because the equilibrium data relevant to these species is not available.

7) Hydration of oxide. The increased adsorption at higher temperatures could be caused by an increase in the surface area of the oxide available due to breakdown of the iron(III) oxide structure and the formation of iron(III) hydroxide.

### C.3. Copper(II) oxide system

#### C.3.a) Results

##### C.3.a.i) Adsorption of octyl hydroxamate.

Copper(II) oxide (surface area, 1,00 m<sup>2</sup>/g) was conditioned for 48 hours with octyl hydroxamate at pH 9,6 at various temperatures. The long conditioning period was required in order to achieve equilibrium at all temperatures. The variation in the hydroxamate adsorption density with time is given in fig.10.

The hydroxamate adsorption density on copper(II) oxide at 20°C reached a value, viz.  $120 \times 10^{-10}$  moles.cm<sup>-2</sup>, that was very much larger than the adsorption density on iron(III) oxide under similar conditions. The adsorption density corresponds to approximately seventeen layers of hydroxamate, if one uses Fuerstenau's<sup>35</sup> value for theoretical monolayer coverage, viz.  $7 \times 10^{-10}$  moles cm.<sup>-2</sup>

At higher temperatures an even larger uptake of hydroxamate by the oxide occurred. Interestingly it was

found that if the adsorption process was conducted at  $40^{\circ}\text{C}$  to point A and then the temperature was increased to  $55^{\circ}\text{C}$  then the rate of uptake of hydroxamate was found to increase to point B.

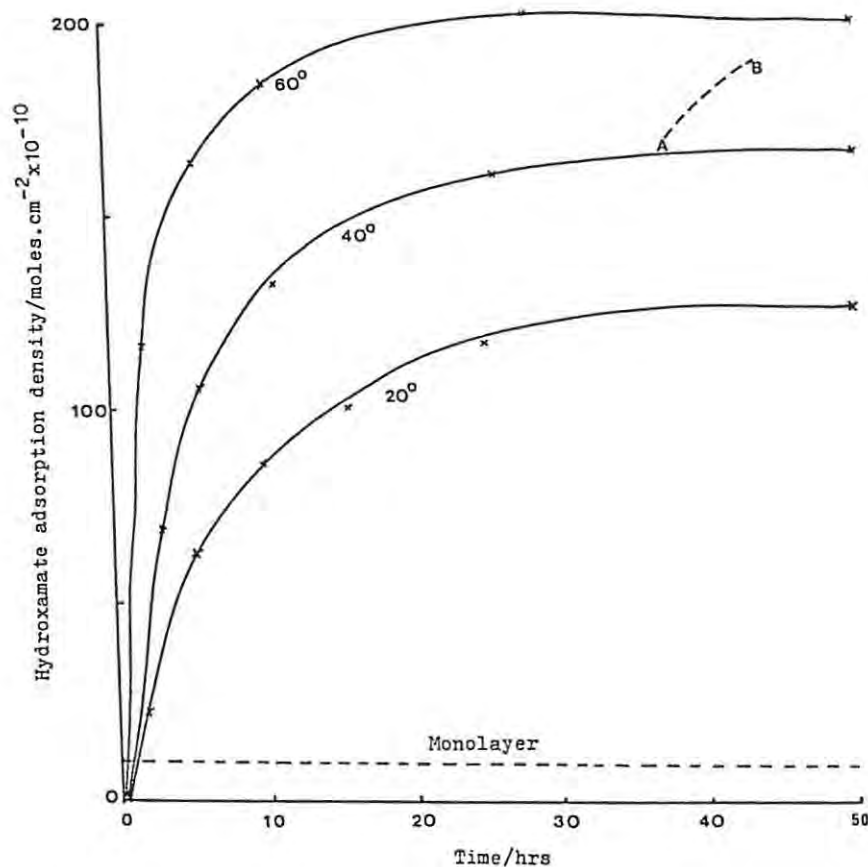


Fig10. Variation of adsorption density with time for CuO-octyl hydroxamate at various temperatures.

The adsorption data after 48 hours can be replotted in terms of the usual adsorption density vs. equilibrium concentration curve as shown in fig. 11 .

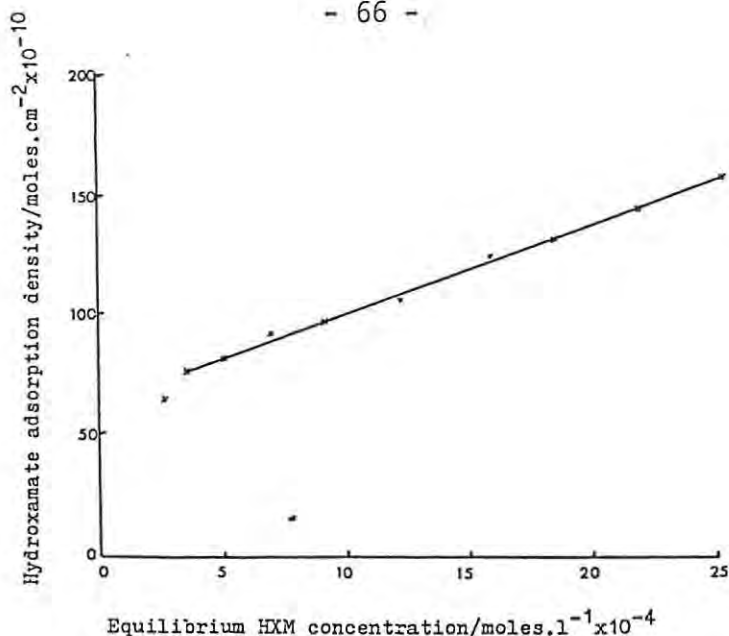


Fig.11. Adsorption isotherm of octyl hydroxamate on CuO at 20°C.

This graph resembles the isotherm derived by Lenormand<sup>36</sup> except that the new data showed a slight increase in adsorption density at higher equilibrium concentrations. He compared his isotherm to the Giles classification of isotherms<sup>48</sup> and decided that the data resembled a high affinity type. He concluded that the hydroxamate chemically adsorbed on malachite. However, the present author considered that because the amount of hydroxamate was so much larger than the theoretical monolayer coverage that it was necessary to consider other possible adsorption processes. By analogy to the iron(III) oxide data it was suspected that a copper hydroxamate precipitate could be responsible for the large uptake of hydroxamate by the copper(II) oxide. This possibility was investigated with the aid of infrared spectroscopy.

3.a.ii) Infra-red study.

The reagent NPBA, was used in this and subsequent studies because it was more soluble. The results for the octyl derivative were expected to be similar.

The results of an infra-red investigation of the copper(II) oxide - NPBA system are shown in figure 12 and in tabulated form in table 7. The following spectra are illustrated.

- a)  $\text{Cu}(\text{NPBA})_2$ . This solid was formed by the addition of a NPBA solution to a copper(II) sulphate solution.
- b) Copper(II) oxide (surface area  $1,0\text{m}^2/\text{g}$ ) was treated with a NPBA solution for 24 hours at a pH 5,5 and at  $25^\circ\text{C}$ .
- c) Copper(II) oxide was treated under the same conditions as for (b) but in this case the oxide was subsequently extracted with dichloromethane.

The spectra illustrated in (b) and (c) were measured using the x 20 scale expansion facility. The significant change in the baseline slope due to the scatter caused by the presence of the oxide in the disc dictated that only a restricted wavenumber range could be measured before the baseline setting needed adjustment. In the case of (c) only the spectrum over certain wavenumber regions were measured.

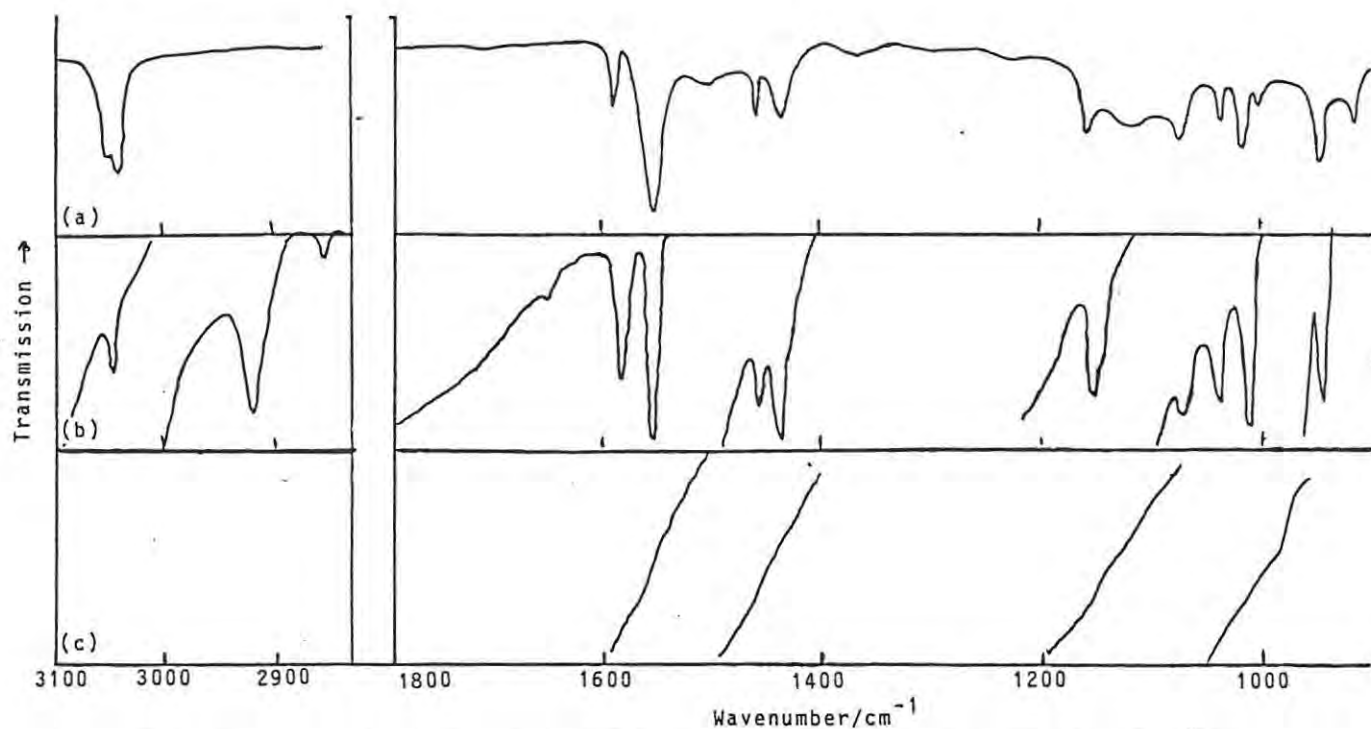


Fig. 12. Infra-red spectra of copper (II) oxide treated with N-phenylbenzohydroxamate. (a)  $\text{Cu}(\text{NPBA})_2$ , (b)  $\text{CuO}$ -adsorbed NPBA/ $25^\circ\text{C}$ , (c)  $\text{CuO}$ -adsorbed NPBA/ $25^\circ\text{C}$ -extracted  $\text{CH}_2\text{CL}_2$ .

Table 7.

Infra-red spectroscopic data of copper(II) oxide conditioned with N-phenylbenzohydroxamate (KBr discs, wavenumber/ $\text{cm}^{-1}$ ).

$\text{Cu}(\text{NPBA})_2$	Copper(II) oxide conditioned $25^\circ/60^\circ$	Copper(II) oxide after extraction.
3040(m)	3045	
2920(w)	2920	
2850(w)	2850	
1582(m)	1580	Z
1550(s)	1548	E
1495(m)		R
1457(m)	1456	O
1430(m, br)	1435	
1156(m)	1155	
1070(w)	1070	
1035(m)	1035	
1012(m)	1010	
1000(w)		
940(m)	938	

s=strong, m=medium, w=weak, br=broad

Copper(II) oxide which was treated with NPBA at pH 5,5 showed absorption peaks which were very similar to those for  $\text{Cu}(\text{NPBA})_2$ . When the treated copper(II) oxide sample was extracted with dichloromethane no absorption peaks associated with  $\text{Cu}(\text{NPBA})_2$  were observed. This evidence therefore strongly supported the proposal that the formation and the adsorption of precipitate could explain the adsorption data. It was therefore decided to attempt to measure the amount of the precipitate formed.

3.a.iii)  $\text{Cu}(\text{NPBA})_2$  formation.

An indirect method was used to show that  $\text{Cu}(\text{NPBA})_2$  was formed at the copper(II) oxide surface. The complex was removed from the oxide by extraction into dichloromethane.  $\text{Cu}(\text{NPBA})_2$  was known to be very soluble in this solvent. The identity and concentration of the complex could then be checked spectrophotometrically by the comparison of the absorbance with that of standard solutions of  $\text{Cu}(\text{NPBA})_2$ . The concentration of  $\text{Cu}(\text{NPBA})_2$  formed when copper(II) oxide was conditioned with NPBA at ambient pH for 24 hours is given in table 8.

The results indicated that the amount of precipitate formed was very large in comparison to the amount formed on iron(III) oxide. In fact the major part of the hydroxamate adsorbed could be explained by the formation of a precipitate of  $\text{Cu}(\text{NPBA})_2$ .

Table 8.

The formation of  $\text{Cu}(\text{NPBA})_2$  on copper(II) oxide at various temperatures. N-phenylbenzohydroxamate ( $1 \times 10^{-3} \text{ mol.l}^{-1}$ , 100ml) Oxide (surface area  $1,00 \text{ m}^2/\text{g}$ , 1,0g)

Temp. °C	$\text{Cu}(\text{NPBA})_2$ (moles. $\times 10^{-5}$ )	Adsorption density calc. from $\text{Cu}(\text{NPBA})_2$ (moles. $\text{cm}^{-2} \times 10^{-10}$ )	Adsorption density calc. by resid. meth.
25	5,82	375	367
65	5,34	356	367

C.3.b) Discussion.

It is clear from the data presented that the adsorption of hydroxamate on copper(II) oxide involved the formation of a copper hydroxamate precipitate. At a constant temperature the concentration of hydroxamate adsorbed and therefore the concentration of precipitate formed reached a constant value after approximately 48 hours. This plateau probably indicates that release of copper(II) ions from the surface has ceased. This may have been achieved by the surface precipitate physically sealing the surface from the solution. An increase in temperature was found to cause an increase in the concentration of precipitate produced. This could have been caused by the displacement of the surface precipitate which would expose fresh copper(II) oxide surfaces. It could also be due to an increase in the

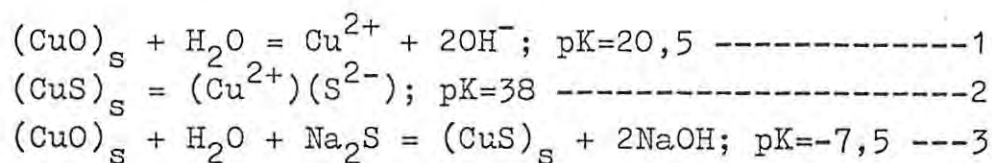
ability of the copper ions to diffuse through the precipitate layer. It was also shown that the adsorption density of hydroxamate was larger at higher equilibrium hydroxamate concentrations. This suggests that a different structural form of precipitate might have formed on the oxide surface. Different forms of precipitate might have different abilities to seal the surface from the solution. The result could also indicate that, at higher hydroxamate concentration, there was a greater tendency for the precipitate to form away from the surface or alternatively to detach from it more easily. The relationship between bulk and surface chelate was investigated further in the detailed work.

#### C.4. Xanthate and sulphidization.

One of the most common ways to treat oxidised copper sulphides and copper oxide ores is first to add sodium sulphide and then to use a xanthate as the collector. The use of xanthates alone has been found to be insufficient to cause these minerals to float. It was considered of interest to investigate the interaction between these reagents and the re-crystallized copper(II) oxide surface, in order that a comparison could be made with the chelating reagent - copper(II) oxide data. It was also hoped that a contribution could be made to the understanding of how the sulphidization process works.

The extent of reaction of sulphide with copper(II) oxide

can be described by combining equations 1 and 2 which describe the solubility of copper(II) oxide and copper(II) sulphide respectively,



A pK of -7,5 for equation 3 indicates that the formation of copper(II) sulphide is very strongly favoured and will result in the dissolution of copper(II) oxide until all the sulphide has been removed.

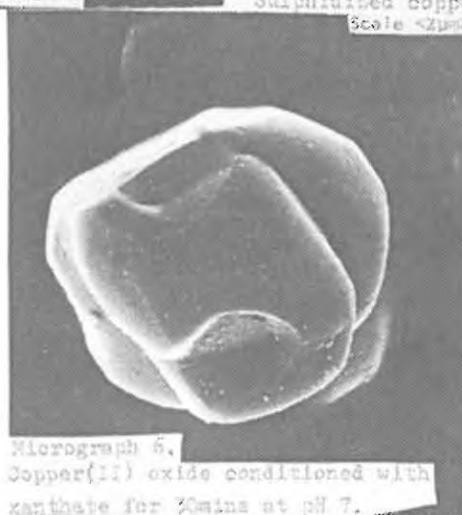
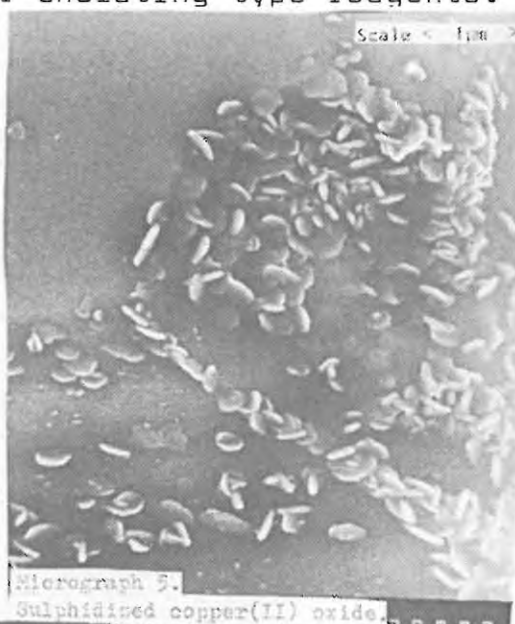
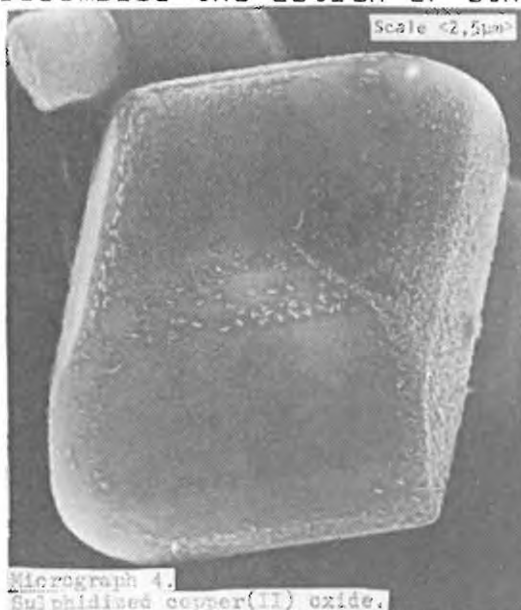
#### C.4.a) Sulphidization procedure.

Re-crystallized copper(II) oxide (1,0 gm, SA = 0,07 m<sup>2</sup>/g) was added to a well stirred solution of sodium sulphide, (100 ml, 3 g/l) at pH 10,0. All traces of sulphide were found to be removed from solution within minutes. Under the SEM it was possible to identify the presence of a surface feature on some parts of the oxide crystal (micrographs 4,5). This feature consisted of a collection of very small, ellipsoid shaped crystallites of copper sulphide. It was possible to cover the entire oxide crystal by the use of higher concentrations of sodium sulphide.

#### C.4.b) Xanthate adsorption.

The treatment of copper(II) oxide particles with potassium ethyl xanthate resulted in the formation of isolated small crystallites on the oxide

surface (micrograph 6). In this regard, xanthate resembles the action of other chelating type reagents.



C.4.c) Reaction between sulphidized copper(II) oxide and xanthate.

Sulphidized copper(II) oxide (1,0 gm) was added to a solution of potassium ethyl xanthate ( $1 \times 10^{-4}$  mol.  $l^{-1}$ , 100 mls) at pH 5,5. The uptake of xanthate by the oxide was monitored directly by passing the solution from the conditioning vessel, via a filter and pump, to a spectrophotometer. It was clear from the results that

the uptake of xanthate increased with sulphidization (fig. 13). In fact, the rate of uptake at pH 10,0 was found to be directly proportional to the level of sulphidization of the surface (fig. 14).

It is concluded from these preliminary experiments that the sulphidization of a copper(II) oxide surface produces a distinct microcrystalline growth of copper sulphide and not a thin uniform layer. These crystals can oxidise rapidly to release copper ions to solution which can then react with the xanthate ion to produce a copper-xanthate precipitate. The importance of the sulphidization process with regard to flotation is that it probably eliminates growth of metal-xanthate precipitate at localised centres and it therefore encourages the precipitate to remain attached to the oxide. Further detailed study of the sulphidization process was not attempted because it was considered too complex to be included within the scope of this study.

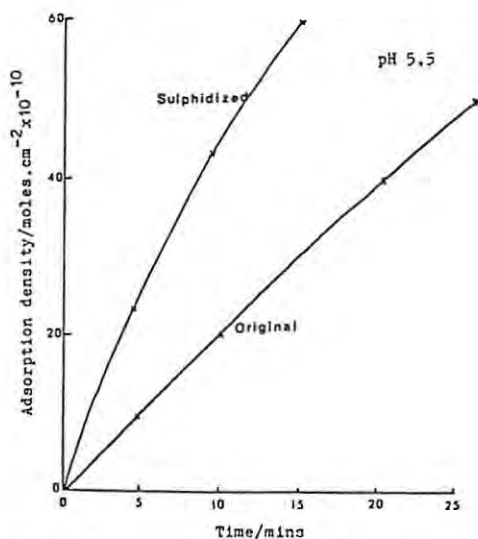


Fig. 13. Adsorption of xanthate by CuO and sulphidized CuO.

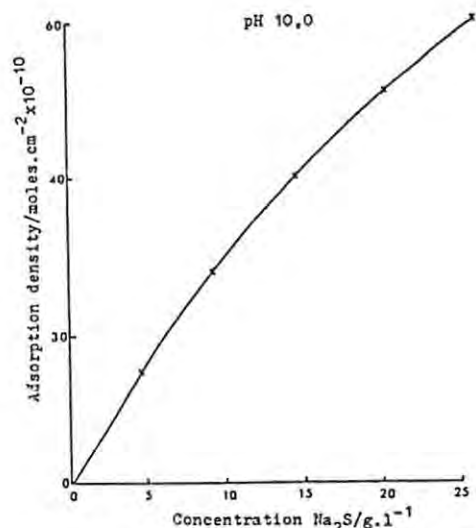


Fig. 14. Variation in xanthate adsorption on CuO with sulphidization level. Time 10mins

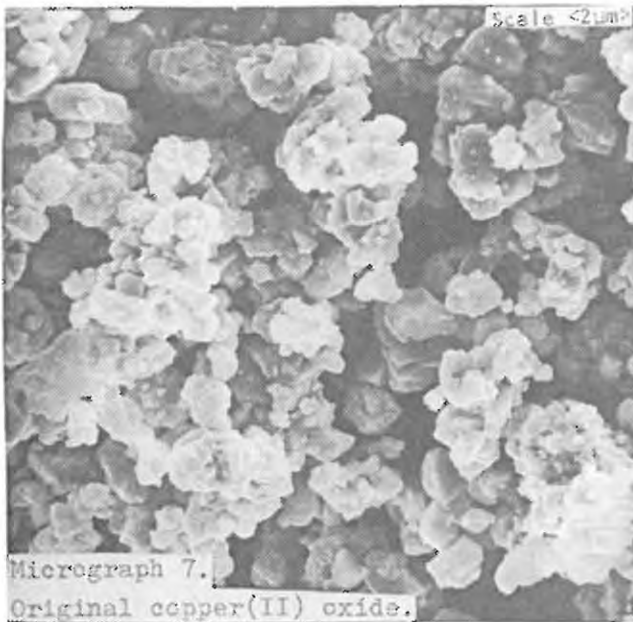
## D. DETAILED WORK

The preliminary work discussed in section C suggested that chelating reagents adsorb on oxide minerals as a metal-chelate precipitate. The present section deals with the attempt to understand the factors which control the rate of formation of the precipitate and the factors which dictate whether it occurred on the oxide surface or in the bulk solution.

### D.1. EXPERIMENTAL

#### D.1.a) Materials

D.1.a.i) Re-crystallized copper(II) oxide. Copper(II) oxide was mixed in equimolar proportions with sodium carbonate and then melted in a platinum crucible heated in a conventional furnace. The melt was kept at  $900^{\circ}\text{C}$  for 20 hours and then cooled slowly. The small, dark, highly reflecting crystals of copper(II) oxide were repeatedly washed with water to remove all traces of sodium carbonate. Batch samples of oxide (50 g each) with surface areas  $0,07 \text{ m}^2/\text{g}$  and  $0,17 \text{ m}^2/\text{g}$  were produced by a slight variation in the cooling rate. Micrograph 7 and 8 show the copper(II) oxide before and after recrystallization.



D.1.a.ii) Copper metal

Standard "Maksal" phosphorous de-oxidised copper cylinders (15 mm diam.) were used. The specifications were, Cu = 99,85%, P = 0,13%.

D.1.b) Analysis

D.1.b.i) Salicylaldehyde and 5-nitrosalicylaldehyde

The concentration in solution of these reagents was measured as follows : The solution was passed directly into a flow cell of a spectrophotometer where the absorption spectrum was monitored continuously at a fixed wavelength. The concentration of reagent was determined from the absorbance by assuming that the Beer-Lambert law applied.

D.1.b.ii) Bis-salicylaldehyde copper(II) (referred to as  $\text{Cu}(\text{SALO})_2$ ). The same method as adopted in the preliminary work for the determination of  $\text{Cu}(\text{NPBA})_2$  was

used (see section C.1.). An extinction co-efficient of  $6667\text{cm}^{-1}\cdot\text{mol}^{-1}\cdot\text{l}$ . was measured.

D.1.b.iii) Bis-8-hydroxyquinolato copper(II) (referred to as  $\text{Cu}(\text{Ox})_2$ ). The same analytical method as adopted for  $\text{Cu}(\text{SALO})_2$  was used, except in this case an extinction co-efficient of  $5091\text{cm}^{-1}\cdot\text{mol}^{-1}\cdot\text{l}^{-1}$ . was measured.

D.1.c) Infra-red studies

It is preferable to measure spectra of the surface of a solid in situ immersed in the liquid phase from which adsorption is taking place. Although there has been considerable progress in the development of techniques for the infra-red examination of surface species in situ,<sup>50</sup> it is still not possible to do this in aqueous media because of the high solvent opacity. This problem can only be overcome by the removal of the liquid. The sample can then be examined directly by diffuse reflectance spectroscopy or indirectly as a pressed KBr disc by transmission spectroscopy. Reflectance techniques suffer from a radiation loss that reduces the sensitivity of the technique. In fact it has been claimed that the intensity of radiation from a "good" diffuse reflector reaching the detector is only about 10% of the intensity measured in transmittance spectroscopy.<sup>51</sup> Furthermore, the measurement of surface species by transmission IR spectroscopy is experimentally very much easier. However, it is necessary with this technique to assume that the presence of the KBr diluent does not

affect the nature of the surface species.

D.1.d) Scanning electron microscope studies

There are a number of problems associated with the use of the S.E.M. to study the formation of a precipitate on copper oxide and/or copper metal. Firstly, it is necessary to remove the solid from the reagent solution because instrument facilities do not offer the option to monitor the reaction in situ. Secondly, the S.E.M. usually requires that samples are coated with a thin gold film in order to increase the conductivity and thirdly that they are viewed under a high vacuum. It is necessary to ensure that these procedures do not change the appearance of the surface features. Fortunately, the two substrates were sufficiently good conductors that it was possible to show by viewing an uncoated sample that this treatment had no effect. In order to prove that the vacuum also had no effect on the sample the standard electron microscope technique of viewing a mould of the sample was used. This confirmed that the vacuum did not alter the precipitate morphology.

D.1.e) Adsorption isotherms

D.1.e.i) Residual method

The concentration of SALO adsorbed on copper(II) oxide could be measured directly by passing the solution, via a filter, into the cell of a UV-visible spectrophotometer. This technique was used only in those experiments in

which dilute SALD solutions and short equilibrium times were employed.

D.1.e.ii) Extraction technique

D.1.e.ii) 1 Apparatus

A number of vessel designs and agitation methods were considered. Eventually the apparatus illustrated in fig. 15 was chosen because it gave the most reproducible results. It also had the following advantages :-

1. the size (150 ml) allowed easy control of the pH and easy recovery of the oxide,
2. it was possible to control the agitation intensity in order to prevent the oxide from accumulating at the liquid surface, and
3. the temperature could be controlled.

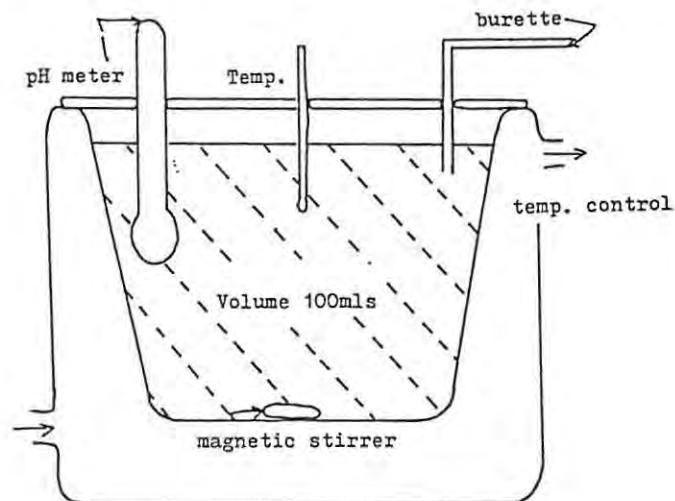


Fig15. Experimental apparatus used for adsorption studies.

D.1.e.ii) 2. Method

Copper(II) oxide (1.0 g) was added to a well stirred solution of chelate (100 ml) kept at a controlled pH and temperature. The ionic strength of the solution was not controlled. After a set conditioning period the amount of bulk and surface chelate was determined.

D.1.e.ii) 3. Separation of bulk and surface chelate

The large difference in specific gravity between copper(II) oxide, viz. 6,5 and bis-chelate copper(II) approx. 1,70 results in a rapid gravitational settling of the mineral before the bulk or dispersed chelate settled. The efficiency of the separation process was investigated in the following experiments :-

- a) the oxide was added to a solution which already contained the precipitate. The precipitate had been produced by the addition of enough copper solution to a chelating reagent solution to produce  $\text{Cu}(\text{chelate})_2$  quantitatively. After a one minute conditioning period the oxide was separated from solution and then the oxide surface checked for any adsorbed precipitate, and
- b) the oxide was pre-conditioned with chelate solution for 5 minutes before the copper solution was added. The result of the first experiment was that the oxide was recovered free of any adsorbed material. However, in the second experiment some precipitate (over and above the amount expected from the pre-conditioning period) was found to have adsorbed on the oxide surface. It was concluded that any procedure to separate bulk and surface

chelate would be a compromise. Nevertheless, a reasonably satisfactory procedure as summarised in fig. 16 was adopted. It is considered that the results were semi-quantitative and that they did reflect trends.

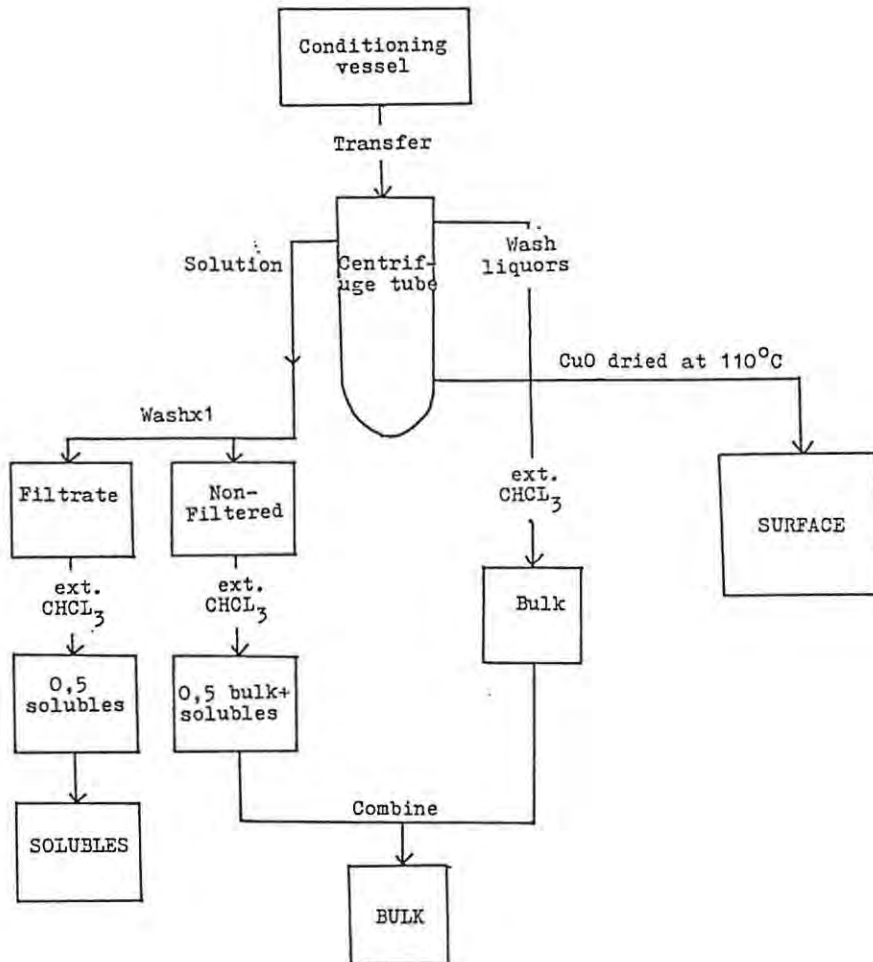


Fig.16. Experimental scheme for separation of bulk from surface copper chelate.

The contents of the conditioning vessel were transferred

to a centrifuge tube which was spun briefly (10 secs, 1000 revs/min) to accelerate settling of the oxide (simple decantation was unsuccessful because of the large carry over of oxide on the solution surface). The solution was then separated into two equal fractions, one of which was filtered through 0,2 $\mu$ m Millipore filters to remove bulk chelate and the other not. The filtered and unfiltered solutions were then extracted with an organic solvent (usually chloroform) which made possible the determination of the concentration of the water soluble copper chelate complexes and the concentration of bulk chelate. Next, the oxide was redispersed and centrifuged at least 8 times in an attempt to eliminate weakly attached surface chelate. The wash solutions from these steps were combined and then extracted with the organic solvent. The concentration of bulk chelate determined in the wash solutions was added to the concentration determined in the original solution to give the total bulk chelate. In the final step the oxide was dried at 110<sup>o</sup>C for 30 minutes. The oxide was then extracted with the solvent to give the concentration of surface chelate. It was important to ensure that the oxide was absolutely dry because it was found difficult to remove the chelate when even small amounts of water were present. The concentration of bulk and surface chelate in the organic extracts was calculated from the extinction co-efficients for the copper chelate complexes.

D.1.f) Precipitation studies

The apparatus used in the experiments in which a copper metal cylinder (diam.15 mm., length 50 mm) was rotated in a chelate solution ( $1 \times 10^{-3}$  mol.l<sup>-1</sup>, 250 ml) is shown in fig. 17.

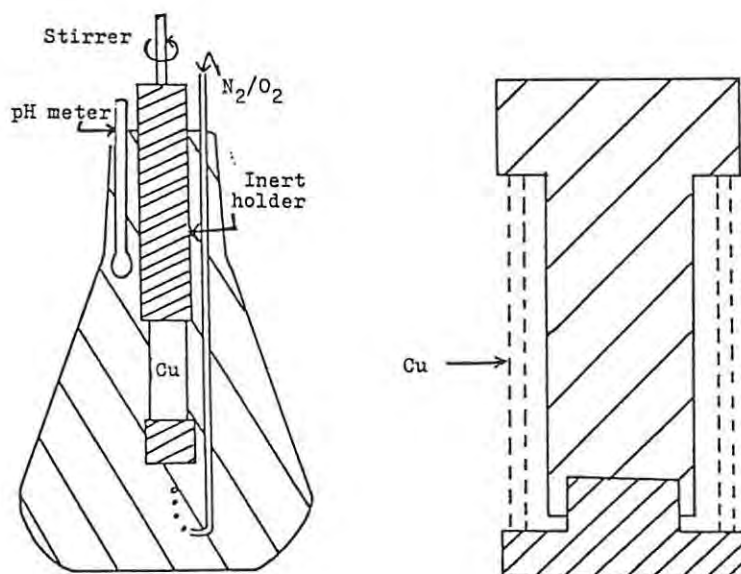


Fig.17. Experimental apparatus used to study metal-chelate precipitation.

The device was rotated (250 revs/min) in the chelate solutions for a set length of time and then carefully removed. The precipitate was either extracted from the metal with an organic solvent or viewed under the S.E.M.

D.2. SOLUBILITY OF RE-CRYSTALLIZED COPPER(II) OXIDE

The variation with pH of the copper concentration of an aqueous solution after contact with re-crystallized copper(II) oxide for 2 hours was measured directly by passing the solution into an atomic absorption spectrophotometer. The results as illustrated in fig. 18. show that the copper concentration decreased rapidly from a maximum at very acidic pH values to a minimum at a pH of between 7,0 and 8,5. At very high pH values the oxide again became significantly soluble.

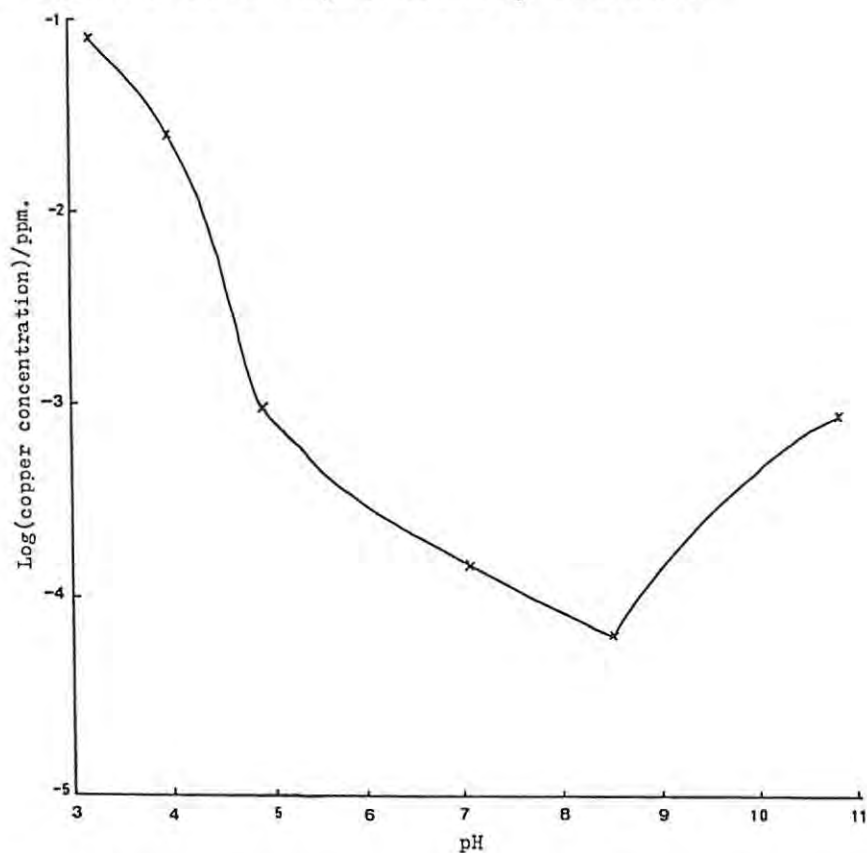
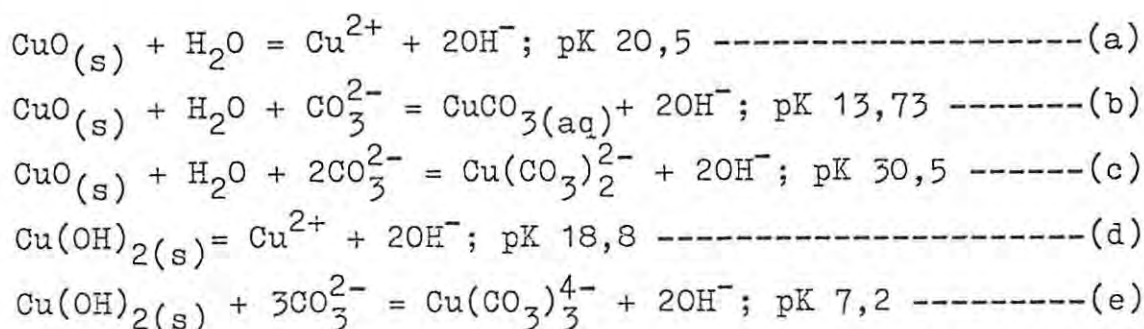


Fig.18. Solubility of re-crystallized copper(II) oxide after 2hours at 25°C

The pH of minimum solubility has been considered to represent the point of zero charge of an oxide. <sup>52</sup>

Consequently, copper(II) oxide can be considered to be

positively charged below pH 7,0 and negatively charged above pH 9,0. Recently Attia <sup>52</sup> combined together various known equilibrium equations, for example equations (a) to (e) below, in an attempt to deduce the solubility of the solids, copper(II) oxide and copper(II) hydroxide in open, aqueous solutions.



The variation with pH of the concentration of copper ions in aqueous solution, as predicted by these equilibrium equations, was read from the original diagrams given by Attia. <sup>52</sup> This concentration is compared in table 9 with the results found after 2 hours conditioning for the re-crystallized copper(II) oxide. The predicted copper concentration and the experimentally determined value both decreased with increasing pH values. However, the solubility of the re-crystallized version at pH 7,0 and pH 9,0 was significantly larger than the theoretically predicted value. It was expected that the solubility would be less than the predicted value because it was unlikely that the solutions would have been in contact

with copper(II) oxide long enough for the final equilibrium to be achieved. A number of reasons can be suggested for the discrepancy between the experimental and theoretical values :-

1. the equilibria were more complex than the equations allowed for,
2. the oxide surface is converted to a hydroxide surface at high pH values, and
3. the concentration of CO<sub>2</sub> in the solution varied from the assumed value.

Table 9.

Comparison between the copper concentration,  $x$ , released from re-crystallized copper(II) oxide as determined experimentally after 2hrs and the equilibrium concentration predicted theoretically,  $x_{pred}$ .

pH	Cu(OH) <sub>2</sub> CuO (Attia's predicted values.)				Re-crystallized CuO (this work)
	No CO <sub>2</sub>	CO <sub>2</sub>	No CO <sub>2</sub>	CO <sub>2</sub>	
	$x_{pred}/ppm$				$x/ppm$
5,0	10 <sup>4</sup>	10 <sup>4</sup>	2x10 <sup>2</sup>	2x10 <sup>2</sup>	1,3x10 <sup>1</sup>
7,0	1	1	2x10 <sup>-2</sup>	2x10 <sup>-2</sup>	9,0x10 <sup>-2</sup>
9,0	6x10 <sup>-4</sup>	1,3x10 <sup>-1</sup>	3x10 <sup>-11</sup>	2x10 <sup>-3</sup>	2,2x10 <sup>-1</sup>
10,5	6x10 <sup>-3</sup>	6x10 <sup>2</sup>	2x10 <sup>-4</sup>	2	1,14

### D.3. RESULTS AND DISCUSSION

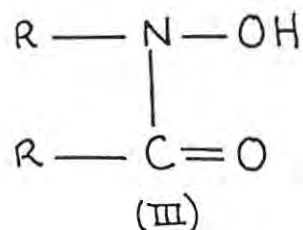
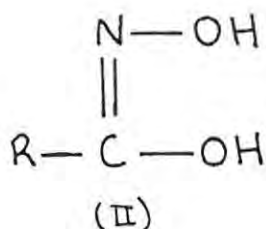
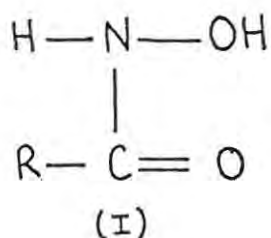
This work is primarily aimed at understanding the mechanism of adsorption of chelating reagents on oxide minerals. It is not directly concerned with the monitoring of the floatability of the oxide, although the underlying assumption is that this function is related to the adsorption process. This assumption does not imply that the adsorption maxima always coincides with flotation maxima (if measured by the residual method) because it has already been documented that this is not always the case.<sup>21-23</sup> However, it is felt that there will be a relationship between the adsorption of reagent at the oxide surface and its floatability, ie. no or little adsorption, no or little flotation. In this study an attempt has been made to investigate some of the factors, such as pH, temperature, surface area and dispersing agents, which it is considered could influence the adsorption process. The rate of the adsorption process, the chemical nature of the adsorbed species and the structural form of the adsorbed material were of particular interest. Furthermore an attempt was made to understand the factors which influence whether a reagent adsorbed on the oxide surface formed a well-attached phase that could influence its floatability or formed a loosely-attached or non-attached phase which was unlikely to enhance its floatability.

The results will be dealt with separately in terms of the reagent used.

#### D3.a) HYDROXAMIC ACIDS

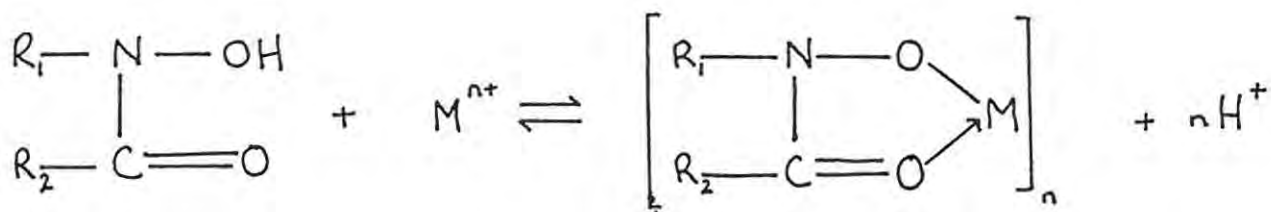
##### D.3.a.i.) General Features

Hydroxamic acids form an important family of chelating reagents which have found extensive use in the solvent extraction and gravimetric analysis of metal ions.<sup>53</sup> Structurally, hydroxamic acids can be represented in their two tautomeric forms (I) and (II).



By substitution of the hydrogen atom attached to the nitrogen atom in (I) by alkyl or aryl groups numerous N-substituted hydroxamic acids of type (III) can be obtained. The pK value of the hydroxyl varies from 7,05 for o-nitrobenzohydroxamic acid to 11,33 for N-phenyl n-butyrohydroxamic acid. <sup>54</sup>

It has been shown by I.R. and U.V. spectral studies <sup>54</sup> and also by an X-ray crystal structure determination <sup>54</sup> that complex formation of hydroxamic acids usually takes place with the replacement of the hydroxylamine hydrogen by the metal ion and ring closure through the carbonyl oxygen.



Curiously, hydroxamic acids form two types of copper hydroxamate precipitates depending on the nature of the substituents. <sup>54</sup> A mono complex,  $(R Cu OH H_2O)_x \cdot H_2O$  (R= hydroxamate) has been isolated using simple aliphatic hydroxamic acids such as acetohydroxamic acid; on the other hand benzohydroxamic acid gave a bis chelate,  $CuR_2$ .

#### D.3.a.ii) N-phenylbenzohydroxamate (NPBA).

This reagent was chosen in this study for the following reasons.

1. It was claimed to be moderately stable in air and light, and at moderate temperatures. <sup>55</sup>

2. The copper complex was soluble in dichloromethane.
3. The dissociation constant for the ligand was well known.<sup>56</sup>
4. The formation constants for the 1:1 and 1:2 copper complexes had been published.
5. The formation of the 1:2 copper hydroxamate precipitate was claimed to be quantitative between pH 3,0 and 6,4.<sup>55</sup> However, the following negative features associated with this reagent were recognized.
  - a) NPBA was only slightly soluble in water (0,04 g/100 ml) and so the concentration range open to study was restricted.<sup>55</sup>
  - b) The reagent has been noted to decompose at very high pH values.<sup>58</sup>

D.3.a.iii) Metal-species distribution

It is advantageous to represent metal-complex equilibria visually in a species distribution diagram. These diagrams can assist in the interpretation of the adsorption isotherms, provided that it is acknowledged that they reflect thermodynamically favoured equilibria and therefore do not take account of kinetic factors. The literature was consulted for the relevant equilibrium constant data. Unfortunately, the only data for the formation of copper hydroxamates were derived in a medium of 50% ( $V/V$ ) dioxane-water.<sup>57</sup> The approximate values for a medium of 100% water were derived by assuming that the variation in the constants with the medium was

approximately the same as that for 8-hydroxyquinolato copper(II) complexes, <sup>59</sup> i.e. the relationship between the medium and the constants was the same in both cases. The relevant literature data and the calculated value for 100% water for NPBA is given in table 10. The acid dissociation constant (K<sub>a</sub>) and the stability constant (β) were defined as follows:

$$K_a = \frac{(H^+)(L^-)}{(HL)}$$

$$\beta_1 = \frac{(CuL^+)}{(Cu^{2+})(L^-)}$$

where (HL) is the concentration of the neutral reagent species and where (L<sup>-</sup>) is the concentration of the reagent anion, and where (CuL<sup>+</sup>) is the concentration of the metal-reagent complex.

Table 10.

Calculation of equilibrium constant data for N-phenylbenzohydroxamate in 100% water from 8-hydroxyquinoline data at 25°C.<sup>59</sup>

Complexing ion	Constant	Value	Medium
8-HYDROXYQUINOLINE			
H <sup>+</sup>	pK <sub>A</sub>	12,33	
Cu <sup>++</sup>	log β <sub>1</sub>	15,00	70% diox.
	log β <sub>2</sub>	14,00	
H <sup>+</sup>	pK <sub>A</sub>	11,54	
Cu <sup>++</sup>	log β <sub>1</sub>	13,49	50% diox.
	log β <sub>2</sub>	12,73	
H <sup>+</sup>	pK <sub>A</sub>	9,70	
Cu <sup>++</sup>	log β <sub>1</sub>	12,10	0% diox.
	log β <sub>2</sub>	10,90	
N-PHENYLBENZOHYDROXAMATE			
H <sup>+</sup>	pK <sub>A</sub>	11,04	
Cu <sup>++</sup>	log β <sub>1</sub>	10,36	50% diox.
	log β <sub>2</sub>	8,78	
H <sup>+</sup>	pK <sub>A</sub>	9,15	
Cu <sup>++</sup>	log β <sub>1</sub>	8,96	0% diox.
	log β <sub>2</sub>	6,53	

The concentration of the various copper hydroxamate complexes was calculated for specific total reagent and total metal concentration by combining the following equations:

$$Cu_{(total)} = Cu^{2+} + CuL^+ + CuL_2$$

$$L_{(total)} = HL + L^- + CuL^+ + 2CuL_2$$

This method used to solve the equations is outlined in the appendix. The species distribution is represented diagrammatically in fig. 19.

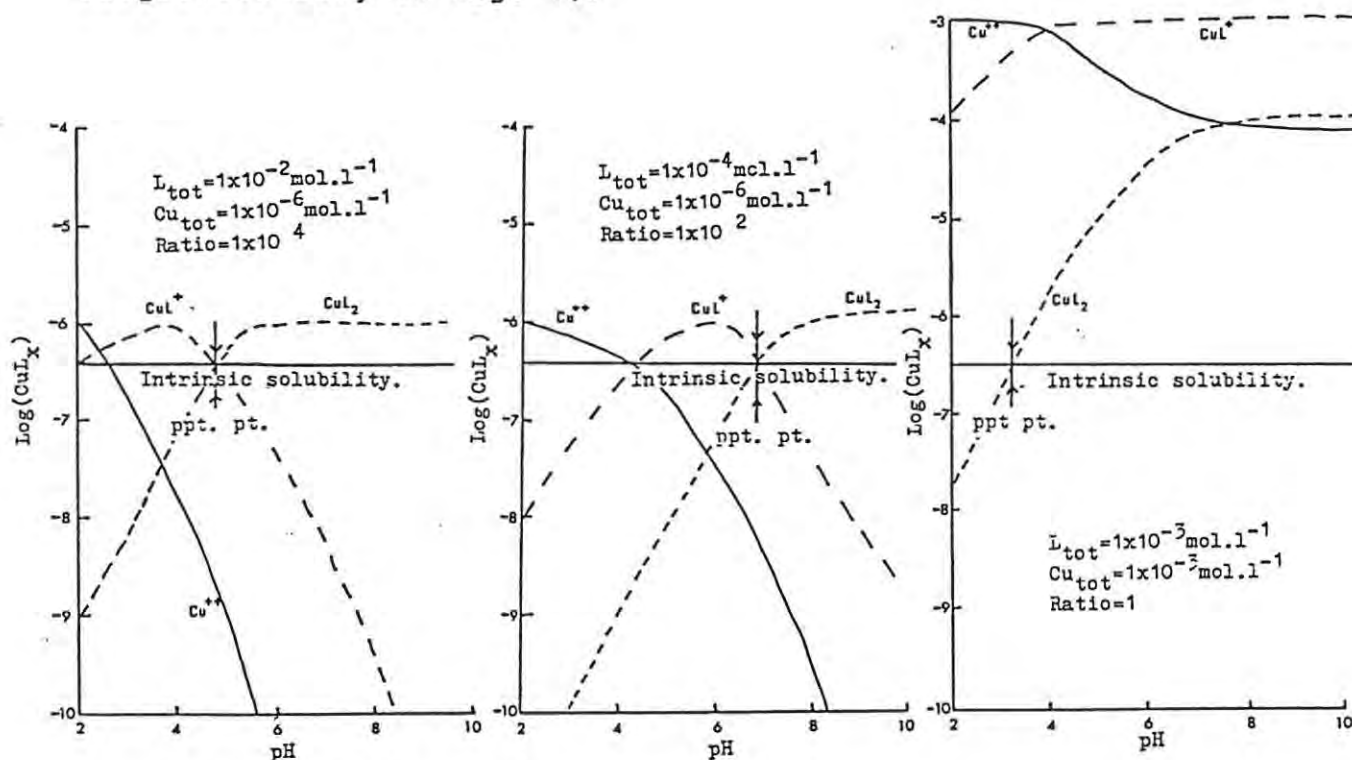
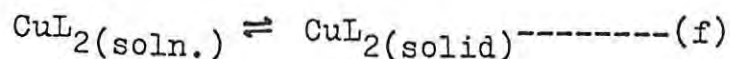


Fig. 19. Species distribution diagram at various copper and N-phenylbenzohydroxamate concentrations at 25°C.

The intrinsic solubility of the  $CuL_2$  species (as defined in equation (f) below) is unknown in the case of the reagent, NPBA.



For the purpose of the construction of this diagram the

value was assumed to be similar to the known value of the 8-hydroxyquinolatocopper(II) complex.<sup>59</sup>

A number of trends are evident in this diagram, viz.

1. the bis complex,  $\text{CuL}_2$ , is favoured at high pH's and at high  $L_{\text{TOT}}:Cu_{\text{TOT}}$  ratios, whereas the 1:1 complex is important at low pH values and low  $L_{\text{TOT}}:Cu_{\text{TOT}}$  ratios, and
2. the point of precipitation of solid  $\text{CuL}_2$  varies from pH 4,7 for high  $L_{\text{TOT}}:Cu_{\text{TOT}}$  ratios to pH 6,8 for low ratios.

#### D.3.a.iv) Adsorption isotherms

A study was made of the concentration of  $\text{Cu}(\text{NPBA})_2$  produced when re-crystallized copper(II) oxide was conditioned with NPBA under different conditions. The following variables were considered; pH, time, surface area, temperature and the presence of dispersing reagents.

#### D.3.a.iv) 1 Time, surface area

The conditioning period required to establish equilibrium between dilute NPBA solutions at set pH values, and copper(II) oxide samples of different surface areas, was determined (fig. 20).

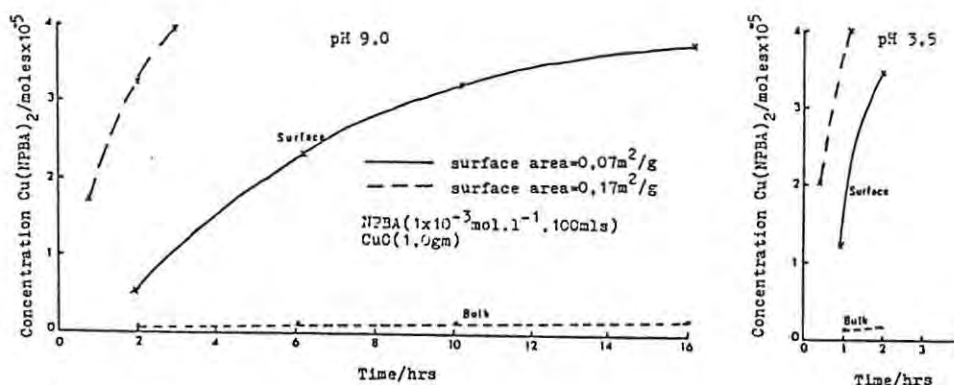


Fig.20. The variation with pH in the concentration of  $\text{Cu}(\text{NPBA})_2$  formed on two different surface area copper(II) oxides.

The following features were evident:

- a) The production of  $\text{Cu}(\text{NPBA})_2$  on re-crystallized copper(II) oxide continued until the residual hydroxamate concentration had dropped to a very low value. This differed from the preliminary adsorption results on the octyl derivative (see section C.3) in which relatively high equilibrium hydroxamate concentrations were found. This variation is considered to arise from the significantly different surface areas of the sample.
- b) The rate of formation of  $\text{Cu}(\text{NPBA})_2$  was dependent on both the pH of the solution and on the surface area of the oxide. The concentration of hydroxamate adsorbed by copper(II) oxide (surface area  $0,07 \text{ m}^2/\text{g}$ ) after 16 hours at pH 9,0 or 3 hours at pH 3,5 was approximately  $100 \times 10^{-2} \text{ moles. cm}^{-2}$ . This is equivalent to over 150 layers of hydroxamate, based on the Fuerstenau<sup>35</sup> calculation that one layer equals  $7 \times 10^{-10} \text{ moles. cm}^{-2}$ .
- c)  $\text{Cu}(\text{NPBA})_2$  was considered to precipitate on the surface of the oxide. The small amount of bulk (or

dispersed) metal-chelate detected was probably caused by copper(II) oxide carry over and could probably also be considered as surface chelate.

D.3. a.iv) 2 Temperature.

The rate of formation of  $\text{Cu}(\text{NPBA})_2$  was found to be temperature dependent (table 11). Oxide conditioned at  $60^\circ\text{C}$  for 10 minutes at either pH 3,5 or pH 9,0 adsorbed enough hydroxamate to form the equivalent of more than fifty theoretical layers. At  $25^\circ\text{C}$  the oxide only adsorbed enough hydroxamate at pH 9,0 to form the equivalent of five layers and at pH 3,5 to produce thirteen layers. These results are explained by the fact that an increased temperature caused a larger dissolution rate of the oxide and therefore a greater tendency for  $\text{Cu}(\text{NPBA})_2$  to form.

Table 11.

The variation with temperature in the concentration of the precipitate,  $\text{Cu}(\text{NPBA})_2$ , formed from N-phenylbenzohydroxamate solutions ( $1 \times 10^{-3} \text{ mol.l}^{-1}$ ) and re-crystallized copper(II) oxide (surface area  $0,17 \text{ m}^2/\text{g}, 1,0 \text{ g}$ ).

pH	Temp./ $^\circ\text{C}$	Time/min.	Concentration/moles $\times 10^{-5}$
9,0	25	10	0,30
	25	60	1,79
	60	10	3,16
3,5	25	10	0,80
	25	30	1,97
	60	10	3,44

D.3.a.iv) 3 PH.

The variation with pH of the concentration of  $\text{Cu}(\text{NPBA})_2$  formed on re-crystallized copper(II) oxide after a 2 hour conditioning period is shown in fig. 21 . The solubility data for copper(II) oxide conditioned in blank aqueous solutions under similar conditions is also included. The copper concentrations were converted from p.p.m. to moles/100 ml in order to allow the direct comparison with the concentration of  $\text{Cu}(\text{NPBA})_2$ .

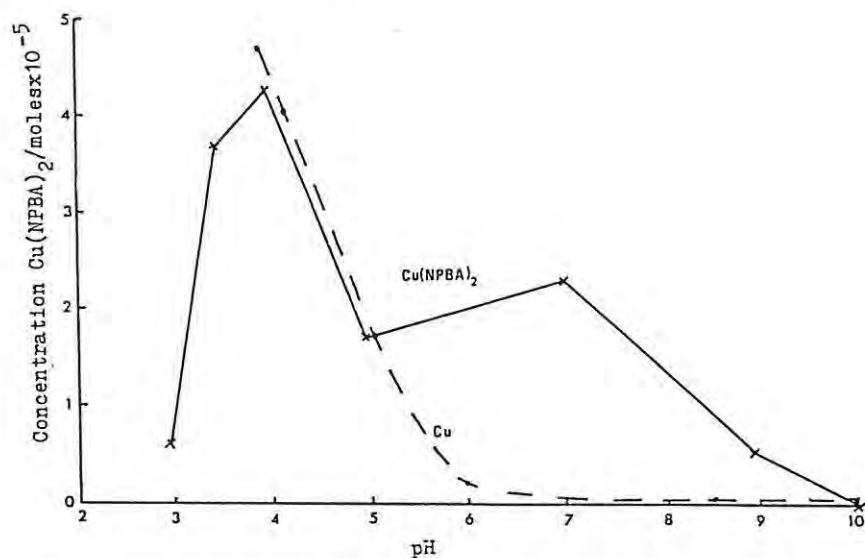


Fig.21. Variation with pH of the concentration of  $\text{Cu}(\text{NPBA})_2$  formed on re-crystallized CuC at  $25^\circ\text{C}$ .  $\text{CuO}(0,07\text{m}^2/\text{gm}, 1,0\text{gm})$   
 $\text{NPBA}(1 \times 10^{-3} \text{mol.l}^{-1}, 100\text{mls})$  Time 2hrs, Temp.  $25^\circ\text{C}$ .

The adsorption results showed the following important features.

1) They resembled the adsorption isotherm derived by Lenormand.<sup>36</sup>

2) There was no  $\text{Cu}(\text{NPBA})_2$  formed on the oxide at a pH 3 and pH 10.

- 3) There were two maxima at pH 4,0 and pH 7,5 in the total concentration of precipitate formed.
- 4) A minimum in precipitate concentration at pH 5,0 existed.
- 5) The concentration of precipitate produced was generally larger at acidic pH values than at basic pH values.
- 6) The concentration of copper ion released from the oxide between pH 4,0 and 5,0 corresponded well to the concentration of  $\text{Cu}(\text{NPBA})_2$  formed over the same pH range. At higher pH values there was significantly more precipitate formed than copper ion released.

These features can be understood with reference to:

i) The metal complex species distribution diagram (fig. 19).

ii) The schematic representation of the variation with pH of the concentration of copper ion released from the oxide and the hydroxamate anion concentration as shown in fig. 22.

iii) The solubility of the  $\text{CuL}_2$  (L = NPBA) precipitate.

The species distribution data indicated that the species,  $\text{CuL}^+$ , predominated at low pH values and low reagent to metal ratios. It is therefore concluded that the formation of this species was responsible for the lack of hydroxamate adsorption at pH 3,0. At pH 10,0 the species distribution diagram predicted that the  $\text{CuL}_2$  complex would predominate. The observation that no

precipitate of  $\text{CuL}_2$  was detected on the oxide at this pH could be due to either competition between hydroxyl and hydroxamate ions for the copper ions or to the decomposition of the reagent. The fact that Lenormand<sup>36</sup> found a similar trend for the octyl derivative suggests that decomposition was not a factor.

The  $\text{CuL}_2$  species was shown in the species distribution diagram to predominate at pH values greater than 4,0. In addition, it was shown that the complex soon precipitates from aqueous solution because it has relatively low intrinsic solubility. The interpretation of the variation in the relative concentration of the precipitate formed on the oxide between pH 3,0 and 9,0 is complicated by the fact that the concentration of the constituents required, vary in opposition to each other with pH as shown in fig.22 .

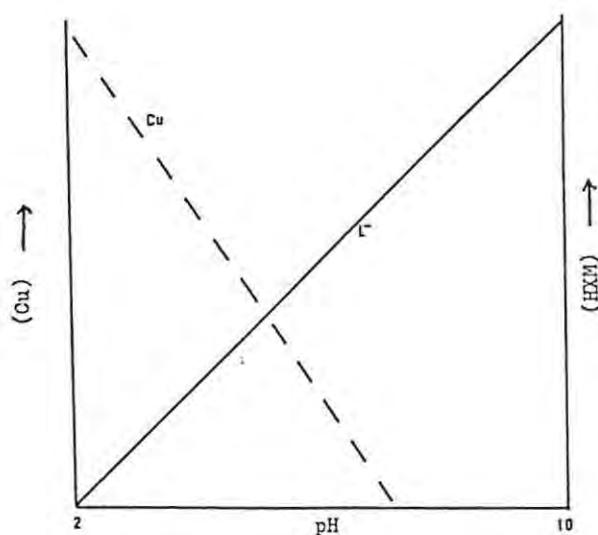
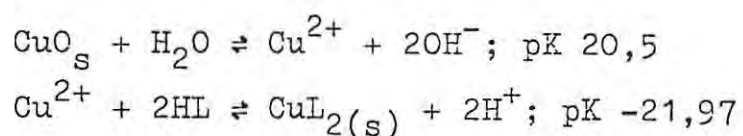


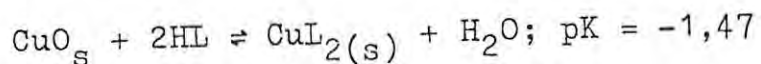
Fig.22. Schematic representation of the variation of the copper and hydroxamate anion concentration with pH.

At acidic pH values the oxide was relatively soluble whereas the concentration of the hydroxamate anion was low. This results in the rate of precipitation of  $\text{CuL}_2$  on the oxide being controlled by the rate of release of copper ions. Consequently, the adsorption data between pH 4,0 and 5,0 could have been predicted from a knowledge of the rate of release of copper ions. However, with further pH increases the concentration of copper released drops significantly and the control of the rate of precipitation shifts to the concentration of the hydroxamate anion. The concentration of precipitate produced on the oxide surface was now larger than the concentration predicted from the solubility of the oxide. The reason for the enhanced formation of precipitate can be most easily appreciated from the comparison between the solubility of the oxide and the precipitate, as expressed in the equations below.



(this equation takes account of the formation constant of the complex and it's intrinsic solubility)

These equations can be combined to give the overall equation to describe the reaction between the reagent and the oxide.



This equation indicates that copper(II) oxide will dissolve in the presence of NPBA in an attempt to establish the equilibrium concentration of  $\text{Cu}^{2+}$  based on the solubility product of the precipitate, ie. the concentration of  $\text{L}^-$  and  $\text{Cu}^{2+}$  are reduced to levels which satisfy this equation. Consequently, the larger the initial concentration of the hydroxamate anion, the greater the rate the copper(II) oxide will dissolve in order to reduce the concentration of the anion, and therefore the greater the rate of precipitation.

D.3.a.iv) 4 Dispersing reagents.

Gum arabic, a polysaccharide which contains some acidic functional groups<sup>60</sup>, was added to the reagent solution in an attempt to monitor it's effect on the growth of the precipitate on copper(II) oxide (fig. 23).

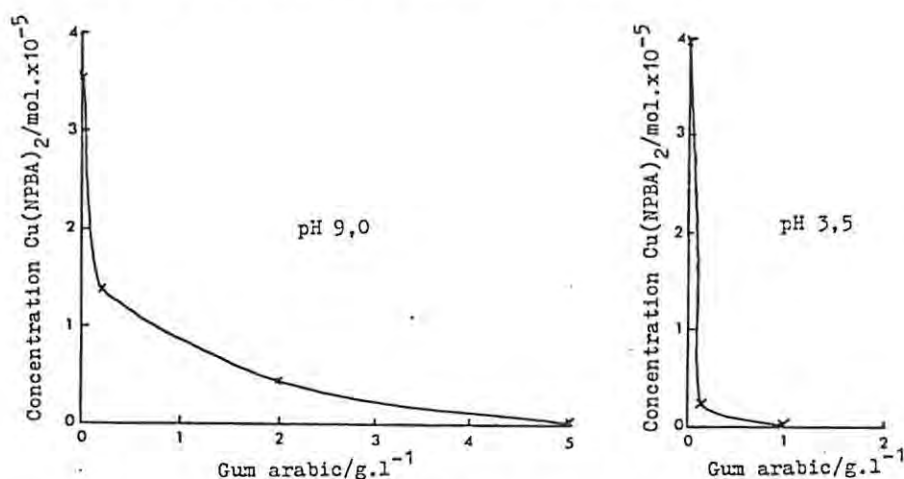


Fig.23. The formation of  $\text{Cu}(\text{NPBA})_2$  on  $\text{CuO}$  in the presence of gum arabic at  $60^\circ\text{C}$ .  $\text{CuO}(0,17\text{m}^2/\text{g}, 1,0\text{gm})$   $\text{NPBA}(1 \times 10^{-3} \text{mol} \cdot \text{l}^{-1}, 100\text{mls})$  Time 10mins, Temp.  $60^\circ\text{C}$

The results showed that the formation of the  $\text{Cu}(\text{NPBA})_2$  precipitate was restricted by the addition of gum arabic. The addition of 0,02 g of the gum to the NPBA solution

(100 ml) at pH 9,0 reduced the concentration of the precipitate produced from  $316 \times 10^{-7}$  moles to  $107 \times 10^{-7}$  moles. The concentration was even further reduced by a larger addition of gum to the solution. At pH 3,5 gum arabic addition of 0,02 g per 100 ml effectively prevented the formation of the precipitate on the oxide surface.

The influence of the presence of gum arabic on the concentration of copper ions released by the oxide was also investigated. It was found that the addition of 0,5 g per 100 ml of the gum to a blank aqueous solution at pH 9,0 increased the copper release from below detectable levels to 0,30 ppm. In the presence of the reagent this concentration was increased still further to 0,50 ppm (table 12).

Table 12.

Solubility of CuO in the presence  
of additives.

Condition	Conc./ppm
pH 9,0	0,0
pH 9,0/NPBA	<0,1
pH 9,0/G.A.	0,3
pH 9,0/NPBA/G.A.	0,5

It is proposed that gum arabic acts by a combination of the following mechanistic pathways:

- a) Some gum arabic adsorbs on the copper(II) oxide and therefore effectively blocks the uptake of chelating

reagent. An increase in the concentration of gum offered would effectively increase the amount of gum adsorbed by the oxide which would result in a more effective prevention of chelate adsorption.

b) The acidic fraction of the gum forms a strong copper complex. This was evident from the increased solubility of the oxide in the presence of the gum. The concentration of precipitate formed could be reduced by competition between the gum and the reagent for the copper ions.

c) Gum arabic could operate by effectively reducing the nucleation and crystal growth of the  $\text{Cu}(\text{NPBA})_2$  precipitate.

#### D.3.a.v) Infra-red spectroscopy

The infra-red absorption peaks associated with  $\text{Cu}(\text{NPBA})_2$  were identified on re-crystallized copper(II) oxide. The results were similar to the preliminary work (see Table 7).

#### D.3.a.vi) Scanning electron microscope study

The scanning electron microscope was used to study the structure of copper precipitates and the structure of the adsorbed material on copper(II) oxide surfaces.

#### D.3.a.vi) 1. Precipitates

The  $\text{Cu}(\text{NPBA})_2$  precipitate was generated by the addition of a dilute copper solution to a NPBA solution controlled at a set pH. A spherulitic type growth of a collection

of long, tabular, well formed crystals was formed at pH 3,5 (micrograph 9). At pH 9,0 the precipitate of  $\text{Cu}(\text{NPBA})_2$  showed no distinct crystal form (micrograph 10).

D.3.a.vi) 2. Copper(II) oxide (Surface Area =  $2,18\text{m}^2/\text{g}$ )

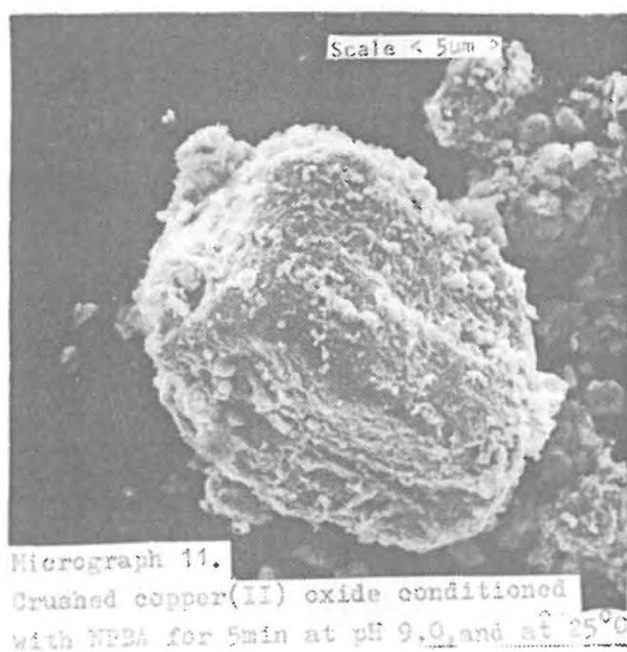
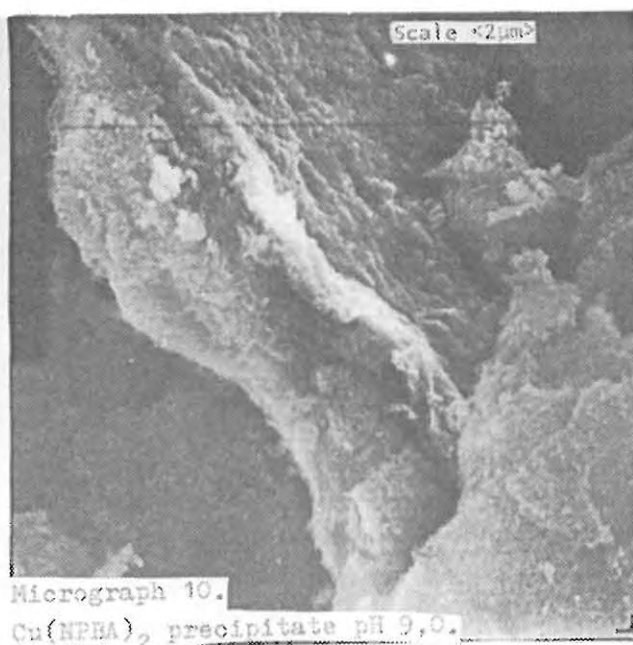
A crushed sample of re-crystallized copper(II) oxide with a high surface area was treated for 5 minutes only at  $25^\circ\text{C}$  with a solution of NPBA ( $1 \times 10^{-3} \text{ mol.l}^{-1}$ ) at pH 9,0. The surface of the copper(II) oxide became effectively coated by a microcrystalline growth (micrographs 11 and 12).

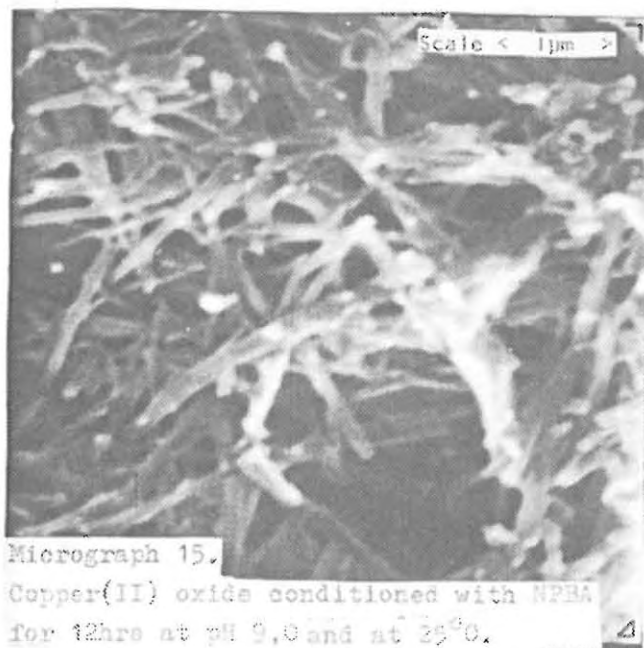
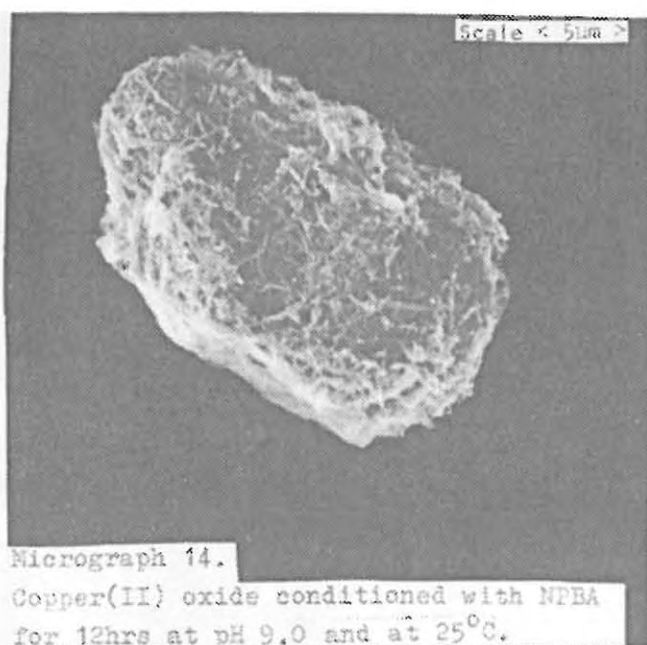
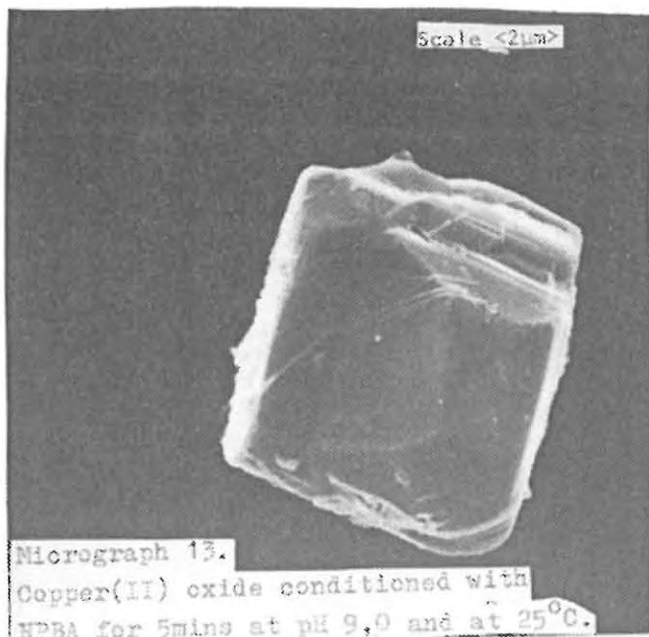
D.3.a.iii) 3. Copper(II) oxide (SA =  $0,07 \text{ m}^2/\text{g}$ ).

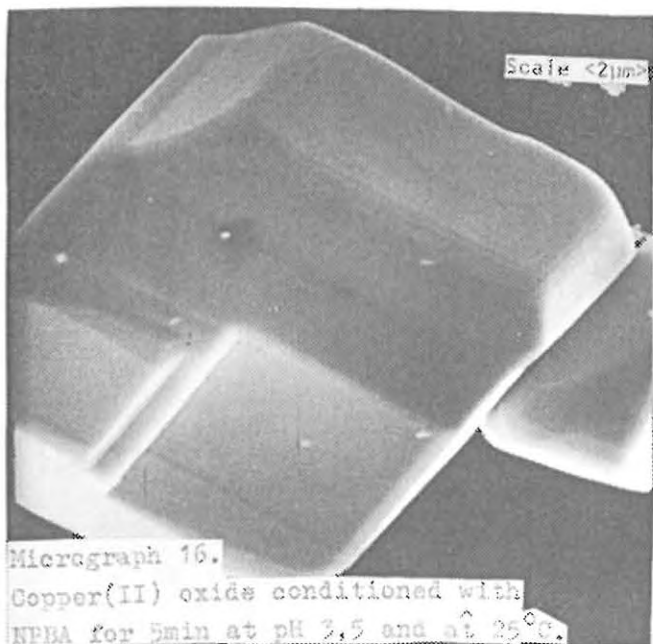
Re-crystallized samples of copper(II) oxide were treated at two pH values for 5 minutes and also for time intervals that allowed maximum formation of  $\text{Cu}(\text{NPBA})_2$ . The initial formation of precipitate at pH 9,0 occurred as long fibres across the surface (micrograph 13). Further growth caused coalescence with the resultant formation of a complete layer on the surface (micrograph 14). Higher magnification shows the weave like structure of the fibres (micrograph 15). A similar study at pH 3,5 indicated that crystal growth on copper(II) oxide was different. Nucleation occurred at a limited number of sites (micrograph 16) from which subsequent growth formed long, thin crystals (micrograph 17 and 18). Interestingly, large areas of the crystal appeared to be unaffected by the presence of the new crystals.

An observation was made under the S.E.M. that has important implications with regard to the mechanism of chelate - oxide interactions. Micrographs 11 and 14 show two crystals of the oxide of approximately the same size conditioned in the one case with a NPBA solution at pH 9,0 for 5 minutes and in the other case at pH 9,0 for 12 hours. The total concentration of chelate formed on the overall 1,0 gm of oxide sample was the same in both cases. However, in the one case the relative surface area of the oxide was  $2,18 \text{ m}^2/\text{g}$  and in the other case only  $0,07 \text{ m}^2/\text{g}$ . More detailed examination of the structure of the surface growth indicated that there were some similarities between them, such as the fact that long fibres existed in both cases, and also some differences, such as the fact that there was less order in the more rapidly precipitated material. If the rate of precipitation on the oxide surface was dependent only on the rate of metal release from the oxide particle then one would have expected that there should have been significant differences in the form and the concentration of the precipitate on the two particles. This is because the one particle was only exposed to solution for 5 minutes whereas the other was exposed for 12 hours. However, the evidence presented suggests that the character of the precipitate was not controlled solely by the particle onto which it precipitates but also by those particles adjacent to it. In the case of the high surface area oxide sample there would be an environment

of high  $\text{Cu}^{2+}$  around the particle studied due to presence of a large number of smaller particles adjacent to it. This environment causes precipitation to occur more rapidly than in the case where all the particles are larger (as in the case of the higher surface area sample) and also possibly to be less specific. Unfortunately, it was not possible to repeat a similar type of experiment at pH 3,5 because it was difficult to control the pH accurately when the high surface area material was used. However, based on the structural form of the precipitate as determined earlier under the S.E.M. (micrograph 9), it was expected that the results would be different from those at pH 9,0. It was also considered possible that in this case most of the precipitate might not be attached to the surface of the oxide.







D.3.b) HYDROXY-OXIMES

D.3.b.i) General features

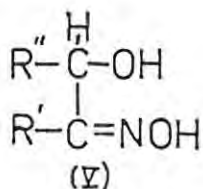
Although the hydroxy-oxime functional group was recognized to be specific for copper ions many years ago<sup>61</sup>, it was only comparatively recently that intense interest has been focussed on this group. Reagents which contain it now form the basis of a series of copper selective extractants which are in use commercially to recover copper(II) from the acidic liquors used in the leaching of low grade ores.<sup>62</sup> Some examples of the trade names of these extractants are :-

1. The General Mills LIX types and
2. The Acorga P5000 type reagents.

There are two very distinct groups into which reagents of this type can be categorised.

D.3.b.i) 1.  $\alpha$ -Acylloximes and related ligands.

These oximes have structure V.

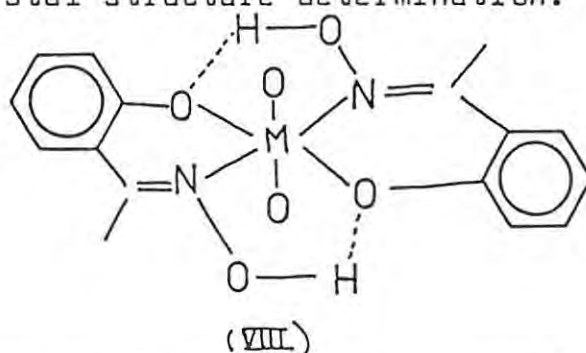


The reagent forms with copper a 1:1 green, water-insoluble complex in the cases where R' and R'' are either straight chain alkyl groups or phenyl groups. These complexes have been proposed



copper quantitatively as  $\text{Cu}(\text{SALO})_2$  in the pH region 3-10. However, between pH 1,5 and 3,0 precipitation is incomplete, and between pH 10,1 and 10,7 the precipitate is found experimentally to redissolve.

The structure of  $\text{Cu}(\text{SALO})_2$  (VIII) has been confirmed by an X-ray crystal structure determination.<sup>67</sup>



Co-ordination of the ligand to the metal occurs via the nitrogen and oxygen atoms. There are two important features to note :-

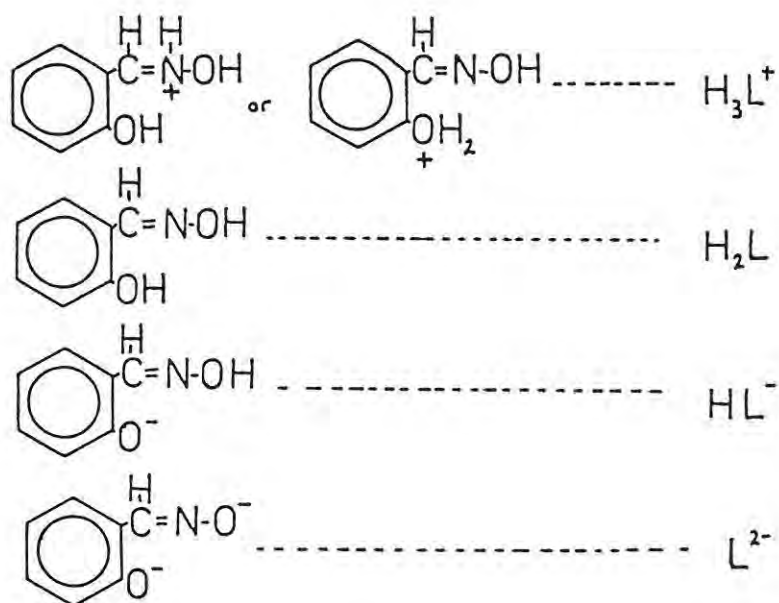
- i) the formation of intramolecular O-H...O bridges between two co-ordinated groups. This has important consequences with regard to the formation of these complexes, and
- ii) the oximic oxygens of molecules above and below the plane interact with the copper atom to form a distorted octahedral geometry about the metal. This is important since the metal is thus effectively unavailable to co-ordinate to water molecules. (Some ligands such as  $\beta$ -hydroxyquinoline can form hydrated solids). The exclusion of water increases the amount of hydrophobicity that the formation of this precipitate can impart to an oxide surface. The formation of a basic 1:1 copper-SALO

precipitate at high pH's has also been noted but there has been little work published about it. <sup>20</sup>

D.3.b.ii) Metal species distribution

D.3.b.ii) 1. Salicylaldoxime (SALO)

Salicylaldoxime can exist in the following forms :-



The relationship between these complexes is well known and so the values could be obtained from the literature. <sup>44,45</sup> Three complexes of SALO with copper ions are considered in the literature, viz.  $\text{Cu}(\text{HL})^+$ ,  $\text{Cu}(\text{HL})_2$ ,  $(\text{CuL}_2)^{2-}$ .

Some researchers have disputed that  $\text{Cu}(\text{HL})^+$  exists in aqueous media. <sup>68-69</sup> The reason put forward to account for the failure to detect the 1:1 species has been that

the 1:2 version has a significantly increased stability due to the extra intramolecular bonds between the coordinated groups. There are a number of determinations of the formation constant of the 1:2 species in dioxane solutions. Ashurst<sup>69</sup> has extrapolated data determined for a series of dioxane solutions in order to determine the theoretical value for a 0% dioxane solution.

There is little information available in the literature about the conditions of formation of either the 1:1 basic copper-SALO precipitate or the soluble species,  $(CuL_2)^{2-}$ . It was therefore decided to investigate the reaction between copper ions and SALO at two pH values. The absorbance of a SALO solution ( $1,1196 \times 10^{-4}$  mol.l<sup>-1</sup>, 100 ml) at a controlled pH was measured over the wavelength range 250 to 450 nm, by pumping the solution through the spectrophotometer cell as shown below in fig. 24.

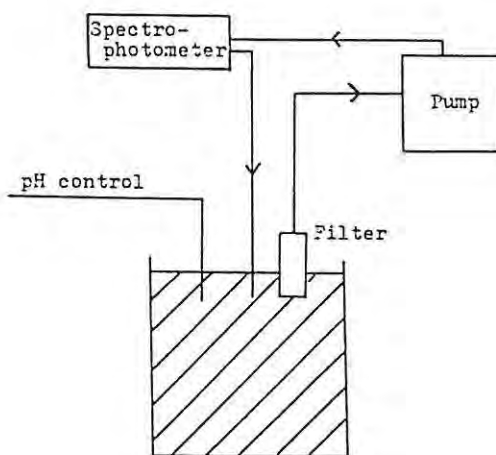


Fig.24. Apparatus to monitor metal-complexation.

A filter was placed in the line in order to remove any solid material. The change in the absorbance on the

addition of small quantities of copper solution ( $4,005 \times 10^{-3} \text{ mol.l}^{-1}$ ) was then monitored. The drop in the absorbance of the reagent at pH 5,5 with copper addition is illustrated in fig. 25. The inset is included to show the data replotted to show the linear relationship between the concentration of copper added and the absorbance.

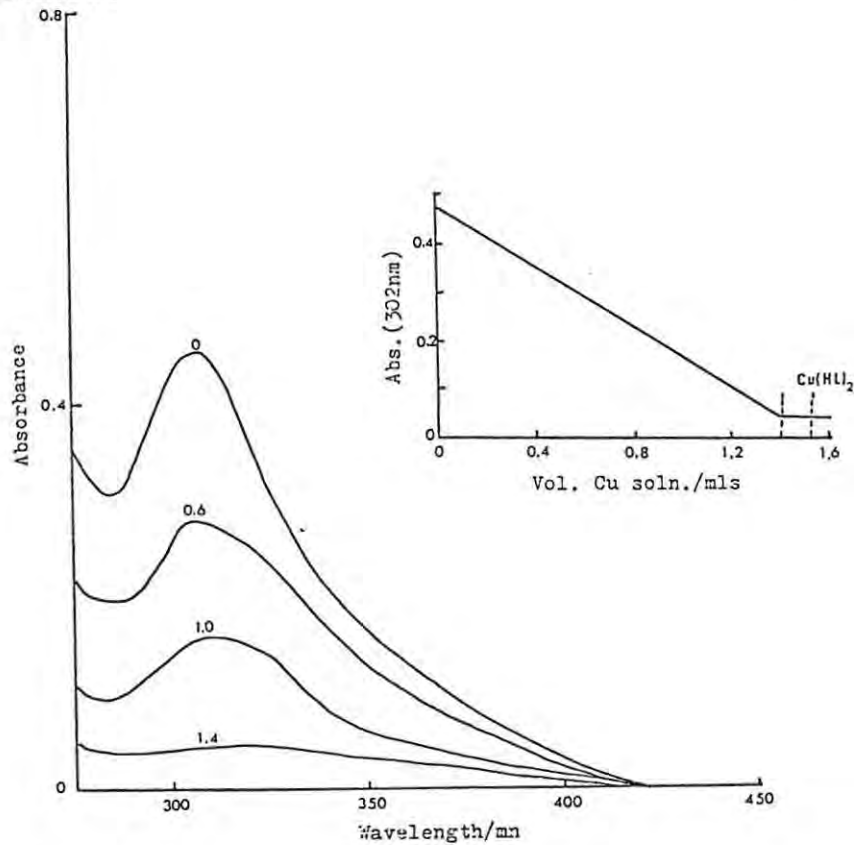


Fig. 25. Titration of SALO against copper solution at pH 5,5.

The calculation of the ratio of the concentration of SALO originally present and the concentration of copper required to reduce the absorbance to zero confirmed that a precipitate of  $\text{Cu}(\text{SALO})_2$  was formed at pH 5,5. The same type of experiment was repeated at pH 10,0 (fig. 26).

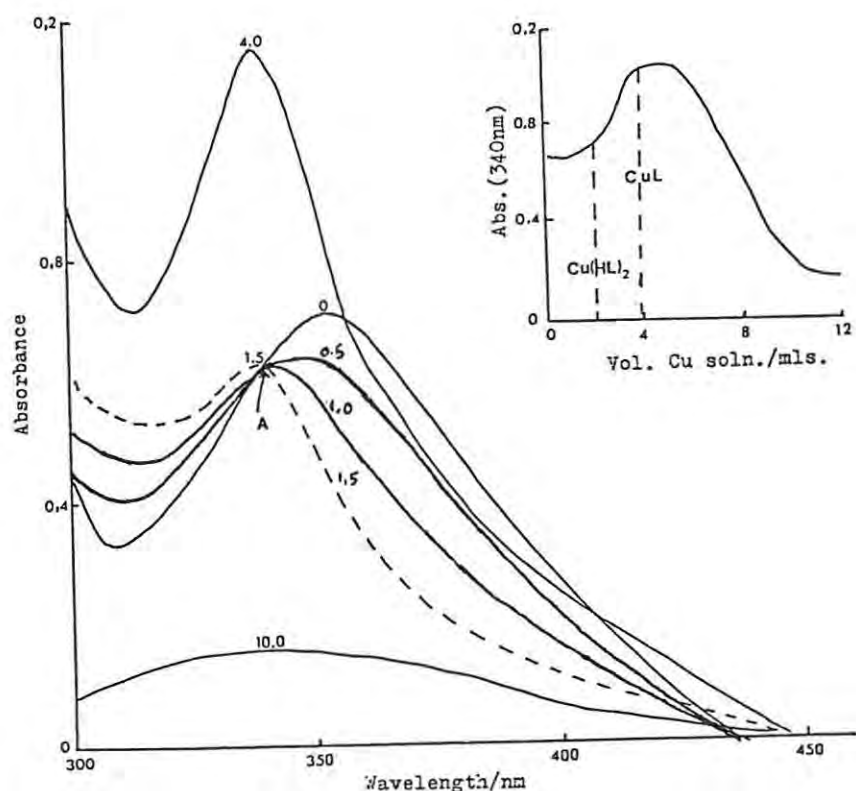
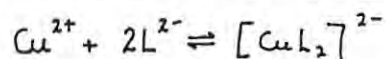
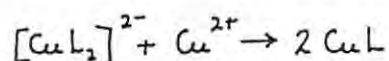


Fig. 26. Titration of SALO against copper solution at pH 10.

At this pH the absorption maximum of the reagent shifted to 355 nm. The addition of up to 1,5 ml of the copper solution ( $4,005 \times 10^{-3} \text{ mol. l}^{-1}$ ) caused the spectrum to move from the reagent maximum at 355 nm to a new maximum at 337 nm. The occurrence of an isosbestic point as shown as point A in fig. 26' indicated that only two species were involved in the equilibrium. On the basis of the measurement of the ratio between the concentration of SALO and copper the following equilibrium is suggested :-



Further addition of copper ions increased the intensity of the maximum at 337 nm, such that the absorption curve deviated from the isosbestic point. This was probably caused by the co-ordination of more copper as shown below.



The addition of still further copper caused the absorbance to decrease gradually. A precipitate could be detected visually and was suspected to be a polymeric form of the CuL complex, viz.  $(\text{CuL})_n$ .

This study has shown therefore that 1) at low copper concentrations,  $\text{Cu}(\text{SALO})_2^{2-}$ , is the most important species at pH 10. No attempt was made to measure the formation constants of this species but for the purpose of the construction of a species distribution diagram an approx value had to be chosen. The value chosen reflected the importance of this species at high pH values, and 2) the basic 1:1 precipitate only forms in the presence of a large excess of copper ions. This solid is therefore unlikely to form on copper(II) oxide since this oxide has a very limited solubility at high pH values. The values chosen for the derivation of the metal complex species distribution are collated in table 13.

Table 13.

Equilibrium constant data used in the calculation of the copper-salicylaldehyde species distribution (fig. 25). The medium was 100% water and the temperature 25°C.

Equilibrium	Value	Reference
$H_3L \rightleftharpoons H_2L + H^+$	$pK_1=1,72$	45
$H_2L \rightleftharpoons HL^- + H^+$	$pK_2=9,18$	45
$HL^- \rightleftharpoons L^{2-} + H^+$	$pK_3=12,08$	45
$Cu^{2+} + 2HL^- \rightleftharpoons Cu(HL)_2$	$\log\beta_2=15,20$	69
$Cu^{2+} + 2L^{2-} \rightleftharpoons (CuL_2)^{2-}$	$\log\beta_2=22,00$	Assumed

The species distribution was calculated using this data in the same manner as outlined in the appendix. The data is presented diagrammatically in fig. 27.

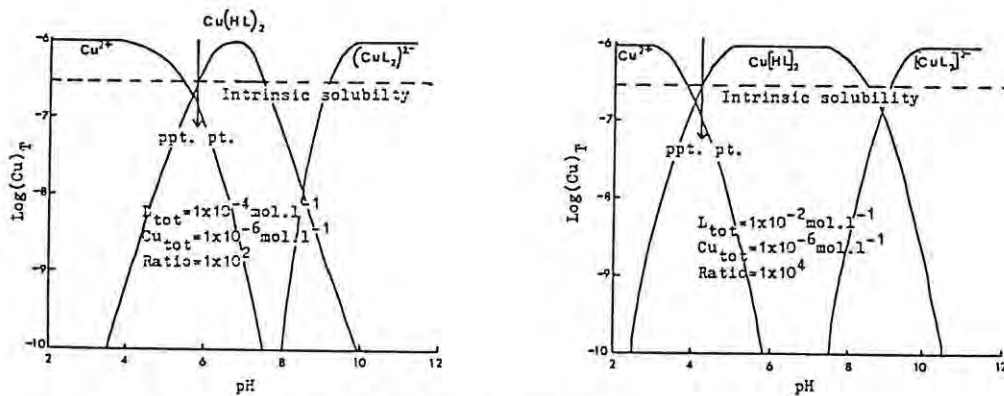


Fig. 27. Species distribution diagram for different total SALO and copper concentrations.

The bis complex,  $\text{Cu}(\text{HL})_2$ , predominates over the neutral pH range. At low pH values and low total reagent concentrations the free metal ion species is more important. The comparison of this diagram with the equivalent distribution diagram of N-phenylbenzohydroxamate (section 3.a) indicates that the two ligands have similar ability to co-ordinate to copper. The intrinsic solubility of  $\text{Cu}(\text{HL})_2$  in water is unknown and so the value given for the similar copper oxinate species was used.<sup>59</sup> The precipitation point varies from pH 4,2 for high  $L_{\text{TOT}}/\text{Cu}_{\text{TOT}}$  ratio solutions to pH 5,8 for low  $L_{\text{TOT}}/\text{Cu}_{\text{TOT}}$  ratio solutions.

D.3.b.ii) 2. Substituted SALO derivatives

The first acid dissociation constant of a series of substituted ligands in solutions containing 75% dioxane have been determined previously.<sup>68</sup> (Table 14)

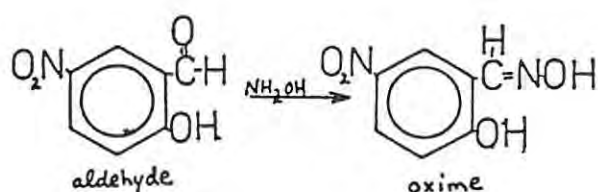
Table 14.

Acid dissociation constants for a series of substituted salicylaldoximes. The medium was 75% dioxane, ionic strength 0,1, temperature 20°C.

Substituent	Value
SALO	10,70
5-methyl	11,06
5-chloro	10,25
5-nitro	8,72

These values illustrate the effect of the electrophilic (chloro and nitro) and nucleophilic (methyl) substituents on electron density of the donor atom. The decrease of the electron density on the donor atom causes the increase of the dissociation of the proton, i.e. the increase of the dissociation constant. In the same study it was also established that the stability constants of the metal complexes showed a similar order, but unfortunately the value for the copper-nitro derivative complex was not determined.

The nitro derivative (referred to as SNSALD) was chosen for use in the present study because it showed very significant differences from the parent ligand. It was considered that ligands too similar to SALD would not show noticeable variations in behaviour. The nitro derivative of SALD was prepared from the aldehyde as follows :-



The derivation of the species distribution diagram requires the values for the acid dissociation constant and for the stability constant of the copper complex. The acid dissociation constant could be measured relatively easily by titration against standard sodium hydroxide. The value determined of  $pK_A = 6,05$  showed a

similar decrease from SALO to that shown for the aldehyde in table 14. In order to be able to infer an approximate value for the stability constant of the nitro-derivative, it was necessary to consult some work on the stability constants of metal complexes of substituted aldehydes. The values referred to are given in table 15.<sup>70</sup>

Table 15.

Equilibrium constants for substituted aldehydes. The medium was 50% dioxane and the temperature 20°C.

Substituent	pK	log $\beta_2$	$(pK_{SALO} - pK_{subst})(\log\beta_{2SALO} - \log\beta_{2subst})$	
None	9,35	12,00	-	-
5-chloro	8,47	10,30	0,88	1,70
5-nitro	5,96	7,90	3,39	4,10

If one accepts the value of the pK for SALO in 0% dioxane as 9,18 and a formation constant of  $\log \beta_2 = 15,20$  then one can calculate, by assuming that the variation between the oxime and aldehydes would be constant, the values for the  $pK_A$  and  $\log \beta_2$  for the nitro derivative in 0% dioxane. In this way the  $pK_A = 6,09$  and the  $\log \beta_2 = 11,0$  were determined. The agreement between the experimentally determined  $pK_A = 6,05$  and the value inferred  $pK_A = 6,09$  lends credence to the assumptions made.

At this stage it should be recalled that the soluble complex,  $(Cu(SALO)_2)^{2-}$ , was shown previously to be an important species at high pH's. Consequently, similar precipitation experiments were performed with the nitro ligand in order to test for the formation of a similar

complex. The controlled addition of the copper solution ( $4,005 \times 10^{-3} \text{ mol.l}^{-1}$ ) to a solution of the 5-nitrosalicylaldoxime ( $1,004 \times 10^{-4} \text{ mol.l}^{-1}$ , 100 ml) at a pH of 10 resulted in a linear decrease in the absorbance at 430 nm (fig. 28).

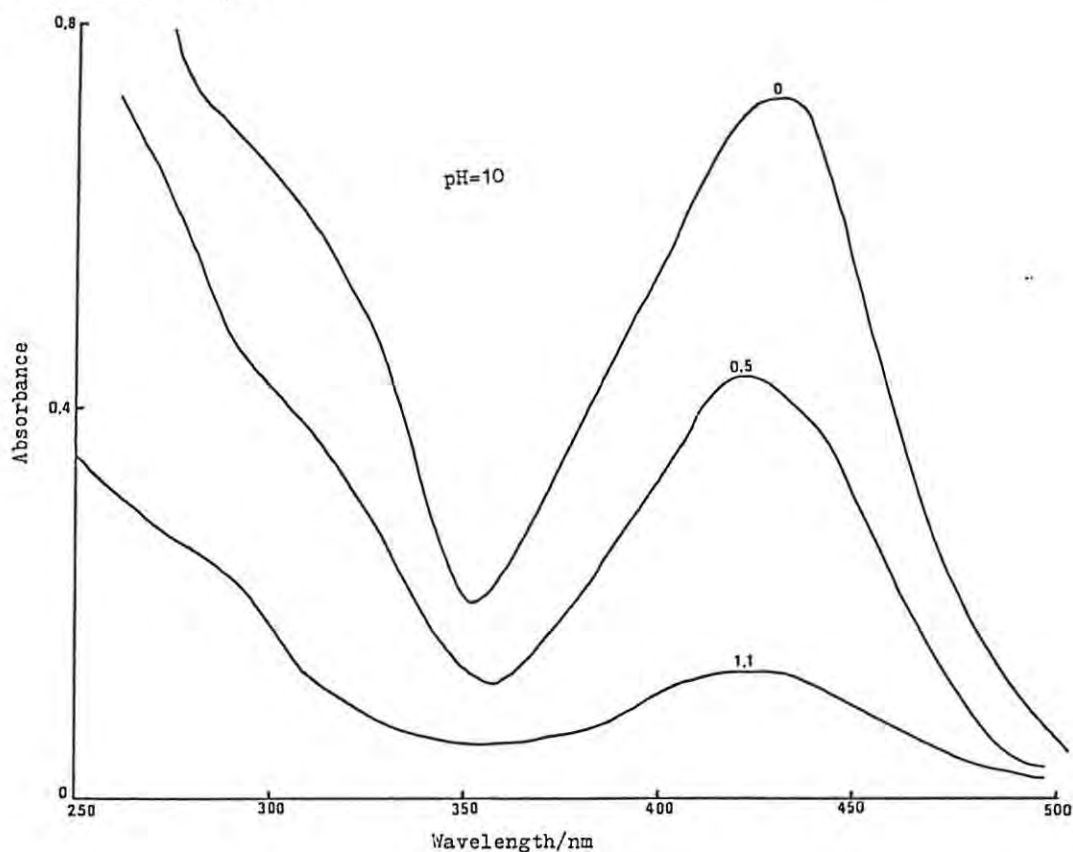


Fig.28. Titration of 5-nitrosalicylaldoxime against copper solution.

The visual detection of a brownish precipitate, and the calculation of the concentration of copper required to reduce the absorbance to zero, indicated that a 1:2 copper-chelate was responsible. Interestingly, the soluble species,  $(\text{Cu}(\text{5SALO})_2)^{2-}$  was not detected under these conditions.

It was found impracticable within the scope of this study

to determine the dissociation constant of the oximic hydrogen accurately. The approximate value was determined by titration and was shown to be very low, viz.  $10^{-11}$ . The cause of the lack of formation of the  $(\text{Cu}(\text{SSALD})_2)^{2-}$  species at high pH's could be either the weak dissociation tendency of the oximic hydrogen or the decreased formation constant of the metal complex. Unfortunately, there was no way of distinguishing between the two and so it was decided to exclude these species from the derivation of the species distribution diagram. The data used to derive the diagram is collated in table 16.

Table 16.

Equilibrium constant data used in the calculation of the copper-5-nitrosalicylaldehyde species distribution (fig. 27).

Equilibrium	Type	Value
$\text{H}_2\text{L} \rightleftharpoons \text{HL}^- + \text{H}^+$	$\text{pK}_a$	6.05
$\text{Cu}^{2+} + 2\text{HL}^- \rightleftharpoons \text{Cu}(\text{HL})_2$	$\log \beta_2$	11.10

The data was processed in the same way as previously in order to calculate the concentration of the free copper ions and the concentration of the copper complex at different total metal and ligand concentrations (fig. 29).

6/21/50

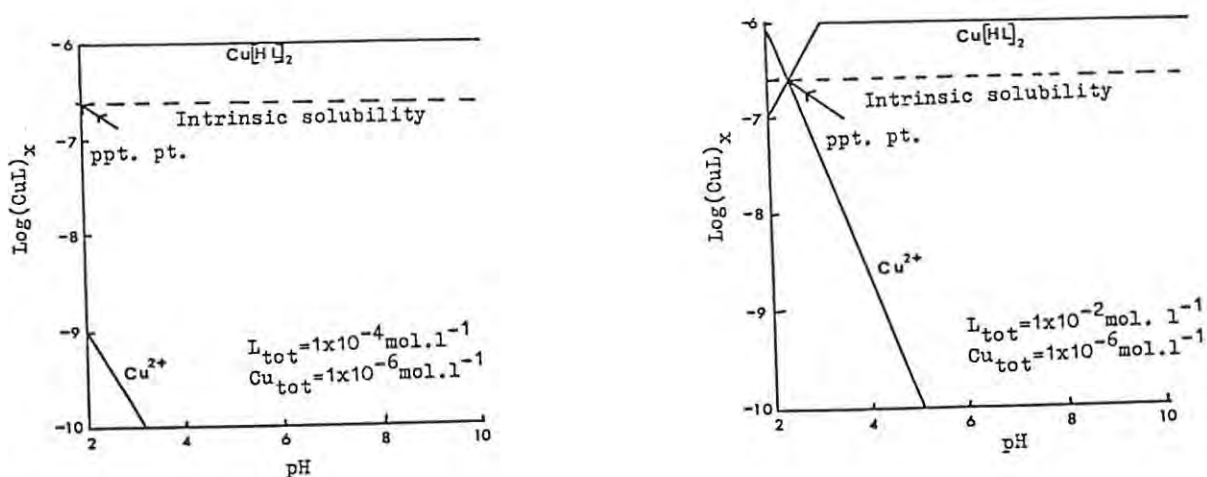


Fig. 29. Species distribution for 5-nitrosalicylaldehyde.

The comparison of these diagrams with the equivalent SALD data shows an interesting feature. It is clear that in the case of the nitro-derivative the formation of the bis-complex is favoured over the free metal ion down to comparatively low pH values. This could have important consequences in adsorption studies since copper(II) oxide becomes increasingly more soluble under acidic conditions.

D.3.b.iii) Adsorption isotherms

In the preliminary work of this study it was confirmed that chelating reagents adsorb on copper(II) oxide through the formation of an insoluble precipitate on the surface. Nagaraj <sup>21-23</sup> has also shown that the precipitate might be present in large amounts in a dispersed form in the bulk solution. Consequently, in most adsorption experiments the concentration of  $\text{Cu}(\text{SALO})_2$  precipitate was determined and not simply the

residual concentration of SALO. However, in the case of experiments with very dilute solutions of SALO and with nitro-substituted derivatives, the concentration of reagent removed from solution was measured directly. A reliable measurement of bulk and surface precipitate was not possible in these examples because the concentration produced was so low.

The following variables were considered in the derivation of adsorption isotherms, viz. time, surface area, pH, temperature, concentration and the presence of substituents in the aromatic ring.

D.3.b.iii) 1. Time, surface area

The concentration of surface  $\text{Cu}(\text{SALO})_2$  and of dispersed precipitate (called bulk) was measured as a function of conditioning time. The results for the copper(II) oxide sample (surface area  $0,17 \text{ m}^2/\text{g}$ ,  $1,0 \text{ gm}$ ) conditioned with salicylaldoxime at  $20^\circ\text{C}$  ( $1 \times 10^{-3} \text{ mol.l}^{-1}$ ,  $100 \text{ ml}$ ) are shown in fig.30.

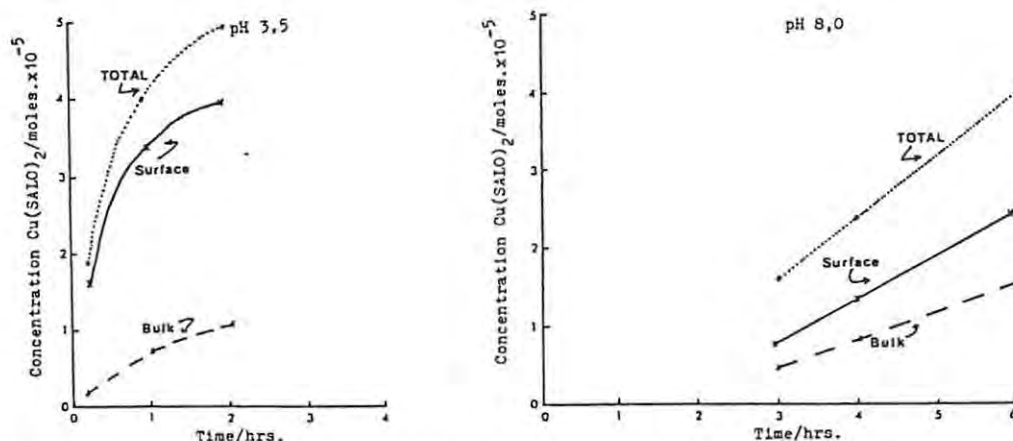


Fig.30. The variation with pH in the rate of formation of bulk and surface  $\text{Cu}(\text{SALO})_2$  on  $\text{CuO}$ .

The following important features were noted :

- a) The formation of the precipitate of  $\text{Cu}(\text{SALO})_2$  was a gradual, continuous process. The reaction only reached equilibrium when the reagent concentration had dropped to a very low value.
- b) The rate of the formation of precipitate was pH dependent. At pH 3,5  $5 \times 10^{-5}$  moles of  $\text{Cu}(\text{SALO})_2$  was produced after a 2 hour conditioning period, whereas at pH 8,0 it took 6 hours to produce  $4 \times 10^{-5}$  moles.
- c) The concentration of surface chelate always exceeded the concentration of bulk chelate. At pH 3,5 after 2 hours conditioning the concentration of surface chelate detected was  $4 \times 10^{-5}$  moles which corresponds to approximately 67 layers of chelate. (A monolayer equals  $7 \times 10^{-10}$  moles. $\text{cm}^{-2}$ ). The concentration of bulk chelate formed under the same conditions corresponded to 16 layers of chelate. The ratio of surface to bulk chelate at pH 3,5 was therefore 4,19. At pH 8,0 after 6 hours conditioning the concentration of surface chelate corresponded to 39 layers whereas the concentration of bulk chelate corresponded to 24 layers. This gives a ratio of surface to bulk of 1,63.
- d) The adsorption results at acidic pH values were similar to the hydroxamate data. In both cases there was a relatively rapid precipitation of copper chelate. However, at basic pH values the rate of precipitation was

significantly larger in the case of the hydroxamate.

D.3.b.iii) 2. pH, concentration

The uptake of SALO by copper(II) oxide was found to be both pH and concentration dependent. The results for copper(II) oxide (surface area  $0,07 \text{ m}^2/\text{g}$ ,  $1,0 \text{ gm}$ ) conditioned with a) SALO ( $1 \times 10^{-3} \text{ mol.l}^{-1}$ ,  $100 \text{ ml}$ ,  $2 \text{ hrs}$ ) and b) SALO ( $1 \times 10^{-5} \text{ mol.l}^{-1}$ ,  $100 \text{ ml}$ ,  $10 \text{ mins}$ ) at  $25^\circ\text{C}$  are shown in fig. 31.

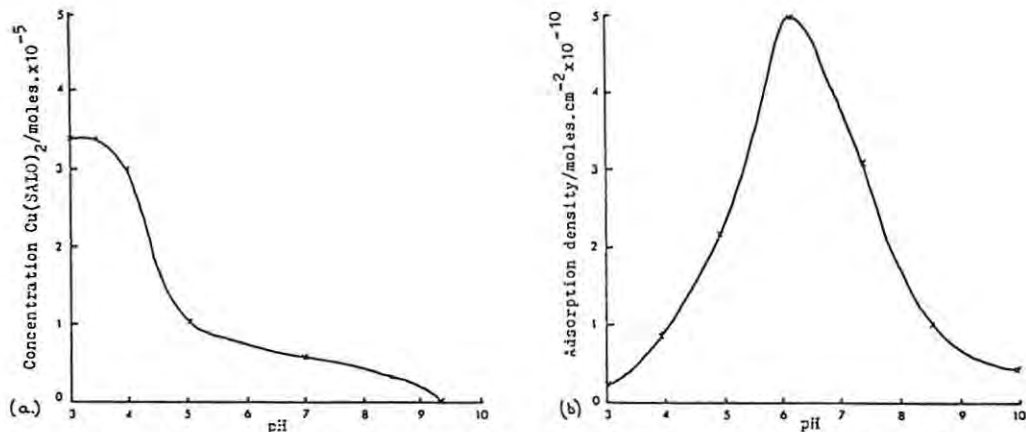


Fig.31. The relationship between the pH and concentration of the SALO solution and the amount adsorbed on CuO.

When high concentrations of reagent were used the maximum formation of  $\text{Cu(SALO)}_2$  occurred at acidic pH values. The amount produced dropped rapidly with increasing pH, such that at pH 9,5 there was very little complex produced. In contrast when very dilute solutions were used the maximum uptake of SALO occurred at neutral pH's. At acidic and basic pH's the adsorption was minor in comparison.

It is of interest to compare the adsorption isotherm for SALO and hydroxamate solutions (see fig. 21). If one

bears in mind that the isotherms are not strictly comparable since they were derived from different batches of copper(II) oxide with different surface areas, it is still possible to infer that, 1) SALO formed a precipitate at lower pH's than hydroxamate and 2) hydroxamate tended to form more precipitate at neutral pH values than SALO.

D.3.b.iii) 3. Temperature

The rate of total precipitation of  $\text{Cu}(\text{SALO})_2$  was found to increase with higher temperatures (fig. 32). This was the same for all reagents studied.

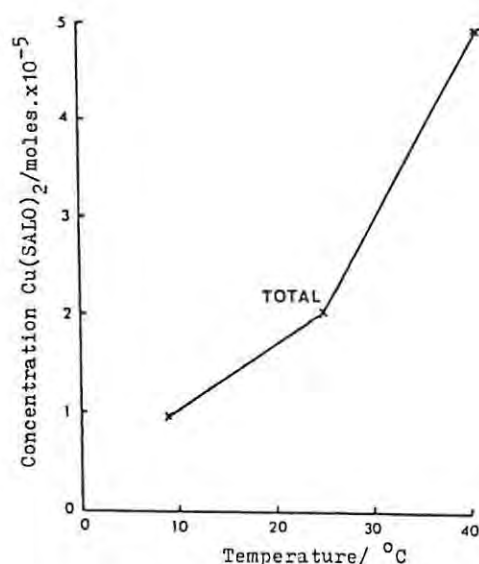


Fig.32. Adsorption of salicylaldehyde on CuO at various temperatures.  $\text{CuC}(0,07\text{m}^2/\text{g})$  SALO ( $1 \times 10^{-3} \text{mol.l}^{-1}$ ) pH 4,0

D.3.b.iii) 4. Comparison between salicylaldehyde and the 5-nitro substituted derivative.

The adsorption of SALO and the nitro-derivative was monitored continuously by passing the solution, via a filter, directly to a spectrophotometer. In this manner

the change in concentration could be monitored continuously. This method was found to be the only feasible manner in which to study the adsorption of the nitro derivative. This was because it was found that the copper chelate of this reagent was insoluble in all organic solvents and so it could not be removed from the surface. An attempt was made to increase the solubility of the copper chelate by incorporating alkyl groups onto the aromatic ring. Although this procedure did overcome the solubility problems of the complex it unfortunately resulted in the reagent itself becoming too insoluble for use.

The adsorption data are reflected in fig. 33.

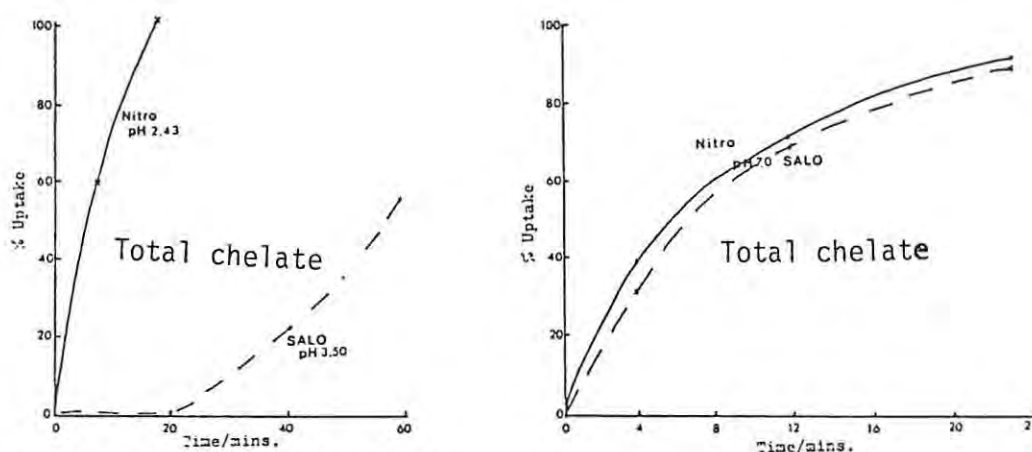


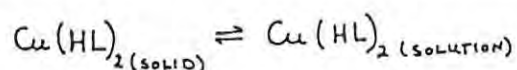
Fig. 33. Comparison between the rate of adsorption of salicyladoxime and 5-nitrosalicyladoxime on CuO.

It was clear that i) the nitro-derivative adsorbs at very low pH's, ii) at low pH's the SALO does not initially become adsorbed, and iii) at neutral pH the two reagents adsorb in a similar fashion.

D.3.b.iii) 5. Discussion

The model proposed to explain the adsorption of chelates on copper(II) oxide was the same as was discussed previously. In this model the adsorption data were considered in terms of the factors which controlled the formation and growth of a 1:2 copper-chelate precipitate. The concentration formed was proposed to be controlled by the dissolution of the oxide and by the complexing ability of the reagents as was reflected in the species distribution diagrams.

The adsorption data for SALO and the nitro-derivative fitted the above model. The results of the adsorption experiments conducted at two different initial concentrations are considered first. Fig. 31 showed that when a very dilute SALO solution was used then maximum uptake occurred at neutral pH values, whereas when a more concentrated solution was considered then maximum uptake occurred at acidic pH's. A large uptake at acidic pH's was expected because the oxide dissolution data had indicated the maximum release of copper ions under these conditions. However, in order to understand the adsorption maximum at neutral pH for very dilute solutions it is necessary to refer to the species distribution diagrams. Although the intrinsic solubility as defined in the equation below is not known, a reasonable value of  $10^{-6,5}$  can be assumed by analogy with



the known value for copper oxinate. <sup>59</sup>

These diagrams indicate that this value is exceeded at pH 5,8 for a  $1 \times 10^{-4}$  mol.l<sup>-1</sup> SALO solution and at pH 4,2 for a  $1 \times 10^{-2}$  mol.l<sup>-1</sup> solution. It can be concluded that copper chelate precipitate was responsible for the uptake of SALO on copper(II) oxide. Comparison of the adsorption data for SALO at neutral and at high pH with the equivalent data for hydroxamate shows that there was less precipitation formed with the former. If the same intrinsic solubility value was used, then at pH values greater than 8, no adsorption would be predicted. The lack of adsorption was caused by the formation of the  $(\text{Cu}(\text{SALO})_2)^{2-}$  species.

It is easy, within the terms of the above model, to explain the increased uptake with higher temperatures. A temperature rise caused an increase in the rate of release of copper ions from the oxide and thus an increased rate of precipitation.

The relationship between the species distribution in solution and the adsorption data was well illustrated in the comparison between the SALO and the nitro-reagent. The adsorption data indicated that at pH 2,43 the nitro derivative was immediately adsorbed from solution whereas the SALO derivative at pH 3,5 was only adsorbed after 20 mins. This is explained by the requirement that for SALO precipitation the copper concentration needed to reach a

high value. The species distribution diagrams confirm that the copper complex of the nitro derivative is favoured to much lower pH's than SALO. No differences occurred between SALO and the nitro derivative at pH 7,0 because under these conditions chelation was strongly favoured for both.

Some refinements to the model are needed to account for the surface to bulk ratio of the chelate as given in fig. 30/. In the first place it is clear that surface chelate formation was favoured over bulk chelate formation. This indicates that initial nucleation of the precipitate took place on the surface of the copper(II) oxide and not in the bulk solution. However, there was a distinct tendency for the surface to bulk ratio to decrease at high pH values. In order to understand this phenomenon it is necessary to consider some experimental data on the flocculation of  $\text{Cu}(\text{SALO})_2$  precipitates. Experiments were conducted in which the precipitate was generated by the addition of a copper solution to the reagent solution at pH 3,5 or at pH 9,0. In the former case the precipitate rapidly flocculated and therefore settled rapidly. However, at pH 9,0 the precipitate was found to be well dispersed. This dispersion was caused by the adsorption by the precipitate of either hydroxyl ions or possibly  $[\text{Cu}(\text{SALO})_2]^{2-}$  ions. It is therefore suggested that the same factors could be partly responsible for the tendency for more bulk chelate to form at high pH's.

D.3.b.iv) Scanning electron microscope study

The scanning electron microscope has proved an extremely useful tool with which to study copper(II) oxide surfaces. This technique has made possible a study of the structural features of the growth present on copper(II) oxide surfaces treated with SALO under different conditions. The micrographs chosen for illustration in this thesis show representative particles (or particle surfaces) of the bulk oxide sample. All the features noted occur on all the surfaces but for obvious reasons it was not possible to display all these particles.

D.3.b.iv) 1. Nucleation

A sample of copper(II) oxide was treated with a SALO solution under conditions such that enough SALO was adsorbed on the surface to give a coverage of approx.  $9 \times 10^{-10}$  moles.cm.<sup>-2</sup> Subsequent examination of this oxide surface under the S.E.M. at very high magnification ( $20 \times 10^4$  times) revealed the presence of small elongated crystallites (micrograph 19).

It is of interest to attempt to relate these crystallites to the molecular dimensions of copper - SALO complexes and thus to the concept of a monolayer coverage. It is assumed initially that the metal ion remains incorporated in the oxide lattice and that the reagent reacts by the displacement of surface ions. From a knowledge of the crystal structure of tenorite, ie. CuO, (the unit cell data are given in table 17) the average area per surface copper atom can be calculated approx. as  $0,10 \text{ nm}^2$ . This value is an approximation since the value will vary depending on

which crystal face oxide cleavage occurs. If each copper atom reacted with a single SALO molecule then there would be  $20 \times 10^{-10}$  moles adsorbed on  $1 \text{ cm}^2$  of the oxide surface. On the other hand if the steric restrictions of the size of the SALO molecule are considered then the maximum number of SALO molecules that could fit in a closely packed fashion on the surface can be calculated, ie. with the molecule protruding from the surface. The area covered by the N and O groups which are involved in chelation to the surface copper ion was determined as  $0,26 \text{ nm}^2$  from the van der Waals radii of these groups. This would give an adsorption density of SALO of  $6,3 \times 10^{-10}$  moles  $\text{cm}^{-2}$ . The area covered by a SALO molecule is similar to the values calculated by others, eg. octyl hydroxamate  $0,25 \text{ nm}^2$ ,<sup>35</sup> ethylxanthate  $0,29 \text{ nm}^2$ ,<sup>71</sup> stearate  $0,20 \text{ nm}^2$ .<sup>72</sup> Other packing configurations such as when the aromatic group lies flat on the surface would give a larger area covered by the atom and thus a lower adsorption density. However, this configuration is unlikely since the co-ordination to the metal ions is constrained by its attachment to other lattice ions.

The occurrence of a single SALO molecule attached to a surface copper atom is unlikely to be detected by the S.E.M. even at the very high magnification used. Consequently since a distinct surface product (or crystallite) was detected on a treated oxide surface (no such feature was detected on the untreated oxide at the same magnification) at an adsorption density which would approximate a uniform monolayer coverage, it is considered that these features represent isolated multilayer

patches of a copper - salicylaloximate precipitate. The other areas on the surface would therefore be unaffected by the reagent. This is illustrated below.



An estimation of the approximate number of molecules of  $\text{Cu}(\text{SALO})_2$  present in the crystallites can be made in two ways. In one method a visual estimate indicated that only about 5% of the area displayed in micrograph 19 was covered by the crystallites. If it is accepted that uniform monolayer coverage approximates to the amount of SALO adsorbed then by simple proportion it can be estimated that the crystallites were made up of at least 20 molecular layers of  $\text{Cu}(\text{SALO})_2$ . The approximate amount of  $\text{Cu}(\text{SALO})_2$  required to give a monolayer coverage can be determined from the unit cell dimensions as given in table 17. An average of  $7 \times 10^{-10}$  moles.  $\text{cm}^{-2}$  was calculated on the area covered by the crystal faces of  $\text{Cu}(\text{SALO})_2$  considered most likely to be orientated towards the oxide surface. For example the area covered by the 100 and 001 crystal faces of  $\text{Cu}(\text{SALO})_2$  are  $0,24\text{nm}^2$  and  $0,84\text{nm}^2$ , respectively. Possible attachment to the surface in these cases could occur via the metal ion or by the hydrogen bonds to the hydroxyl group.

In the other method an attempt was made to estimate the volume of material adsorbed on the oxide surface. This requires unfortunately an assumption of the depth of crystallites

which is almost impossible to estimate visually from the micrograph.

The crystallite size was estimated as -

Length	0,03 $\mu\text{m}$
Width	0,004 $\mu\text{m}$
Depth	0,0001 $\mu\text{m}$

The volume was determined as  $1,2 \times 10^{-20} \text{ cm}^2$  (assuming a rectangular shape).

The volume of one molecule of  $\text{Cu}(\text{SALO})_2$  can be calculated as  $3,34 \times 10^{-22} \text{ cm}^2$  from the density which has been determined as  $1,67 \text{ g/cm}^2$ . This indicates that there are 36 molecules in the crystallites.

In conclusion of this section it appears from the evidence that a uniform monolayer of SALO adsorbing on the surface of copper oxide is insufficient to explain all the data. However, it is recognised that the evidence does not exclude the possibility that the formation of the crystallites goes through a stage that involves an attachment of a SALO molecule to the surface. It is suggested in this thesis that the adsorption data is better explained in terms of nucleation and crystal growth theory. Nucleation occurs at isolated high energy sites on the surface. Once nucleation has occurred then subsequent crystal growth occurs at these sites.

Table 17.

Crystallographic details for tenorite.

Monoclinic symmetry.

Unit-cell dimensions.

$$a = 4,68, b = 3,42, c = 5,13 \text{ \AA}^0$$

$$V = 81,08 \text{ cm}^3$$

$$D = 6,52 \text{ g/cm}^3$$

Number of CuO molecules = 4.

Crystallographic details for Cu-SALO chelate.

Monoclinic symmetry.

Unit-cell dimensions.

$$a = 13,98, b = 6,08, c = 8,00 \text{ \AA}^0$$

$$D = 1,67 \text{ cm}^3$$

Number of molecules = 2.

D.3.b.iv) 2. Crystal growth

Copper(II) oxide was treated with SALO solutions under conditions which allowed the study of the nature of the crystal growth after nucleation.

a. Time The nucleation sites were visible under the S.E.M. at a magnification of 2000 times (micrograph 20). Further growth resulted in these nuclei increasing in size to produce a uniform, rectangular shaped crystallite (micrograph 21). There appeared to be no generation of new nuclei. Interestingly, the crystallites occurred as isolated patches on the surface and not as a uniform coverage and, therefore leaving a fair proportion of the surface unaffected by SALO.

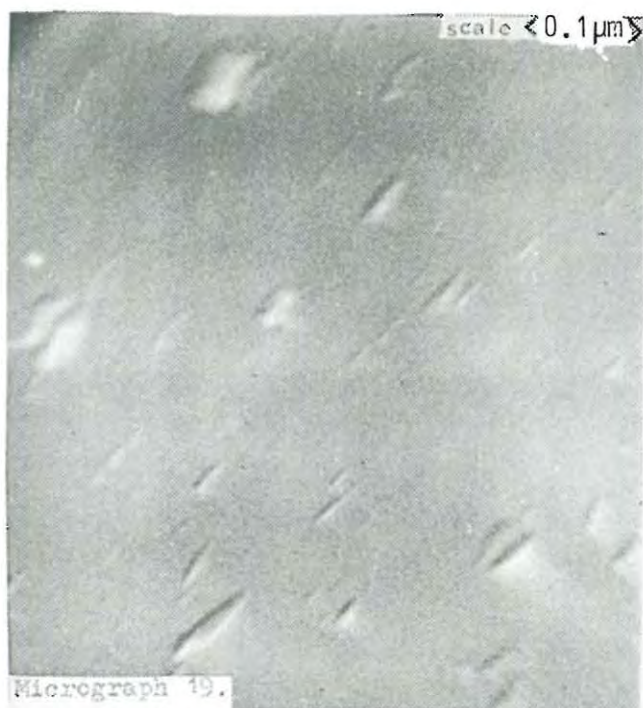
b. Surface area

It is possible, by the variation of the surface area of an oxide, to change the number of copper ions entering solution for a known mass of oxide in a set length of time. Crystal growth on oxides of different surface areas should reflect the effect of this change. The results did indeed show that for a copper(II) oxide sample of surface area  $0,07 \text{ m}^2/\text{g}$  the crystallites were larger (micrograph 22) than for a sample of surface area  $0,17 \text{ m}^2/\text{g}$  (micrograph 23). The crystallites were well formed in both cases.

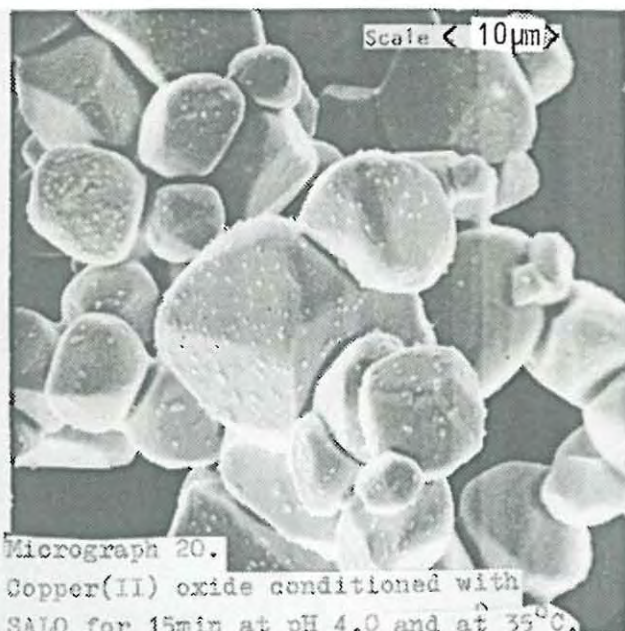
c. Reagent types

A comparison was made of the surface growth on copper(II) oxide treated with SALO and with the nitro derivative at acidic and neutral pH values. SALO formed isolated patches of flat, rectangular shaped crystals (micrograph 24). In contrast the nitro-derivative formed a fibrous, mat-like structure across most of the oxide surface

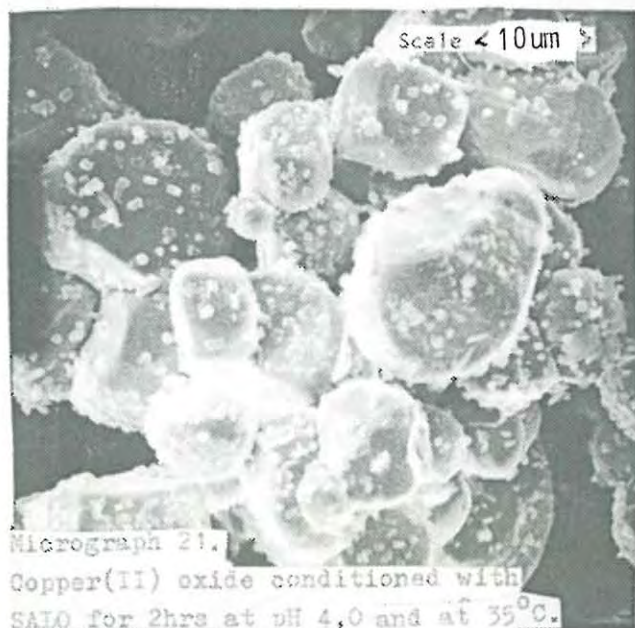
(micrograph 25). Closer examination of a sample treated briefly with the nitro-reagent revealed that the initial growth occurred as long, orientated blades (micrograph 26). An important difference between the nitro derivative and SALD is that the surface growth of the former reagent is more continuous and therefore it is expected to function as a better reagent in the flotation process. It is suspected that the reason for the difference in the structure of the precipitate was related to the chemical nature of the two reagents. The presence of the nitro-group on the aromatic ring could have restricted the development of the uniform crystal lattice. It was also possible that the degree of supersaturation of the copper complex in solution before precipitation was very much higher in the case of the nitro derivative. It is known that precipitates grown from highly supersaturated solutions tend to grow preferentially in one direction, ie. they are fibrous. This point will be developed further in the section dealing with 8-hydroxyquinoline.



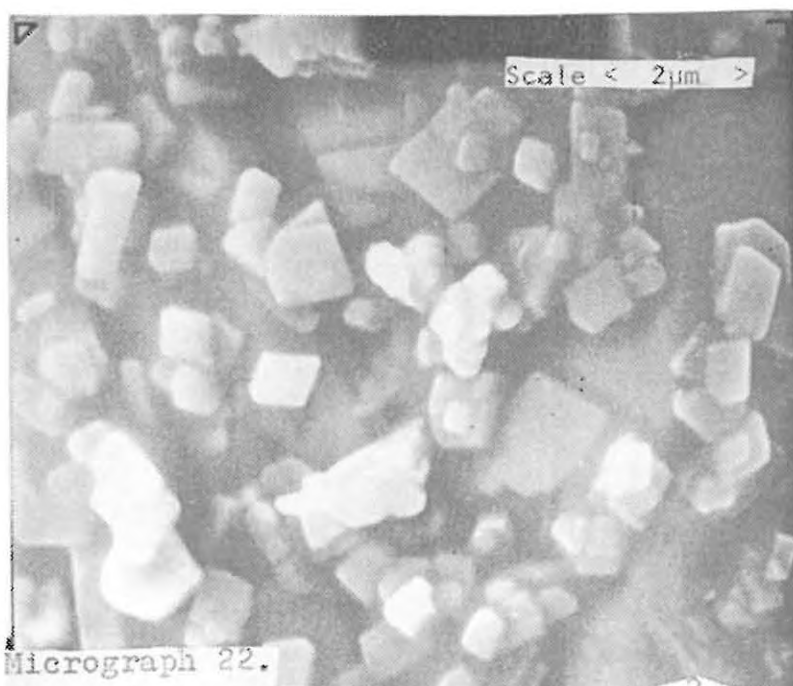
Micrograph 19.  
Copper(II) oxide conditioned with SALO  
to give theoretical monolayer coverage.



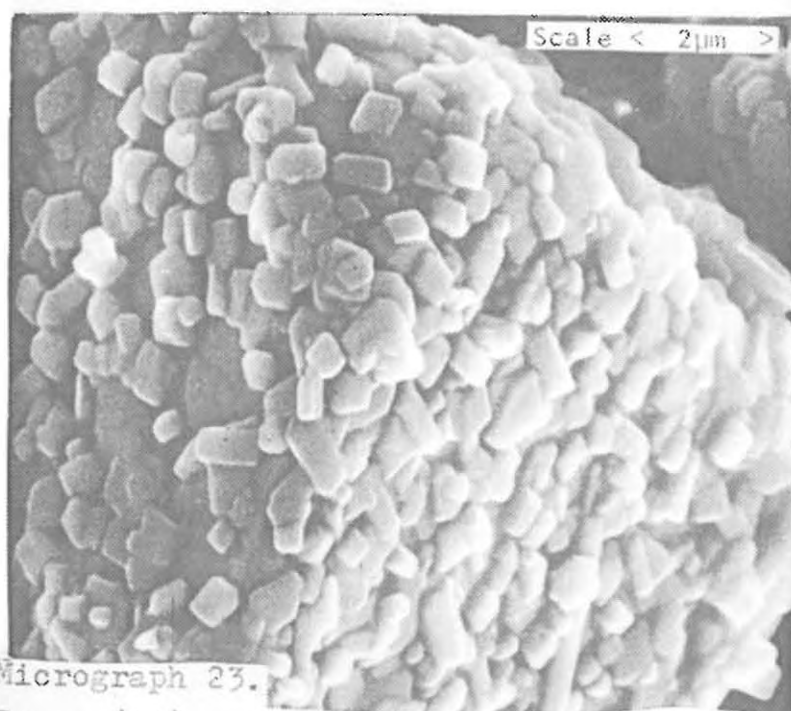
Micrograph 20.  
Copper(II) oxide conditioned with  
SALO for 15min at pH 4.0 and at 35°C.



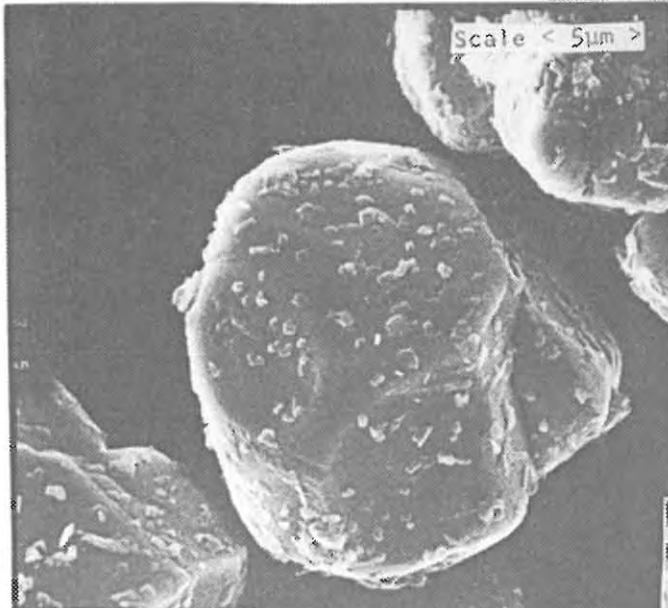
Micrograph 21.  
Copper(II) oxide conditioned with  
SALO for 2hrs at pH 4.0 and at 35°C.



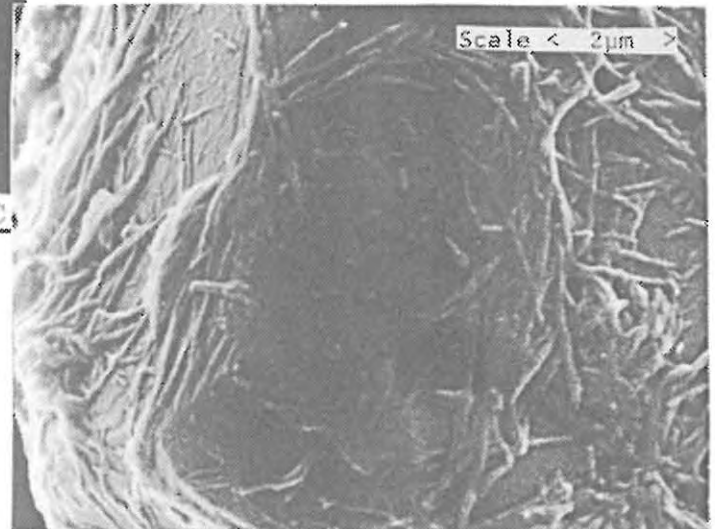
Micrograph 22.  
Copper(II) oxide, surface area  $0,07\text{m}^2/\text{g}$ ,  
conditioned with SALO for 3hrs at pH 3,5  
and at  $25^\circ\text{C}$ .



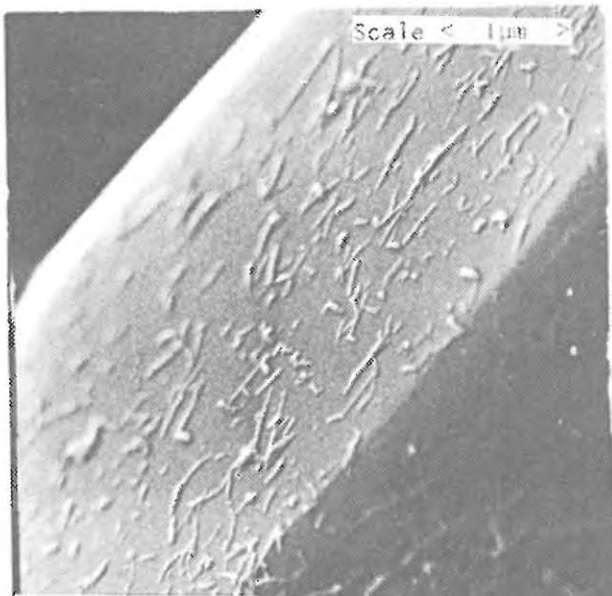
Micrograph 23.  
Copper(II) oxide, surface area  $0,17\text{m}^2/\text{g}$ ,  
conditioned with SALO for 1,5hrs at  
pH 3,5 and at  $25^\circ\text{C}$ .



Micrograph 24.  
Copper(II) oxide conditioned with  
SALO for 40mins at pH 4,0 and at 25°C.



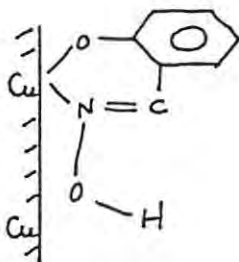
Micrograph 25.  
Copper(II) oxide conditioned with  
5-SALO for 40mins at pH 4,0 and at 25°C.



Micrograph 26.  
Copper(II) oxide conditioned with  
5-SALO.

D.3.b.v) Infra-red study

Cecile et al <sup>17-20</sup> have studied in detail the infra-red spectra of SALO species adsorbed on a high surface area sample of malachite. At a low surface coverage they detected absorption peaks at positions similar to those of the 1:1 basic copper salicylaldoximate precipitate. At higher surface coverages they found that there was good agreement between the spectra of the adsorbed species and the 1:2 copper salicylaldoximate precipitate. Since the major difference between the 1:1 and 1:2 precipitates was caused by the loss of the oximic hydrogen, they concluded that the SALO adsorbed initially as shown below.



They considered that there was some form of interaction between the oximic hydroxyl group and the surface which caused a shift of the N-O stretching bands to the higher energies associated with the basic species.

In the present study experiments were conducted on copper(II) oxide with the view to confirming whether the same interaction occurred. It was found necessary to

increase the surface area to  $2,18 \text{ m}^2/\text{g}$  in order to detect absorption peaks at low surface coverage. This surface area was still very much lower than the  $50 \text{ m}^2/\text{g}$  material used by Cecile<sup>17-20</sup>. The data from an infra-red investigation of the copper(II) - SALO system are shown in figure 34 and table 18. The following spectra are illustrated.

- a)  $\text{Cu}(\text{SALO})_2$ . A copper(II) sulphate solution was added to a SALO solution at pH 5 until a precipitate formed.
- b)  $\text{Cu}(\text{SALO})\text{OH}$ . A copper(II) sulphate solution was added to a SALO solution at pH 11 until a dark green precipitate formed.
- c) Copper(II) oxide (surface area  $2,18 \text{ m}^2/\text{g}$ ) was added to a  $2,5 \times 10^{-4} \text{ mol.l}^{-1}$  SALO solution at neutral pH and at  $20^\circ\text{C}$ . Complete adsorption of the SALO would have given an adsorption density of  $11 \times 10^{-10} \text{ moles.cm}^{-2}$ . This low coverage approximates the amount required to form a monolayer of reagent on the oxide surface.
- d) Copper(II) oxide (surface area  $2,18 \text{ m}^2/\text{g}$ ) was added to a  $1 \times 10^{-3} \text{ mol.l}^{-1}$  SALO solution at neutral pH and at  $20^\circ\text{C}$ . The amount of SALO adsorbed of approximately  $45 \times 10^{-10} \text{ moles.cm}^{-2}$  was equivalent to multilayer coverage.

In addition, the possible assignments as given by Ramaswami<sup>73</sup> for  $\text{Cu}(\text{SALO})_2$  are given in table 18.

The spectra in these cases were adjusted to take account of the varying background in order to increase the visual clarity.

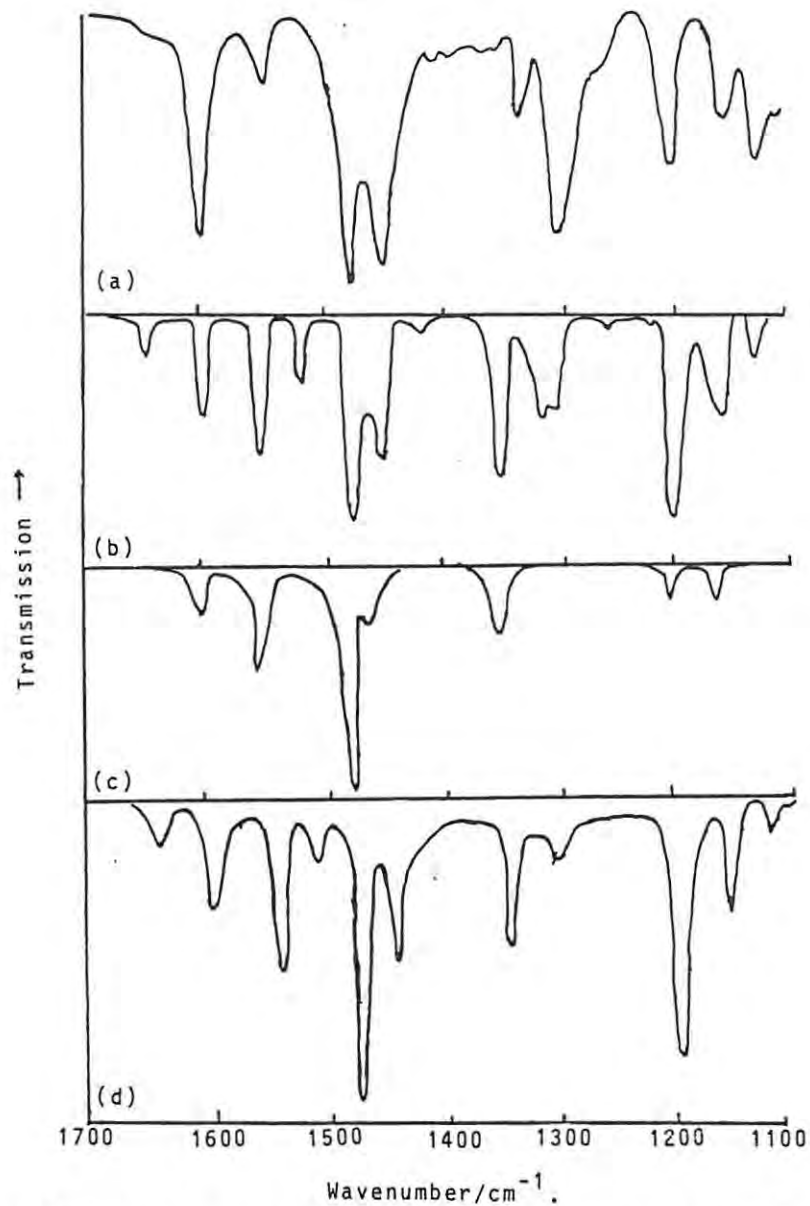


Fig.34, Infra-red spectra of copper(II) oxide treated with Salicylaldoxime.

- a)  $\text{Cu}(\text{SALO})_2$ , b)  $\text{Cu}(\text{SALO})\text{OH}$ , c)  $\text{CuO}$ -adsorbed SALO/low coverage
- d)  $\text{CuO}$ -adsorbed SALO/high coverage.

Table 18.

Infra-red spectra of copper(II) oxide conditioned with salicylaldoxime.

Bis-salicyl- aldoximato- Cu(II).	Mono-salicyl- aldoximato- Cu(II).	Low coverage	High coverage	Possible assignment
1645(s)			1650	OH deform. vib. C-N stretch coupl with C-C stretch.
1600(s)	1599(vs)	1600	1600	
1545(vs)	1545(s)	1550	1545	
1510(s)			1512	Ortho disubst. benzene.
1470(vs)	1475(vs)	1470	1470	
1445(vs)	1440(vs)	1450	1445	
1405(w)	1400(s)			
	1380(s)			
	1355(s)			CH vibr. in plane
1335(vs)	1325(s)	1340	1340	
1303(s)				
1290(s)	1290(vs)		1305	
1250(w)	1250(w)			
1215(w)				N-O stretch.
1190(vs)	1195(a)		1195	

vs=very strong, s=strong, w=weak.

The results show that there was a very good correlation between the infra-red absorption peaks of the surface species present on copper(II) oxide with a high surface coverage of SALO and the bis-SALO copper(II) complex. The only peaks of the bis-complex that were not observed were those of weak intensity. However, at low surface coverages the absorption peaks of the bis complex at  $1650\text{ cm}^{-1}$  and  $1510\text{ cm}^{-1}$  were not detected. These peaks were also not observed for the 1:1 basic copper complex and were probably associated with the presence of the N-OH bonds. There was no complete agreement between the 1:1 complex and the surface species since the peaks at  $1400\text{ cm}^{-1}$ ,  $1380\text{ cm}^{-1}$  and  $1290\text{ cm}^{-1}$ , for instance, were not detected. In addition, some of the wavelength positions were slightly shifted.

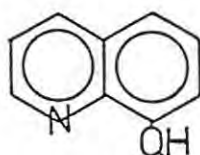
It has been previously shown that it was possible to identify isolated patches of precipitate on the surface of copper(II) oxide which had been treated with SALO to generate a theoretical monolayer coverage. This evidence would appear to eliminate the simple monolayer coverage of SALO concept as was envisaged by Cecile.<sup>17-20</sup> The change in the absorption spectra of the surface species on moving from the first few layers to many layers could result from a structural change in the bis-SALO precipitate. The copper(II) oxide surface could constrain the development of the precipitate and thus force the development of a crystal lattice not usually

adopted. Subsequent growth would occur in the most favourable form which would be similar to the precipitate generated from copper and SALO solutions.

D.3.c) 8-HYDROXYQUINOLINE

D.3.c.i) General features

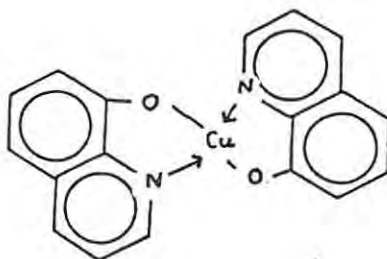
The class of compounds containing a hydroxyl group and a heterocyclic nitrogen atom capable of forming a 5- or 6-membered chelate ring with metal ions have proved useful as analytical reagents.<sup>74</sup> The most important of these is 8-hydroxyquinoline, commonly known as oxine.



Oxine has been used in the gravimetric analysis of copper solutions. It is claimed that this reagent quantitatively precipitates copper ions from solution over the pH range 2,7 to 14,4.<sup>74</sup> It has also been used in the solvent extraction of metal ions from solution. In fact the major constituent of the commercial Kelex type copper extractants is oxine.<sup>75</sup>

The reaction between oxine and copper in aqueous solution produces the hydrated complex;  $\text{Cu}(\text{Ox})_2 \cdot 2\text{H}_2\text{O}$ . In this complex the two oxine ligands form a square around copper with the two water molecules taking up axial positions.<sup>76</sup>

An anhydrous version of copper oxinate can be produced by heating the hydrate at  $110^\circ\text{C}$ . This form of  $\text{Cu}(\text{Ox})_2$  has the ligands bound in a plane to the copper:



Weak bonding to the oxygen atoms of adjacent molecules completes the distorted octahedral co-ordination <sup>77</sup>. (this is a similar structure to  $\text{Cu}(\text{SALO})_2$ ). If the form is heated at above  $200^\circ\text{C}$  it rearranges to a more stable form. This modification has the ligands in a trans configuration around the metal but the arrangement is not co-planar since the nitrogen atoms are twisted out of plane to allow approach of the fifth ligand, an oxygen atom from a second molecule of  $\text{Cu}(\text{Ox})_2$ . This gives copper a rather distorted square pyramidal configuration and the structure can be regarded as containing essentially isolated dimer units. <sup>78</sup> The form is also recovered from chloroform extracts of the copper oxinate.

#### D.3.c.ii) Metal-species distribution

A recent review of 8-hydroxyquinoline has discussed and critically evaluated the published data on the dissociation and solubility of oxine and its metal chelate. <sup>59</sup> The values for the acid dissociation constant and the stability constant of the copper complex were extracted from this review. The values are listed in Table 19.

Table 19.

Equilibrium constant data at 25°C used in calculation of the copper-8-hydroxyquinolate species distribution (fig.32).

A refers to oxinate.

Equilibrium	Type	Value	Medium
$H_2A \rightleftharpoons H^+ + HA^-$	$pK_1$	5,02	0,9KCl
$HA \rightleftharpoons H^+ + A^-$	$pK_2$	9,70	0,9KCl
$Cu^{2+} + A^- \rightleftharpoons CuA^+$	$\log\beta_1$	12,10	0,1 Na <sup>+</sup>
$Cu^{2+} + 2A^- \rightleftharpoons CuA_2$	$\log\beta_2$	23,00	0,1 Na <sup>+</sup>
$CuA_2(Solid) \rightleftharpoons CuA_2(Soln.)$	pS	6,48	0,1 Na <sup>+</sup>

The species distribution (fig. 35) for different total metal and ligand concentrations could be derived using these data as was shown previously (see appendix).

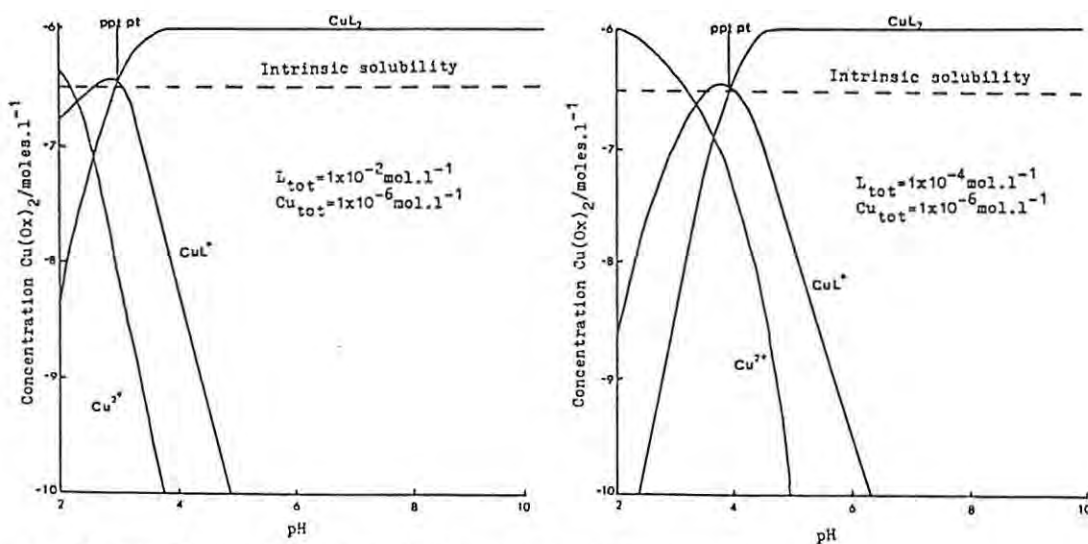


Fig.35 Species distribution for copper-8-hydroxyquinoline complexes at different total metal and ligand concentrations.

The following important features are noteworthy :

- a) The  $\text{CuL}^+$  species is important at low pH values.
- b) The pH at which the amount of  $\text{CuL}_2$  exceeds the intrinsic solubility, ie. the precipitation point, changes from 3,8 for solutions with a ligand to copper ratio of  $10^2$  to pH 2,6 for a solution with a ligand to copper ratio of  $10^4$ .
- c) Oxine does not form a soluble metal complex species at high pH values.

It is beneficial to the understanding of the adsorption characteristics of the organic ligands studied to compare the  $\log \beta_2$  values. This gives another measure of the complexing ability of the ligand for copper ions. (Table 20).

Table 20

Comparison between  $\log \beta_2$  values  
for copper-chelate complexes.

Ligand	$\log \beta_2$
N-phenylbenzohydroxamate	15,49
Salicylaldoxime	15,20
8-hydroxyquinoline	23,00

The magnitude of the value for oxine is very much greater than either of the other two chelating reagents.

One therefore expects differences in the rate of formation of the bis-chelate precipitates on copper(II) oxide surfaces at high pH values.

D.3.c.iii) Adsorption isotherms

The adsorption of oxine by copper(II) oxide was studied at different pH values and temperatures. In addition, the effect of the surface area of the oxide and the presence of a dispersing agent was investigated. Previous results had indicated that for chelate-copper(II) oxide interactions, it was possible to account for all the adsorption in terms of the formation of the bis-chelate precipitate. Consequently, in the derivation of the adsorption isotherms for the oxine-copper(II) oxide system the amount of  $\text{Cu}(\text{Ox})_2$  was determined.

D.3.c.iii) 1. Time

The rate of formation of  $\text{Cu}(\text{Ox})_2$  depended on both the pH of the solution and the surface area of the oxide. The concentration of  $\text{Cu}(\text{Ox})_2$  formed at  $20^\circ\text{C}$  on copper(II) oxide (surface area  $0,07 \text{ m}^2/\text{g}$ ;  $1,0 \text{ g}$ ) from a) Oxine ( $1 \times 10^{-3} \text{ mol.l}^{-1}$ ,  $100 \text{ ml}$ ) at pH 3,5 and b) Oxine ( $1 \times 10^{-3} \text{ mol.l}^{-1}$ ,  $100 \text{ ml}$ ) at pH 9,25 is shown in fig 36. The concentration of  $\text{Cu}(\text{Ox})_2$  formed at  $20^\circ\text{C}$  on copper(II) oxide (surface area  $0,17 \text{ m}^2/\text{g}$ ;  $1,0 \text{ g}$ ) from c) Oxine ( $1 \times 10^{-3} \text{ mol.l}^{-1}$ ,  $100 \text{ ml}$ ) at pH 3,5, and d) Oxine ( $1 \times 10^{-3} \text{ mol.l}^{-1}$ ,  $100 \text{ ml}$ ) at pH 9,25 is shown in fig. 37.

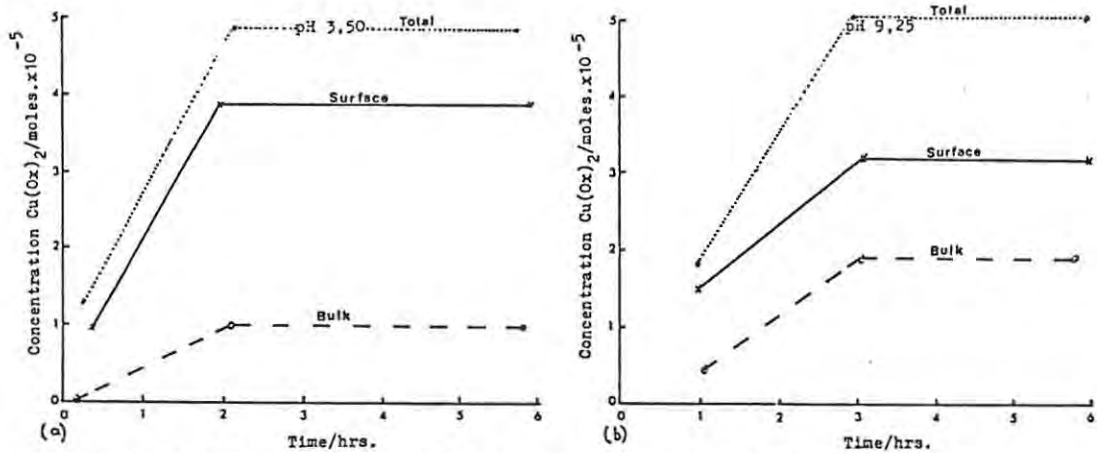


Fig.36: Relative rate of formation of copper oxinate at the oxide surface and in the bulk<sub>2</sub> solution. Copper(II) oxide(surface area 0,07 m<sup>2</sup>/g).

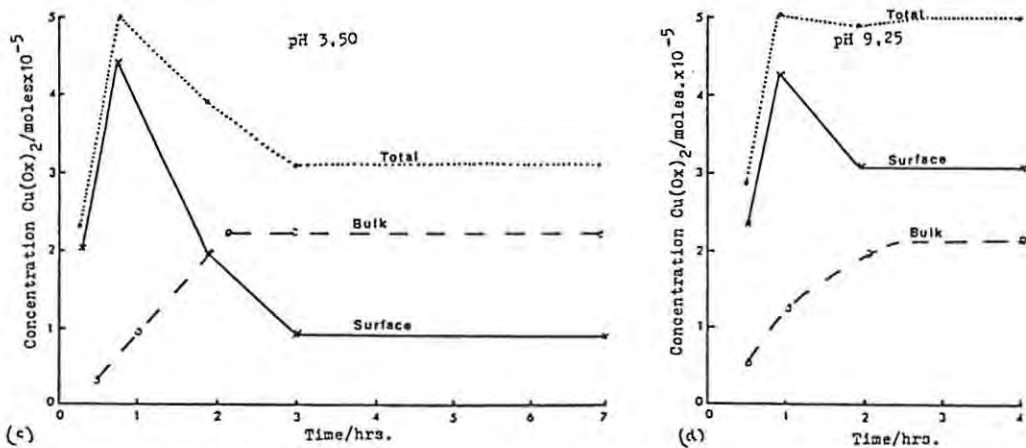


Fig.37: Relative rate of formation of copper oxinate at the oxide surface and in the bulk solution. Copper(II) oxide(surface area 0,17m<sup>2</sup>/g). The experimental details are referred to in the text.

The following important features were noted :-

a) Copper(II) oxide sample (surface area 0,07 m<sup>2</sup>/g).

1. The total concentration of copper oxinate formed increased with time until all the reagent was consumed. The eventual concentration of  $5 \times 10^{-5}$  moles of  $\text{Cu}(\text{Ox})_2$  corresponded to an equivalent of approximately 200 layers of chelate. Further conditioning at either pH 3,50 or pH

9,25 did not affect the concentration of copper oxinate on the surface or in the bulk solution.

2. The rate of formation of total chelate was greatest at acidic pH values hence  $5 \times 10^{-5}$  moles of  $\text{Cu}(\text{Ox})_2$  were produced in 2 hours at pH 3,50 and in 3 hours at pH 9,25.

3. The concentration of surface chelate exceeded the concentration of bulk chelate at both pH values. However, the relative ratio between the surface and bulk chelate changed from 3,90 at pH 3,50 to 1,68 at pH 9,25. The actual concentration of bulk chelate detected at pH 3,50 corresponded to 40 layers of chelate. At pH 9,25 this value increased to an equivalent of 80 layers of chelate.

b) Copper(II) oxide sample (surface area  
0,17 m<sup>2</sup>/g)

1. In the initial stages of the conditioning process at pH 3,50 the concentration of total chelate produced, increased rapidly. This process continued until the reagent concentration had dropped to a very low value. At this stage most of the chelate was recorded as surface chelate. Subsequent further conditioning of the oxide resulted in a decrease in the concentration of total chelate and of surface chelate. At the same time the concentration of bulk chelate increased, such that it eventually exceeded the concentration of surface chelate.

The ratio between surface and bulk chelate changed from 6,0 after 1 hour to 0,45 after 3 hours. The significant decrease in the concentration of the total chelate suggests that under these conditions some of the precipitate of  $\text{Cu}(\text{Ox})_2$  redissolves. The species distribution diagram indicates that the soluble species,  $\text{Cu}(\text{Ox})^+$ , is important at acidic pH values. It is therefore considered possible that the continued release of copper ions at pH 3,5 caused the mono species to become more stable than the bis complex. This feature and the change in the relative ratio between the bulk and surface chelate will be discussed later.

2. At pH 9,25 the rate of the total precipitation of  $\text{Cu}(\text{Ox})_2$  was again a relatively rapid process that continued until the reagent was nearly totally consumed. Subsequent further conditioning was found to have no effect on the total concentration of  $\text{Cu}(\text{Ox})_2$  but it did have an effect on the ratio between the surface and bulk chelate. The ratio decreased from 4,3 after 1 hour conditioning to 1,4 after 2 hours. The decrease in surface chelate can not be attributed to the dissolution of the precipitate. Other factors which will be discussed later were considered to be responsible.

3. There was significantly more bulk chelate detected at pH 3,5 in the experiments with the higher surface area oxide. At pH 9,25 the final concentration of bulk chelate was approximately the same in both cases.

D.3.c.iii) 2. pH

The variation in the overall concentration of  $\text{Cu(Ox)}_2$  produced in the copper(II) oxide-oxine system after a 2 hour conditioning period at different pH values is reflected in fig. 38.

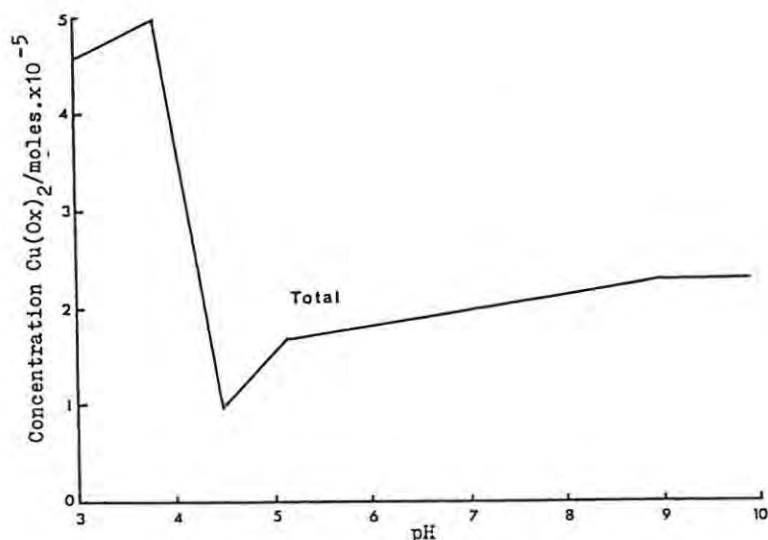


Fig.38. The variation with pH in the total amount of copper oxinate produced after a 2 hr. contact between  $\text{CuO}(0,07\text{m}^2/\text{g})$  and oxine solution ( $1 \times 10^{-3} \text{mol.l}^{-1}$ ) at  $20^\circ\text{C}$ .

The following features were evident :-

- 1) The rate of precipitation was at a maximum at pH 3,5.
- 2) At more acidic pH values the rate decreased to some degree.
- 3) At more basic pH values the rate decreased significantly to a minimum at pH 4,5. Further pH increase caused the rate to gradually increase through to pH 10,0.
- 4) The adsorption isotherm resembled the hydroxamate and salicylaldoximate system in the acidic regions. It differed at higher pH values in that the rate of

precipitation was greatest at pH 10,0.

The adsorption data can be explained in terms of the model discussed previously for the hydroxamate system. In summary, this model suggested that the isotherm could be subdivided in four pH regions :

1) A region (very low pH values) in which soluble copper complexes are found. These species do not adsorb on the oxide.

2) A region (between pH 3,5-4,5) in which  $\text{CuL}_2$  precipitates rapidly. The rate of precipitation is controlled by the rate of release of metal ions.

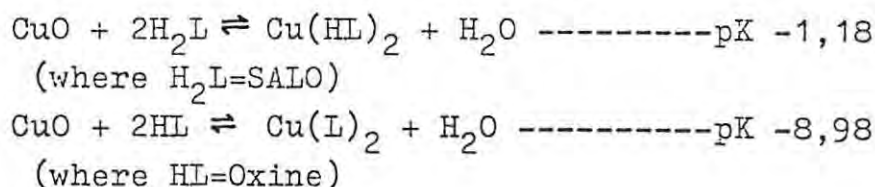
3) A region (between pH 5,0-8,0) in which the precipitation of  $\text{CuL}_2$  is somewhat slower. The precipitation rate usually exceeds the rate of release of copper ions from blank solutions. The rate is rather controlled by the degree of solubility of the precipitate.

4) A region (above pH 8,0) in which the reagent and hydroxyl ions compete for copper ions.

In the case of the oxine data the presence of region 1 can be inferred from the species distribution diagram. The soluble species,  $\text{Cu(Ox)}^+$  and  $\text{Cu}^{2+}$  predominate at pH values below 3 and at low  $L_{\text{TOT}} : \text{Cu}_{\text{TOT}}$  ratios. The precipitation point of  $\text{Cu(Ox)}_2$  as read from the species distribution diagrams for a total reagent concentration of  $1 \times 10^{-2} \text{ mol.l}^{-1}$  were ; NPBA pH 4,7, SALO pH 4,2, Oxine

pH 3,2 and 5NSALO pH 2. Region 2 was therefore expected to extend to lower pH values for oxine and 5NSALO than for NPBA or SALO.

Oxine differs from the other reagents in that region 3 and 4 are combined. The complexing ability of oxine for copper ions as is reflected in the formation constants given in Table 20 is significantly greater than the other reagents. Oxine is thus more readily bonded to copper than hydroxyl ions at high pH values. This can be re-illustrated by the comparison between the solubility of the oxide and the precipitates of  $\text{Cu}(\text{SALO})_2$  and  $\text{Cu}(\text{Ox})_2$  as shown below.



The equilibrium constant for the dissolution of the oxide and the formation of the precipitate is much greater in the case of oxine.

#### D.3.c.iii) 3. Temperature

The overall rate of formation of precipitate was again found to be temperature dependent (fig.39).

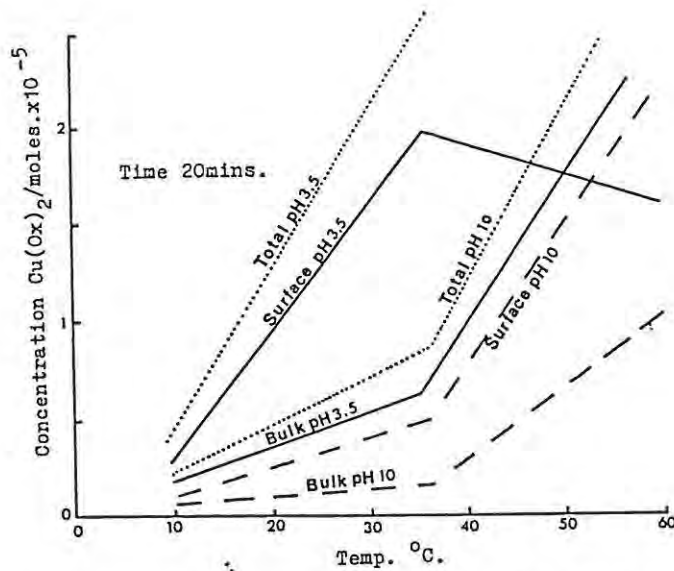


Fig.39. The variation with temperature in the concentration of copper oxinate formed (bulk and surface) from the  $\text{CuO}$ -Oxine system.

However, in this case at pH 3,5 the ratio between the concentration of surface and bulk chelate changed significantly at higher temperatures. The ratio changed from 3,25 at  $25^{\circ}\text{C}$  to 0,77 at  $55^{\circ}\text{C}$ . At pH 10,0 there was no change in the ratio of bulk to surface chelate. It is considered that the reason for the change in the tendency to form bulk and surface chelate is connected to the structure of the precipitate formed. This aspect is discussed later in section D.3.c.v) 3.

D.3.c.iii) 4. Dispersing reagents

The addition of gum arabic to the chelating reagent solution at pH 9,25 was found to reduce the formation of surface chelate and at the same time to increase the concentration of bulk chelate, fig.40. The extent to which the concentration of surface chelate was reduced was linearly related to the concentration of gum arabic added. In addition, the presence of gum arabic appeared to increase the overall concentration of copper oxinate produced at this pH. At pH 3,50 the concentration of surface chelate was also reduced by gum arabic addition to the conditioning solution. However, in this case the extent of reduction for equivalent concentrations of gum was more severe. This suggests that gum arabic coats the surface and reduces nucleation of the precipitate at the oxide surface. Heterogeneous nucleation requires the presence of another surface to assist in the overcoming of the energy barrier required to bring molecules together to form nuclei. Gum arabic could act by adsorbing at the high energy sites on the oxide surface, eg. dislocations etc., and could thus reduce nucleation of the precipitate at these points.

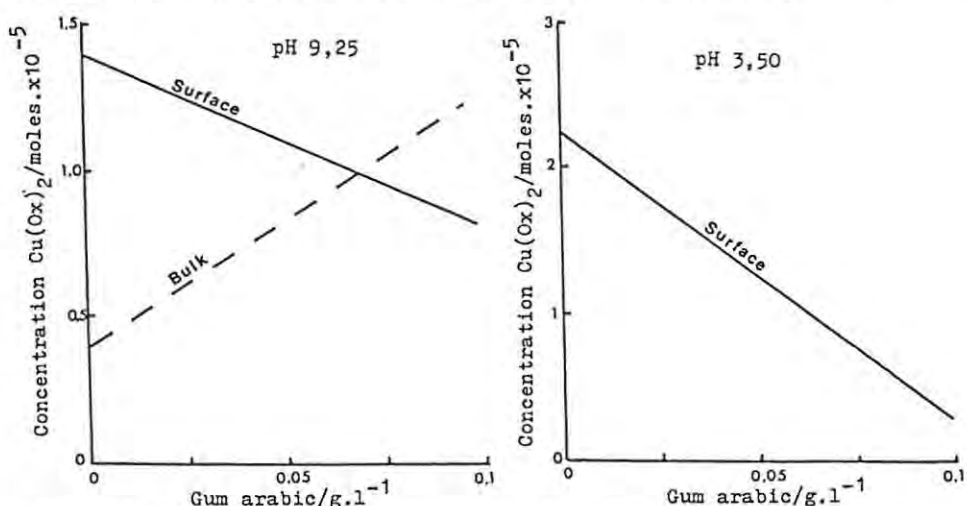


Fig. 40. Adsorption of 8-hydroxyquinoline by CuO in the presence of gum arabic. CuO(0,17m<sup>2</sup>/g, 1,0gm) Oxine(1x10<sup>-3</sup>mol.l<sup>-1</sup>, 100mls) time 30mins, temp. 20°C

D.3.c.iii) 5. Discussion

The model for the adsorption process as developed up to this stage can account reasonably well for the variations in the overall metal-chelate precipitate formation. However, it does not offer an adequate explanation for the formation of bulk and surface chelate. In addition, the model cannot be used to understand the change in the ratio between bulk and surface chelate with conditioning time. It was necessary to consider the results of infra-red spectroscopic data and S.E.M. data in order to rationalise these features.

D.3.c.iv) Infra-red spectroscopic study

An attempt was made with the aid of infra-red spectroscopy to confirm the chemical nature of the adsorbed species on copper(II) oxide conditioned with oxine. In this regard, the literature spectra were consulted, the spectra of freshly precipitated and aged precipitate measured, and the spectra of the adsorbed species on a high surface area material determined.

D.3.c.iv) 1. Copper oxinate precipitates

An attempt was made with the aid of infra-red spectroscopy to confirm the chemical nature of the adsorbed species on copper(II) oxide conditioned with oxine solution ( $1 \times 10^{-3}$  mol.l<sup>-1</sup>, pH 10). In one case the precipitate was separated rapidly from solution by filtration (called freshly precipitated material), whereas in the other case the precipitate was kept in contact with the solution for

2 hours (called aged precipitate). The infra-red spectra of these solids were measured as KBr discs. Some parts of the spectra are represented in fig. 41.

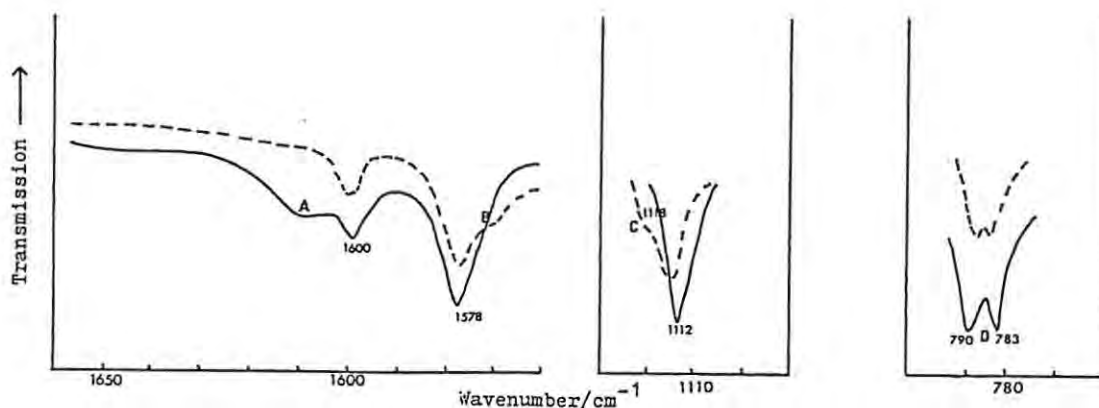


Fig. 41. Infra-red spectra of copper oxinate precipitates.  
 ----- refers to fresh precipitate  
 ——— refers to aged precipitate

The sample of aged copper oxinate differed from the freshly precipitated material in that i) a broad band appeared at A, ii) the splitting of the band at B disappeared, iii) the shoulder on the band at C disappeared and iv) there was a larger separation between the peaks between  $791\text{ cm}^{-1}$  and  $783\text{ cm}^{-1}$ . It was suspected that the broad band at A was associated with a hydroxyl group which would indicate that the spectral changes could be due to the hydration of the copper oxinate. In this regard the infra-red spectra of the literature data on the hydrated species,  $\text{Cu}(\text{Ox})_2 \cdot 2\text{H}_2\text{O}$ , and the anhydrous version,  $\text{Cu}(\text{Ox})_2$ , were consulted.<sup>79</sup> The details of the spectra over the same wavenumber range are represented in table 21.

Table 21.

Literature data<sup>79</sup> for infra-red spectra of copper oxinate precipitates. (Wavenumber/cm<sup>-1</sup>)

Cu(Ox) <sub>2</sub>	Cu(Ox) <sub>2</sub> ·2H <sub>2</sub> O
785	781
	788
804	805
819	818
1118	1109
1500	1495
1570	1560
1590	1590
	1610

A comparison between the above spectra and the spectra of fresh and aged precipitate led to the conclusion that the former resembled a mixture of the anhydrous and hydrated copper oxinates, whereas the latter was similar to the hydrated version. For example, the peak at 1118 cm<sup>-1</sup> associated with the anhydrous version occurred as a shoulder in the spectrum of the fresh precipitate but not at all in the spectrum of the aged version. In addition, the splitting between the peaks which occurred between 791 cm<sup>-1</sup> and 783 cm<sup>-1</sup> increased from 5 cm<sup>-1</sup> to 7 cm<sup>-1</sup> probably because of the decrease in the intensity of the anhydrous peak at 785 cm<sup>-1</sup>.

D.3.c.iv) 2. Copper(II) oxide (surface area 2,18 m<sup>2</sup>/g)-  
Oxine system.

A sample of the original oxide was ground further in an agate mortar in order to increase the surface area of the material. A high surface area material was required for this experiment because it was intended to study the species adsorbed initially. The concentration adsorbed by the original oxide (SA = 0,07 m<sup>2</sup>/g) was so low that it was only detectable after the material had been in contact with the solution for some time.

The infra-red spectrum of a copper(II) oxide sample conditioned briefly (< 5 mins) with a 1x10<sup>-3</sup> mol.l<sup>-1</sup> oxine solution at pH 10 was identical to the spectrum obtained for the anhydrous copper oxinate precipitate.

D.3.c.iv) 3. Copper(II) oxide (surface area 0,07 m<sup>2</sup>/g) -  
Oxine system

Copper(II) oxide was conditioned 2 hours at pH 10 with a 1x10<sup>-3</sup> mol.l<sup>-1</sup> oxine solution. The adsorbed surface species was again found to resemble the anhydrous species, Cu(Ox)<sub>2</sub>, although in this case there was also evidence for the formation of some of the hydrated version. The I.R. spectrum of the bulk precipitate was different from the surface species in that it more closely resembled the hydrated species (fig.42 ).

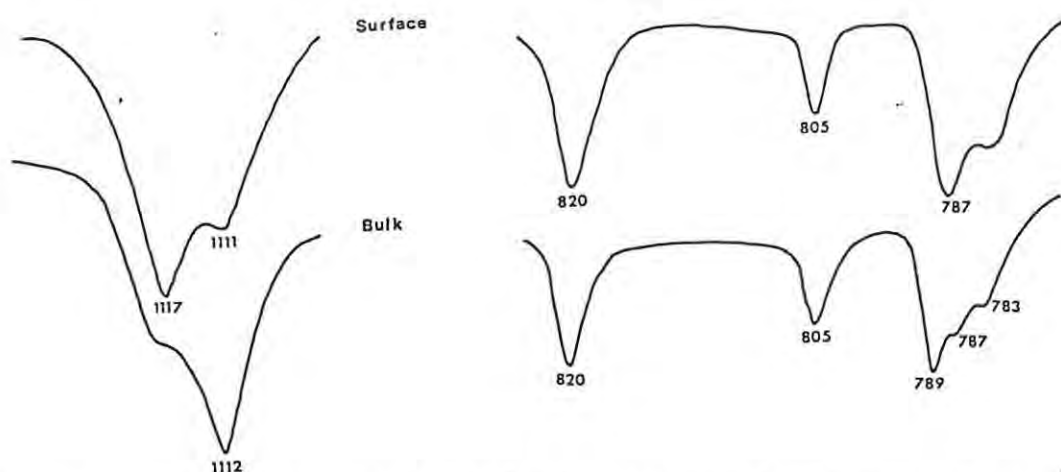


Fig.42. The infra-red spectra of bulk (or non-attached) and surface copper oxinate isolated from the CuO-Oxine system.

D.3.c.iv) 4. Discussion

The infra-red data on copper oxinate precipitates suggests that the initial precipitate formed from solution was the anhydrous version,  $\text{Cu}(\text{Ox})_2$ , and that this species then slowly hydrated to form  $\text{Cu}(\text{Ox})_2 \cdot 2\text{H}_2\text{O}$ . In a similar fashion it was shown that the species formed initially in the copper(II) oxide- Oxine system was the anhydrous version and that this species also subsequently became partially hydrated. It is considered feasible that this hydration of the copper oxinate could be responsible for the significant increase in the bulk-chelate and the decrease in the surface-chelate which was noted in some experiments when the oxide was conditioned for an extended period. Hydration of surface species could result in their detachment because this process probably involves a rearrangement in crystal structure which causes a rupture of the bonds responsible for the attachment of the precipitate to the surface. This possibility was investigated further with the aid of the scanning electron microscope.

D.3.c.v) Scanning electron microscope study

The scanning electron microscope was used to determine the physical appearance of the precipitate on the oxide surface. In this study it was hoped to be able to distinguish the reason for the detachment of surface chelate from high surface area material and not from lower surface area material (see fig. 36,37).

D.3.c.v) 1. Low surface area copper(II) oxide investigation (surface area 0,07 m<sup>2</sup>/g).

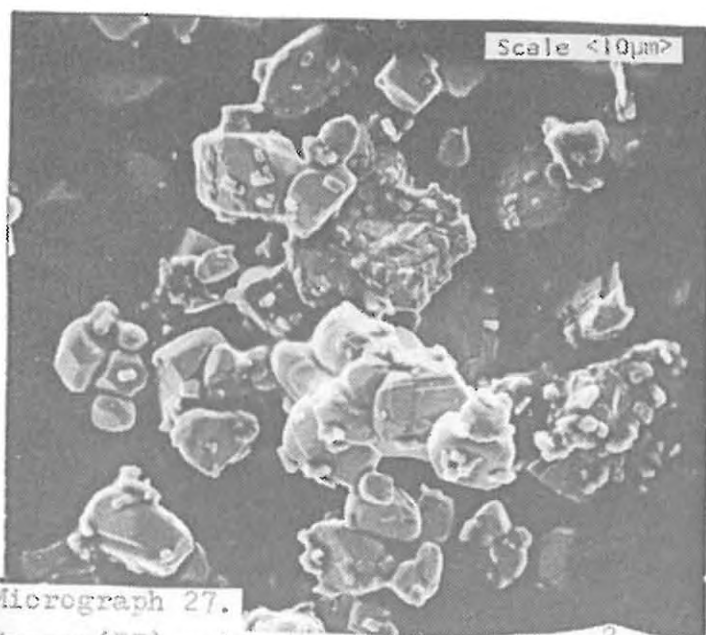
The oxide was treated with  $1 \times 10^{-3}$  mol.l<sup>-1</sup> oxine solution at pH 3,5 for 30 mins. At a magnification of only 1000 times, relatively large hexagonally shaped platelets were visible on the oxide surface (micrograph 27,28). Some of the platelets were very well formed but they only occurred in isolated patches on the oxide surface with the result that large areas of the oxide were unaffected by the crystal growth.

D.3.c.v) 2. High surface area copper(II) oxide investigation (surface area 0,07 m<sup>2</sup>/g).

a) The oxide was treated with a  $1 \times 10^{-3}$  mol.l<sup>-1</sup> oxine solution at pH 3,5 for 30 minutes (micrographs 29,30). The following features were noted under the S.E.M.,

- 1) the oxide particles tended to adhere together to form aggregates (micrograph 29), and
- 2) three types of surface growth were visible, (micrograph 29).

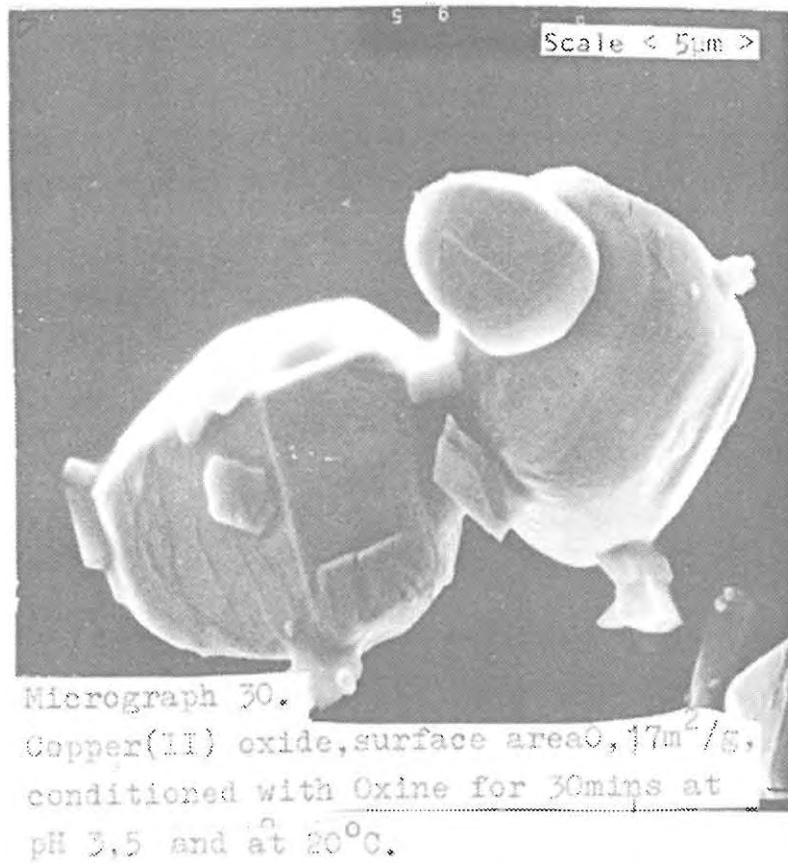
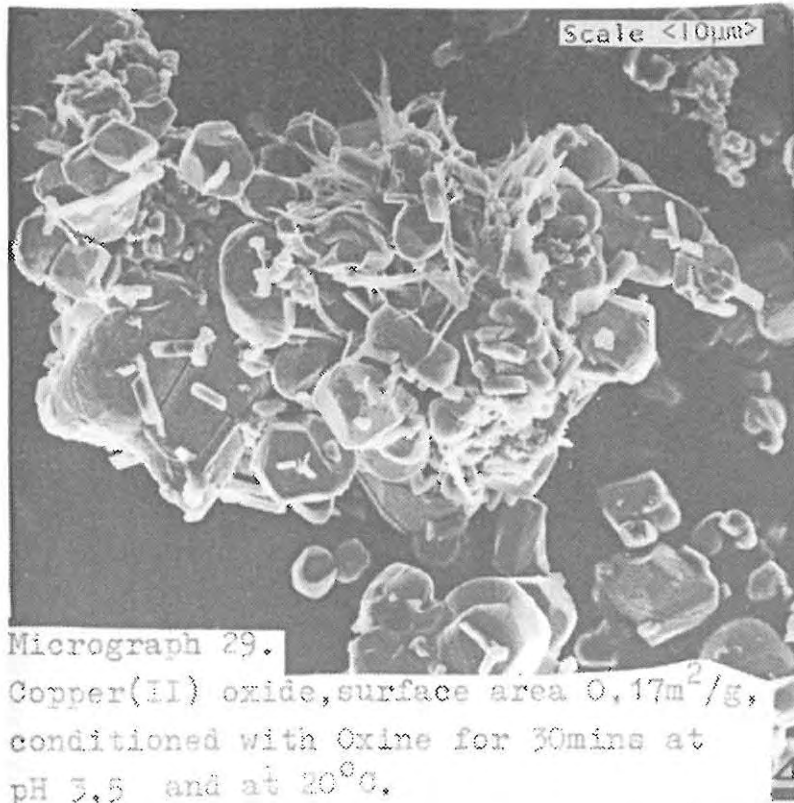
- i) hexagonally shaped crystallites, similar to those detected in micrograph 27.
  - ii) a fibrous type growth which appeared to grow across the surface. This feature is enlarged in micrograph 30, and
  - iii) a whisp-like feature that appeared to grow away from the particle surface (micrograph 29).
- b) The same oxide sample was viewed again under the S.E.M except in this case, the oxide was treated for 4 hours in a  $1 \times 10^{-3}$  mol.l<sup>-1</sup> oxine solution at pH 3,5. It was noted that most of the precipitate had disappeared from the surface and only minor amounts of the hexagonally shaped platelets remained (micrograph 31).

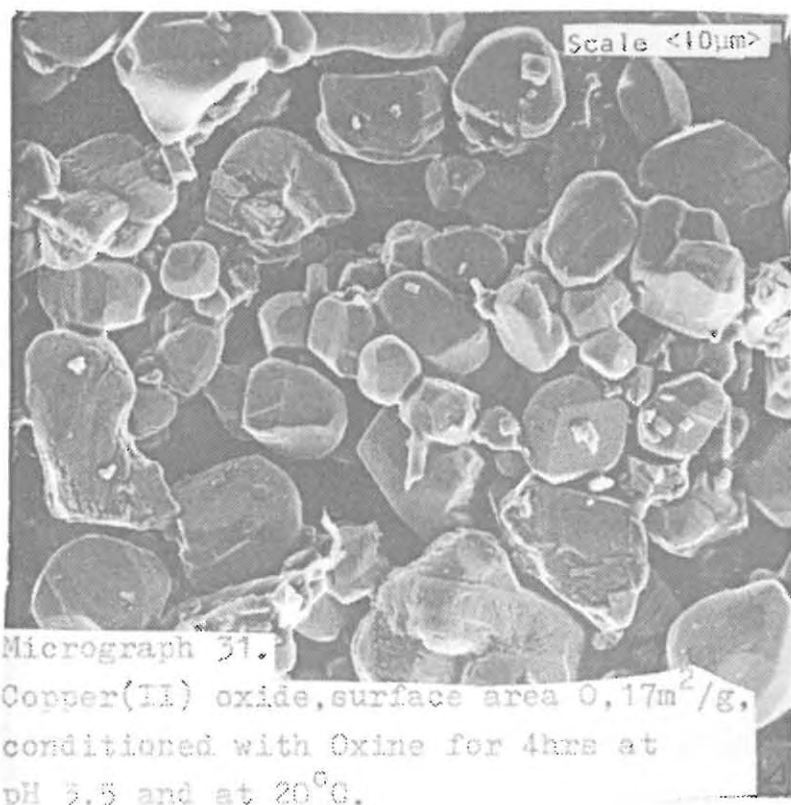


Micrograph 27.  
Copper(II) oxide, surface area  $0,07\text{m}^2/\text{g}$ ,  
conditioned with Oxine for 2hrs at pH 3,5  
and at  $20^\circ\text{C}$ .



Micrograph 28.  
Copper(II) oxide conditioned with Oxine  
for 2hrs at pH 3,5.





### 3. Discussion

When the rate of precipitation of  $\text{Cu}(\text{Ox})_2$  on the oxide was slow, then well formed, hexagonally shaped platelets were formed. These platelets did not appear to detach from the surface easily, possibly because :

- a. they were relatively large and therefore hydrated slowly (the infra-red evidence had suggested that copper oxinate precipitates hydrate with time) or
- b. they were grown slowly and therefore were more intimately associated with the surface.

However, in the case where precipitation was rapid, as for when a high surface area oxide was used, then other physical forms of copper oxinate were preferred. It is suggested that these, forms eg. the fibrous form, were not as stable with regard to remaining attached to the surface. This could possibly be due to the higher surface area of the fibrous form which would therefore hydrate relatively rapidly. It could also be due to the fact that the rapid nature of the precipitation excluded intimate attachment of the precipitate to the oxide surface.

It was concluded that at this stage the model for chelate adsorption on copper(II) oxide had to be extended to include a factor which would take account of the structural type of precipitate formed. With this in mind some of the factors which control metal-chelate precipitation were investigated in more detail.

#### E. METAL-CHELATE PRECIPITATION STUDIES

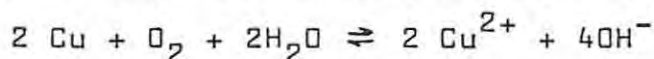
A more fundamental study of metal-chelate precipitation on copper(II) oxide was complicated by the fact that a variable such as pH, controlled both the oxide dissolution and also the formation of the precipitate. Consequently, it was extremely difficult to investigate the relationship between the amount of copper released from the oxide and the nature of the precipitate, and also to determine the factors responsible for the formation of bulk chelate. In order to do this, other systems were considered for which the control of copper release was to some extent independent of the pH. Copper metal was found to be the most suitable in this regard.

The factors which control the nucleation and crystal growth of a precipitate from solutions of the relevant species has been fairly well studied and theoretical models exist to account for most experimental data.<sup>80-82</sup>

There has also been some work reported on the precipitation onto an inert solid. However, there has been little work published on the formation of precipitates on solids, in which one of the species required to form the precipitate, comes from the solid itself. A novel way to study this phenomenon (in a practicable way) is to use a substrate which releases copper ions in a controlled manner.

In this regard copper metal is ideal because it oxidises

in an aqueous environment as follows: <sup>83</sup>



The release of copper ions from the metal at a set pH can be controlled by the variation in either the  $\text{O}_2$  content of the solution or the surface area of the metal.

### E.1. Precipitation from well stirred solutions

#### E.1.a) 8-Hydroxyquinoline

##### E.1.a.i) Polished copper metal

The amount of copper oxinate formed on highly polished copper metal after a 12 hour conditioning in well stirred oxine solution was measured. In addition, the surface of the metal was viewed under the S.E.M. in order to determine the precipitate morphology.

##### E.1.a.i) 1 Adsorption study

The relationship between the pH of the oxine solution and the amount of copper oxinate produced is shown in Fig. 43.

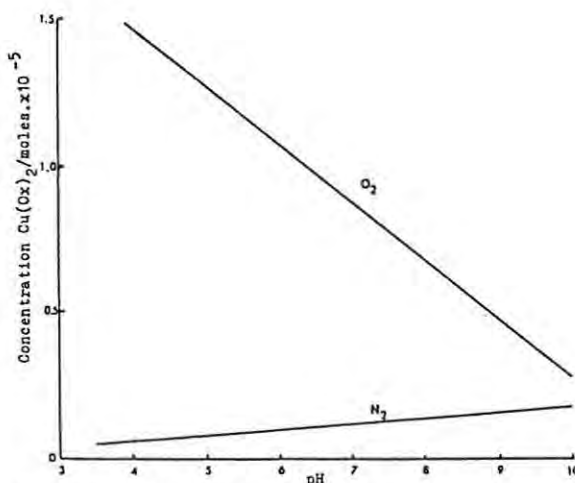


Fig. 43. Adsorption of 8-hydroxyquinoline on copper metal at various pH values.  
Oxine ( $1 \times 10^{-3} \text{mol.l}^{-1}$ , 250mls) time 12hrs, temp.  $20^\circ\text{C}$ .

The results clearly confirmed that it was possible to

control the release of copper ions and thus also to control the precipitation of copper oxinate. This experiment has simulated to some degree the conditions present in the low surface area oxide system because in both experiments the precipitation was controlled by the slow release of copper ions from the surface. It was also noted that no bulk chelate was detected in the copper metal experiment. Obviously, nucleation and crystal growth were favoured at the point of copper ion release.

E.1.a.i) 2 Scanning electron microscope study

Well formed, hexagonal shaped platelets of copper oxinate were formed on polished copper metal treated with oxine at either pH. These platelets grew from small nuclei into large crystallites that eventually covered the entire metal surface (micrograph 32,33).

E.1.a.ii) Etched copper metal

The surface area of the metal was increased by etching the metal surface with concentrated nitric acid. This treatment had the effect of increasing the rate of release of copper ions from the surface (although there was no direct evidence of an actual increase in  $\text{Cu}^{2+}$  it was inferred from the greater rate of precipitation of metal-chelate on the surface).

E.1.a.ii) 1 Adsorption study

The formation of metal-chelate precipitate on etched copper metal was found to be controlled by the concentration of the oxine and not by the amount of copper released (fig. 44).

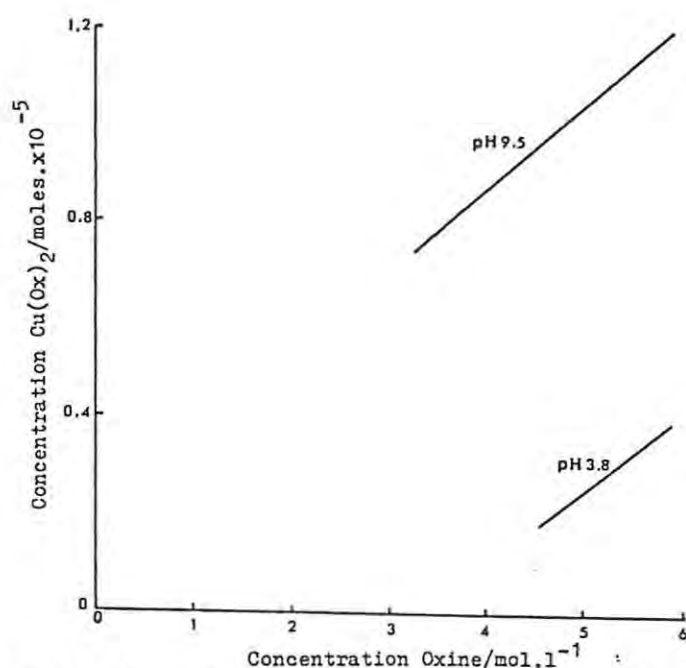


Fig.44. Adsorption of 8-hydroxyquinoline on copper metal at various oxine concentrations.  
Time 30mins, temp. 20°C.

This type of adsorption simulated the high surface area - oxine system. However, again there was no bulk chelate detected.

E.1.a.ii) 2 Scanning electron microscope study

There were significant differences in the crystal morphology of copper oxinate precipitates grown on etched copper metal. When acidic oxine solutions were used two types of crystal habit were adopted, viz. hexagonal platelets and fibrous (micrograph 34). The former habit

was identified in the previous experiment. However, when basic oxine solutions (and therefore higher concentrations of oxinate anion) were used only the fibrous type material was detected (micrograph 35). The physical appearance of the fibrous material was found to be dependent on the concentration of the oxine solution (micrograph 36). The higher the concentration of the oxinate anion the finer the fibres that grew on the metal. The finer fibres sealed the metal surface more effectively with the result that the total uptake of metal chelate by the metal was less than in the case of the coarser fibrous growth. This is illustrated in fig. 45.

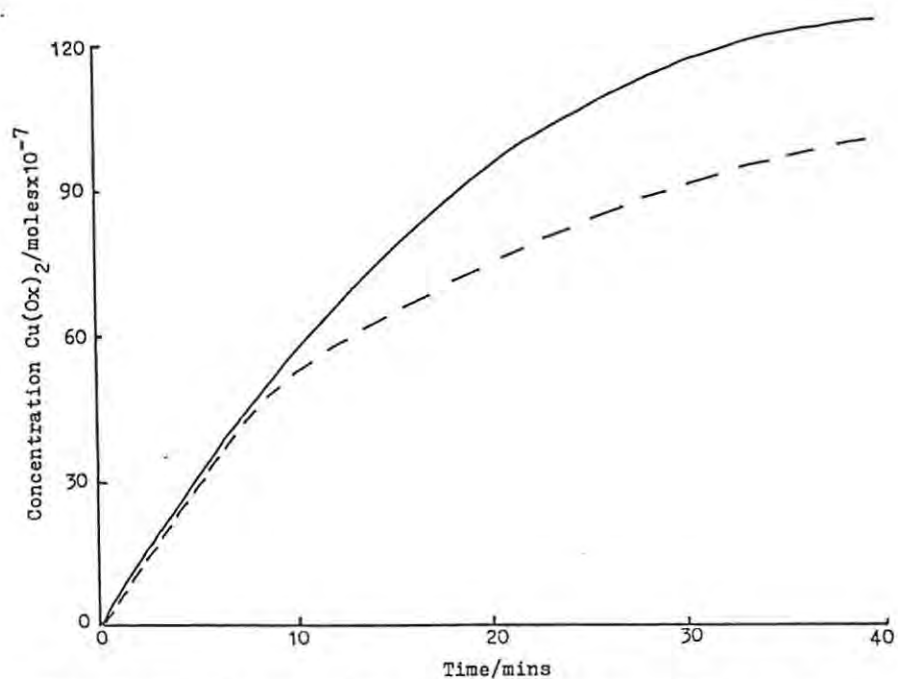
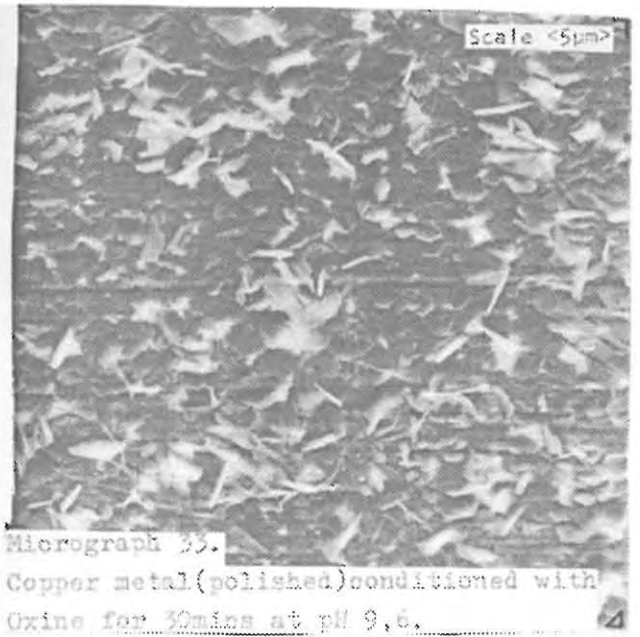
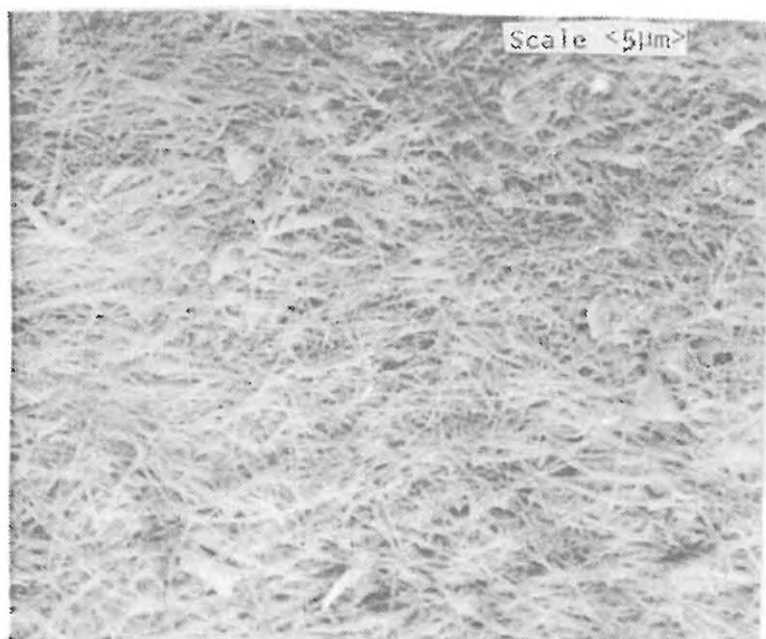


Fig. 45. Variation with time in the concentration of  $\text{Cu(Ox)}_2$  formed at pH 9,50 on copper metal.  
— refers to initial oxine concentration of  $5,7 \times 10^{-4} \text{ mol.l}^{-1}$   
----- refers to initial oxine concentration of  $2,0 \times 10^{-3} \text{ mol.l}^{-1}$





Micrograph 36.  
Copper metal (etched) conditioned with  
Oxine for 10 mins at pH 9,6 and at 25°C.



Micrograph 37.  
Copper metal (etched) conditioned with  
SALO solution at pH 7,5 for 1hr

E.1.b) Salicylaldoxime

The same type of experiments were conducted with SALO as the reagent. The precipitate of copper-salicylaldoximate on the metal always occurred as uniform, well-formed crystallites as shown in micrograph 37. There was no difference in the precipitate produced on polished and etched metal or from solutions at various pH's.

E.1.c) Conclusion

Walton has specified that the most important single feature in determining precipitate morphology is the degree of supersaturation.<sup>80</sup> At low degrees of supersaturation precipitation crystals are expected to be well formed, the shape depending on the crystallographic structure and surface energetics. At higher supersaturations growth is modified, high-energy planes emerging and dendritic crystals being produced. At high supersaturations colloidal phenomena are observed. It is possible to apply this theory to the results of the copper metal study and thus also to the oxide system. Well formed hexagonal platelets of copper oxinate should only be formed from solutions where the degree of supersaturation was low. This was indeed found to be the case because hexagonal crystals were noted only where the copper ion concentration was low (low surface area), and where the oxinate anion concentration was low. Fibrous type (equivalent to the dendritic form in the Walton model) precipitates were predicted to form only at higher

supersaturations, i.e. where the copper release or oxinate anion concentration was increased.

The fact that no colloidal phenomena were observed in these experiments (this would correspond to bulk chelate) could be caused by the fact that the supersaturation level never reached very high values.

The results of the SALO experiments can also be explained in terms of the degree of supersaturation. A lower supersaturation level was expected for SALO than for oxine since the  $\log \beta_2$  value (or solubility product) for the latter was much greater than the former. One therefore predicts that SALO would form well formed crystallites on copper metal and on copper(II) oxide surfaces.

#### E. 2. Diffusion controlled growth of precipitate

It was noted that when copper tubes were placed in well stirred oxine solutions that copper oxinate occurred only on the surface of the metal and not in the bulk of the solution. However, in experiments in which the tube was placed into undisturbed solutions bulk chelate was detected. Table 22 shows the distribution between bulk and surface chelate for undisturbed, oxygenated and aerated oxine solutions, and also for stirred solutions at two pH values after a 20 minute period.

Table 22.

Concentration of bulk and surface chelate (in moles  $\times 10^{-7}$ )  
produced on copper metal under various experimental conditions.

	pH 3,80		pH 9,50		Condition
	Bulk	Surface	Bulk	Surface	
Air	2,6	8,1	2,9	8,7	Non-stirred
O <sub>2</sub>	23,2	0,9	2,4	9,0	Non-stirred
Air	0,0	51,9	0,0	109,2	Stirred

At pH 9,50 precipitate formation was favoured on the surface of the metal, although a small amount did detach when the tube was removed from the solution. The crystal form of the precipitate was both as hexagonal platelets and as a fibrous form (micrograph 38).



However, when the tube was placed in non-stirred,

oxygenated solutions at pH 3,8 bulk chelate rather than surface chelate preferentially formed. The growth of this precipitate away from the surface was recorded photographically as shown below (photograph A and B).



Photograph A.  
Initial growth of  $\text{Cu}(\text{Ox})_2$  on  
copper metal.



Photograph B.  
Subsequent growth of  $\text{Cu}(\text{Ox})_2$   
on copper metal.

The diffusion layer around the copper cylinder was large because of the stationary nature of the solution. It is suggested that the relative diffusion rates of the metal ion and the oxinate anion species within this layer controlled whether the precipitate was recorded as surface or bulk chelate. At basic pH values there are two factors in favour of precipitation occurring on the surface. Firstly, at this pH the effective concentration of the oxinate anion was large and therefore the diffusion rate of oxinate to the surface was rapid enough to replace the concentration removed as the precipitate. Secondly, the diffusion of copper ions from the metal surface was restricted by the presence of excess hydroxyl

ions. However, at acidic pH values the concentration of oxinate anion was lower and so that at any one moment the diffusion rate of oxine to the surface was expected to be insufficient to replace the concentration of anion removed by the formation of the precipitate. In addition, the copper ions were not restricted from diffusing away from the surface. The net result of these factors was that crystal growth occurs in the direction of greatest concentration of oxinate anion which in this case was away from the surface.

A large diffusion layer around copper(II) oxide particles could exist if:- 1) the solution was not well stirred and 2) the solid had a high porosity which restricted access of the solution to all of the solid. In these cases bulk chelate would be expected to form rather than surface chelate.

F. ATTEMPTS TO MEASURE SURFACE HYDROPHOBICITY

This study was primarily concerned with the attempt to understand the mechanism of adsorption of chelating reagents on oxide minerals. A knowledge of the adsorption process should assist in the determination of the best conditions under which these minerals could be recovered by flotation. In an attempt to relate the adsorption data to the tendency for a mineral, to float, it was considered important to measure the relative hydrophobicity of oxide samples coated with the different chelating reagents under different conditions. In this regard, three types of experiments were performed, viz.

1. Bubble pick-up method on copper(II) oxide particles,
2. Single bubble stream flotation method on copper(II) oxide particles, and
3. Contact angle measurement on chelate coated copper metal.

F.1. Bubble pick-up method

This method has been proposed as a useful micro-technique for monitoring the relative hydrophobicity of mineral surfaces.<sup>84</sup> A bubble attached to the end of a microsyringe was lowered through the solution into a carefully prepared indentation in the mineral particle bed. After a set length of time the bubble was removed and the amount of solid attached to it recorded. Unfortunately it was found that this method was very

subjective and very difficult to duplicate with re-crystallized copper(II) oxide. The amount of oxide attaching to the bubble could very easily be varied by a suitable choice of deformation of the bubble and pressure of application. The main reason for this behaviour was probably connected to the very smooth surface and fine particle size of the oxide particles which appeared to be sufficiently hydrophobic to attach to the bubble in the absence of reagent.

#### F.2. Single bubble stream flotation method

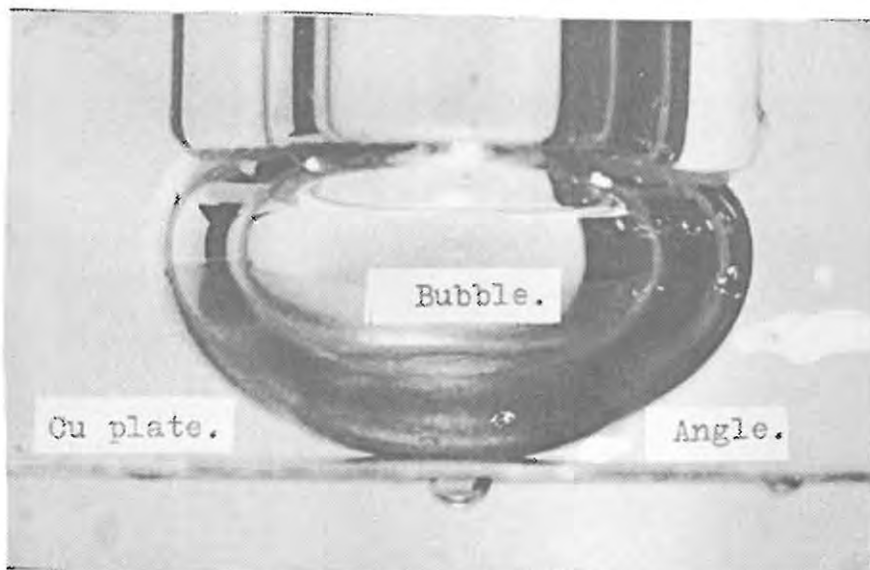
The apparatus used in this section was developed at MINTEK as an alternative to the more traditional Fuerstenau type flotation cell.<sup>85</sup> In this system a single bubble stream of nitrogen is passed through a mineral pulp kept in suspension by a centrifugal pump. At the surface the mineral laden bubbles are diverted to the sides from where the mineral can be recovered. Unfortunately there were practical problems associated with the use of this apparatus to float the re-crystallized copper(II) oxide. The turbulence created by the upward movement of the air bubbles resulted in rather high solid collection in the absence of reagent. The particle size of the oxide was apparently too small for use in this kind of flotation cell.

#### F.3. Contact angle measurement on copper metal

An air bubble attached to the end of an open tube (diam. 0,5 mm) was lowered through the solution onto a copper plate as shown below. The copper plate was pre-conditioned with the chelating reagent.

The angle of attachment was measured later from the photograph. The bubble was then lowered to a level that

ensured a large contact area and then raised back to the original position where the angle was again measured (angle 2).



The results are listed in table 23.

Table 23.

Contact angle measurement

	Uncoated Cu	Oxine	SALO	5-nitroSALO	Potassium ethylxanthate
Angle 1/degrees	15	18	30	25	17
Angle 2/degrees	15	15	66	32	32

The measurement of a contact angle in the above manner is not meant to be an absolute method but rather to give an indication of a trend. Angles of  $15^\circ$  were reported because, with the method used, it was almost impossible to distinguish angles between  $0^\circ$  and  $15^\circ$ . In addition, those contact angles between  $15^\circ$  and  $20^\circ$  were considered to indicate that the hydrophobicity of the surface was so low that no attachment between the bubble and the metal occurred, i.e. that the surface was hydrophilic. A significant hysteresis between the two contact angles also indicated hydrophobicity.

The low contact angle on copper metal indicates that the metal is hydrated to some degree. This agrees with previous findings that copper metal is not naturally floatable.<sup>86</sup> In addition air oxidized copper metal has a surface layer consisting of a mixture of copper(I) and copper(II) oxide which would be expected to make the surface hydrophilic.<sup>87</sup>

A bubble contact angle greater than  $30^\circ$  is considered to indicate that a significant change has occurred at the metal surface due to reagent adsorption. Ethyl xanthate was expected to have a contact angle of  $66^\circ$  as has been previously found. It is suggested that the fact that the measured angle was much smaller could have been caused either by variations in the experimental techniques used or by changes in the form and concentration of the adsorbate on the surface.

The most significant feature of the contact angle data was that oxine adsorption did not appear to increase the hydrophobicity (and thus the contact angle) of the metal surface, whereas the other reagent did. This agreed with the

adsorption data for copper(II) oxide-oxine system. In this case it was shown that the adsorbed copper oxinate became hydrated with time when left in contact with water. Oxine was therefore predicted not to function as a collector for oxide minerals unless an additive, such as fuel oil, was added. This is in fact what has been concluded by other researchers from the results of studies to develop a commercial process to recover oxidised zinc and lead ores in Italy.

G. SUMMARY OF THE MODEL FOR THE ADSORPTION OF CHELATING REAGENTS ON OXIDE MINERALS

The adsorption process can be divided into various stages; oxide dissolution, metal complexation, precipitation and post-precipitation processes.

G.1 Step 1. Oxide dissolution.

A measure of the tendency for a metal oxide to dissolve in aqueous media can be derived from the consideration of the solubility product data of the relevant metal hydroxides. The concentration of metals ions released at equilibrium at pH 4 and the charge to radius ratio for the metal ion is also given in table 24.

Table 24.

Solubility of various metal hydroxides.

Hydroxide	pK <sub>sp</sub>	LogM <sup>x+</sup> <sub>mol.l<sup>-1</sup></sub>		
Al(OH) <sub>3</sub>	31,6	-1,60	INSOL	5,9
Ca(OH) <sub>2</sub>	4,9	15,10	SOL	2,0
Cr(OH) <sub>3</sub>	30,3	-0,30	SEMI-SOL	4,8
Cu(OH) <sub>2</sub>	19,7	0,30	SEMI-SOL	2,8
Fe(OH) <sub>3</sub>	37,9	-7,90	INSOL	4,7
Ni(OH) <sub>2</sub>	16,8	3,20	SOL	2,9
Zn(OH) <sub>2</sub>	15,6	4,40	SOL	2,7

It is clear that ferric hydroxide is significantly less soluble in aqueous media than copper hydroxide. The differences in the solubilities between Ca<sup>2+</sup>, Cu<sup>2+</sup>, Fe<sup>3+</sup> and Zn<sup>2+</sup> hydroxides can be understood with reference to the simplistic electrostatic concept of bonding. The high charge to radius ratio for the ferric ion results in

a stronger attraction for the hydroxyl ions than in the case of, for instance, the zinc ion.

#### G.2. Step 2. Metal - chelate complexation

The chelating reagents used in this study contained active groups which are classified, like the hydroxyl ion, as hard bases (see INTROD.) Consequently, the formation constants for metal-chelate complexation vary with the metal ion in the same manner as the solubility products of the hydroxides. The ferric ion therefore forms a more stable complex with oxine than the copper ion. However, iron(III) oxide releases very few ions to solution and therefore there is very little metal-complexation in solution in this case. By comparison copper(II) oxide releases a relatively large concentration of copper ions to solution and therefore metal-complexation in solution is a very important factor in the adsorption process.

The greater stability of the copper complex of 8-hydroxyquinoline as compared to O-O type chelating reagents (eg. hydroxamate) can be attributed to the fact that the basic character of the oxine nitrogen is greater than that of the carbonyl oxygen. However, it does not follow that the copper complex of  $\alpha$  aminophenol, which shows approximately the same basicity as oxine, has the same stability. In the  $\alpha$  aminophenol group the coordination to a metal is restricted by the presence of

the hydrogen atoms which exert a steric blocking effect. Also, the greater resonance interaction possible in the oxine chelates as compared with the  $\alpha$  aminophenol and salicylaldoxime could account for the greater stability.

### G.3. Step 3 Precipitation

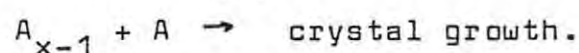
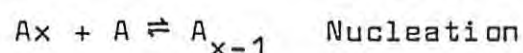
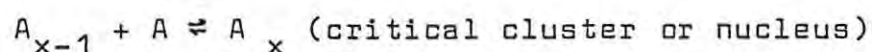
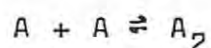
The variation in the concentration of copper-chelate complexes with changes in the pH, concentration and temperature of the solution can be derived from the values of the acid dissociation constant of the ligand and the formation constants of the copper complexes. It is possible with the aid of this data and the knowledge of the intrinsic solubility of the neutral bis-chelate copper complex to determine the conditions which favour metal-chelate precipitation.

Precipitation is a complex phenomenon that is affected by many variables some of which are difficult to control. Walton<sup>78</sup> has listed a number of relevant factors that affect precipitation.

- 1) the number of impurities in the solution.
- 2) catalysis by active sites in the container walls, electrodes, stirrer etc.
- 3) the method of mixing of reactants.
- 4) the rate of stirring.
- 5) temperature.

Nevertheless, it is possible to consider precipitation to occur in two stages, viz. nucleation and crystal growth.

The interaction between metal ions and chelate molecules leads to the formation of a cluster which can become sufficiently large to become consolidated into small crystallites or nuclei upon which irreversible crystal growth ensues.



The presence of a substrate can lower the energy barrier to nucleation and hence catalyse the nucleation process. Copper(II) oxide acts as a very effective site onto which the precipitate can heterogeneously nucleate. It is likely that the copper(II) oxide surface contains surface defects such as dislocations and edges which are more likely to catalyse nucleation.

Crystal growth is controlled by the degree of supersaturation of metal complex. This in turn is controlled by the rate of release of metal ions from the oxide surface, the chelate anion concentration, the formation constant of the precipitate, the intrinsic solubility of the precipitate and the efficiency of the stirring of the oxide-chelate vessel. A low degree of supersaturation can be caused by a limited release of copper ions (eg. low surface area oxide), a low pH, a relatively low formation constant or a relatively high intrinsic solubility. High supersaturations are

generated by the use of a high surface area oxide, a high pH or a reagent with a high formation constant. The precipitation crystals produced on the oxide surface from solutions of low supersaturations are well formed and are in isolated patches (points of nucleation).

Higher supersaturations produce a more fibrous type precipitate by dendritic type growth. The precipitate tends to cover larger areas of the surface. Very high supersaturations can cause the precipitate to nucleate homogeneously and form a colloidal or bulk precipitate. In Nagaraj's experiments part of the cause of the formation of so much bulk precipitate could be the very high degree of supersaturation.

It is possible by the use of additives such as gum arabic to interfere with the precipitate growth and to cause nucleation to occur in solution and not on the surface.

#### G.4. Step 4. Post-Precipitation processes.

The metal-chelate precipitate is subject to a number of physical and chemical processes which can tend to disperse it from the oxide surface. The most obvious physical process involves the detachment of precipitate because of attrition between the various oxide particles. This factor would be dependent on the structural form of the precipitate. It is considered that the precipitate which occurs on the surface as a fibrous layer (see micrographs for SNSALO) is less likely to detach because

of attrition than a precipitate which occurred in isolated patches which protrudes from the surface.

The chemical processes that operate on the precipitate are specific. For example, copper oxinates are believed to convert slowly from the anhydrous to the hydrated form. The nature of this conversion is such that the attachment to the surface is lost and the precipitate is dispersed in the bulk of the solution. The rate of this conversion is dependent on the physical state of the precipitate with the fibrous form hydrating faster than the well formed crystals. In the case of SALO it is suggested that the precipitate can adsorb ions from solution and therefore it can act as its own dispersant.

#### H. ADSORPTION RESULTS IN RELATION TO THE FLOTATION PROCESS

At this stage it is possible to make an intuitive assessment of the adsorption results with regard to the flotation process. It is considered that in this process there are two important features, viz. a) the concentration of precipitate adsorbed on the oxide and b) the physical nature of the precipitate. The former factor is concerned with the need for the oxide particle to attain sufficient hydrophobicity such that it preferentially attaches to introduced air bubbles. The latter factor determines whether the precipitate remains adhered to the oxide surface for a period long enough for the particles to be floated.

The classical idea of the adsorption on oxide minerals was that the organic reagent combined with surface metal ions by the displacement of other adsorbed species such as  $H_2O$  to form a uniform layer. The organic reagents used were designed such that one portion of the molecule was responsible for attaching to the metal ion and the other part was directed to impart to the oxide a hydrophobic nature. In the case of copper oxides it has now been shown that the adsorption process involves precipitation of the species which is formed between the organic reagent and metal ions. The precipitation occurs at the source of metal ions, ie. at the oxide surface. This process resulted in the formation of isolated patches of adsorbed material on the oxide particle.

These patches corresponded to the nuclei from which crystal growth proceeded.

It is considered that the form of the precipitate is an important factor in the control of the recovery of the oxide minerals by the flotation process. The type of precipitate formed is suggested to dictate whether it can withstand the physical displacement forces in the flotation cell. Precipitate morphology can vary from well shaped crystallites to fibres depending on the rate of precipitation. This is in turn determined by the degree of supersaturation of the metal complex. In addition, it is suggested that the presence of isolated patches of crystalline precipitate on the oxide surface might not be sufficient to impart enough overall hydrophobicity to the oxide particle. A fibrous type precipitate which grows laterally across the surface would be expected to overcome this problem to some extent. However, in some cases this type of precipitate appeared to detach from the surface relatively easily.

In conclusion, the results suggest that the most satisfactory conditions to aim for in the flotation circuit are those that produce a strongly adhering crystalline precipitate with a high surface coverage of the mineral surface, ie. to use conditions which produce solutions of low theoretical supersaturation.

It is suggested that the reagent does not adsorb as a uniform monolayer on the surface but rather as patches

of multilayers. However, there is no indication at this stage what degree of surface coverage with these nuclei would be required for floatability. It is recognised that the reagent concentration level used in this study would be uneconomic but it is suggested that the reagent could be modified to increase its hydrophobicity. Furthermore, it is considered that under the above conditions that the amount of reagent required for flotation could be reduced by the elimination of the large losses due to the reagent being consumed to produce non-attached or bulk copper chelate.

## I. FUTURE WORK

There are a number of research avenues considered worthy of further investigation.

1) An extension of the range of oxides covered to include oxides such as titanium(IV) oxide, tin(IV) oxide and zinc(II) oxide.

2) The use of the nitro derivative of 8-hydroxy-quinoline.

3) A study of the effect, of the addition of alkyl substituents onto the aromatic ring in salicylaldoxime, on the crystal morphology of the copper precipitates. The aim would be to relate the degree of supersaturation to the crystal shape.

4) Extend the study of the precipitation of metal chelates on different sizes of copper(II) oxide crystals. This would entail the production of a batch of oxide with as low a surface area as possible. Some of this oxide would be crushed into different particle sizes and then mixed with some of the original uncrushed material. The oxide would then be studied under the scanning electron microscope to determine any differences in the metal-chelate precipitate on the original oxide particles.

5) A more detailed study of the effect of additives such as gums, starches etc. on the adsorption.

6) A more in-depth analysis of the sulphidization process.

7) Further work on the factors which control the precipitation phenomenon.

J. APPENDIX

1. Calculation of the species distribution

Let:

$L_{TOT}$  = total reagent concentration

$Cu_{TOT}$  = total metal concentration

HL = Concentration of hydroxamic acid

$L^-$  = Concentration of hydroxamate anion

$CuL^+$  = Concentration of 1:1 copper hydroxamate complex

$CuL_2$  = Concentration of 1:2 copper hydroxamate complex

$$K1 = \frac{(H)(L^-)}{(HL)} \text{ -----(1)}$$

$$K2 = \frac{(CuL^+)}{(Cu^{2+})(L^-)} \text{ -----(2)}$$

$$K3 = \frac{(CuL_2)}{(CuL^+)(L^-)} \text{ -----(3)}$$

Then

$$L_{TOT} = HL + L^- + CuL^+ + 2CuL_2 \text{ ..... 4}$$

$$Cu_{TOT} = Cu^{2+} + CuL^+ + CuL_2 \text{ ..... 5}$$

Substituting into equation (2) in order to eliminate  $CuL^+$  and  $CuL_2$  terms gives -:

$$Cu_{TOT} = Cu^{2+} + K2 \times (Cu^{2+}) \times (L^-) + K2 \times K3 \times (Cu^{2+}) \times (L^-)^2 \text{ ..... 6}$$

$$Cu^{2+} = Cu_{TOT} / (1 + K2 \times (L^-) + K3 \times K2 \times (L^-)^2) \text{ -----(7)}$$

Thus

$$Cu^{2+} = Cu_{TOT}/(A) \quad \text{----- (8)}$$

Substitute equation (4) into equation (1)

$$L_{TOT} = \frac{(H) \times (L^-) + L}{K1} + \frac{K2 \times Cu_{TOT} \times (L^-)}{A} + \frac{K3 \times K2 \times (L^-)^2}{A} \quad \text{---- (9)}$$

Multiply through by A

$$L_{TOT} \times (A) = \frac{(H) \times (L^-) \times (A)}{K1} + (L^-) \times (A) + K2 \times Cu_{TOT} \times (L^-) + K3 \times K2 \times (L^-)^2 \quad \text{----- (10)}$$

Resubstituting the expression for A and multiplying the equation out and then collecting together the terms of the cubic equations,  $ax^3 + bx^2 + cx + d$ .

$$\text{Thus } a = ((H \times K3 \times K2)/K1) + K3 \times K2$$

$$b = ((H \times K2)/K1) + K2 + 2 \times K3 \times K2 \times Cu_{TOT} - L_{TOT} \times K3 \times (K)$$

$$c = (H/K1) + 1 + K2 \times Cu_{TOT} - L_{TOT} \times K2$$

$$d = -L_{TOT}$$

The cubic equation was solved for  $L^-$  by using the Newton-Rampson method to solve polynomial equations. This method involved assuming as a first approximation to the obtained from the solution to the following expression,

$$L_2 = L_1 - \frac{f(L)}{f'(L)} \quad \text{----- (12)}$$

$f(L)$  = the value of the original cubic expression calculated by substituting  $L_1 = L_{TOT}$

$f'(L)$  = the value of the first derivative of this expression as calculated by substituting  $L_1 = L$  .

Successive approximations of L can be determined by iterating this procedure until there was little change in

the value of  $L$ . Substitution of  $L^-$  into equation 7 enabled the  $\text{Cu}^{2+}$  concentration to be determined. The concentration of  $\text{CuL}^+$  and  $\text{CuL}_2$  could be derived by substitution into equation 2 and 3.

REFERENCES

1. BURKIN, A.R., Chem. Ind., 690(1983).
2. LEJA, J., "Surface Chemistry of Froth Flotation", Plenum press, New York(1982).
3. BARZYK, W., Malysa, K., and Pomianowski, A., Int. J. Miner. Process., 8, 17(1981).
4. HARRIS, P.J. and FINKELSTEIN, N.P., N.I.M. Rep. No 1896(1977).
5. FINKELSTEIN, N.P. and POLING, G.W., Min. Sci. Eng., 9, 4, 177(1977).
6. DE CUYPER, J., Erzmetall., 30, 3, 88(1977).
7. BOWDISH, F.W. and CHEN, T.P., Trans.A.I.M.E., 226, 21(1963).
8. WRIGHT, A.J. and PROSSER, A.P., Trans.I.M.M., 74, 259(1964).
9. BOWDISH, F.W. and STAHMANN, W.S., Trans.A.I.M.E., 238, 118(1967).
10. SOTO, H. and LASKOWSKI, J., Trans.I.M.M., 82, C153(1973).
11. CASTRO, S., SOTO, H., GOLDFARB, J. and LASKOWSKI, J., Int. J. Miner. Process., 1, 151(1974).
12. CASTRO, S., GOLDFARB, J. and LASKOWSKI, J., Int. J. Miner. Process, 1, 141(1974).
13. BUSTAMANTE, H. and CASTRO, S., Trans. I.M.M., 84, 167(1975).
14. QUEIROLO, C. and CASTRO, S., Trans I.M.M., 85, C166(1976).
15. CASTRO S., GAYTAN, H. and GOLDFARB, J., Int. J. Miner. Process, 3, 71(1976).
16. BUSTAMANTE, H., SPARROW, G.J. and WARREN, L.J., Chem.Aust., 48, 10, 375(1981).
17. BARBERY, G., CECILE, J.L., and Plichon, V.M., Proc.12th Int. Miner. Process.Congr, Inst. Min. Metall. 19-34, Sao Paulo(1977).
18. CECILE, J., PhD thesis, Pub.Bureau de Recherces Geol.et Minieres, Orleans, Cecex(1978).

19. CECILE, J., Report of the Bureau de Recherches Geol et Minieres, Orleans, Cedex(1980).
20. CECILE, J.L., CRUZ, M.I., BARBERY, G. and FRIPIAT, J.J., J. Coll, Interface Sci., 80, 2, 589(1981).
21. NAGARAJ, D.R. and SOMASUNDARAN, P., Trans. A.I.M.E., 226, 1891(1980).
22. NAGARAJ, D.R. and SOMASUNDARAN, P., in "Recent Developments in Separation Science", V, CRC Press, Florida, 81-94(1979).
23. NAGARAJ, D.R., PhD thesis, Columbia Univ. New York(1979).
24. BELL, C.F., "Principles and applications of metal chelation", Oxford Chem. Series, Clarendon Press(1977).
25. VIVIAN, A.C., Mining Mag., 36, 348(1927).
26. HOLMAN, B.W., Bull. I.M.M., 315, 53(1930).
27. DE WITT, C.C. and VON BATCHELDER, F., J.Am. Chem. Soc., 61, 1247(1939).
28. RINELLI, G, and MARABINI, A.M., Proc. Xth Int. Miner. Process. Congr. Paper 20, p493, Ins. Min Metall. London (1973).
29. MARABINI, A.M., Trans. I.M.M., 84, C177(1975).
30. MARABINI, A.M., Trans. I.M.M., 87, 76(1978).
31. PETERSON, H.D., FUERSTENAU, M.C., RICKARD, R.S. and MILLER, J.D., Trans. A.I.M.E., 232, 388(1965).
32. PALMER, B.R., GUTIERREZ, G. and FUERSTENAU, M.C., Trans A.I.M.E., 258, 257(1975).
33. SCOTT, J.W. and POLING, G.W., Can. Metal. Quat., 12, 1(1973).
34. FUERSTENAU, M.C., HARPER, R.W. and MILLER, J.D., Trans. A.I.M.E., 247, 69(1970).
35. RAGHAVAN, S. and FUERSTENAU, D.W., J. Coll. Interface Sci., 50, 2, 319(1975).
36. LENORMAND, J., SALMAN, T. and YOON, R.H., Can Metall. Quat., 18, 125(1979).

37. KIERZNICKI, T., MAJEWSKI, J. and MZYK.J., Int. J. Miner. Process., 7, 311(1981).
38. ATADEMIR, M.R., KICHENER, J.A. and SHERGOLD, H.L., Int. J. Miner. Process., 8, 9(1981).
39. MUKAI, S. and WAKAMATSU, T., Proc. 11th Int. Miner. Process. Congr., 671, Inst. Min Metall. Cagliari (1975).
40. BOGDANOVIĆ, I.S. et al., Proc. Xth Int. Miner. Process. Congr., Paper 7. p 553. Inst. Min. Metall., London(1973).
41. RYBOI, V.I., Chem. Abs., 86, 7441d(1977).
42. KOCHKIN, V.I., Chem. Abs., 79, 20997q(1973).
43. TRAHAR, W.J., Trans. I.M.M., 79, C64(1970).
44. SILLEN, L.G. and MARTELL, A.E., "Stability constants" Chem. Soc. special pub. No 17, London(1964).
45. SILLEN, L.G. and MARTELL, A.E., "Stability constants", supp. No. 1, Chem. Soc. special pub. No. 25, London(1971).
46. PERRIN, D.D., "Masking and Demasking of chemical reactions", Chem. Anal., Vol.33, Wiley Intersci., New York(1970).
47. BASOLO, F. and JOHNSON, R.C., "Coordination Chemistry", Pub. W.A. BENJAMIN Inc., New York(1970).
48. GILES, C.H., MacEWAN, T.H., NAKHWA, S.N. and SMITH, D., J.Chem. Soc. 3973(1960).
49. ASBRINK, S. and NORRBY, L.J., Acta Cryst., Sect. B 26, 8(1970).
50. ROCHESTER, C.H., Adv. Coll. Interface Sci., 12 43(1980).
51. FULLER, M.P. and GRIFFITHS, P.R., Am. Lab., 10(10), 69(1978).
52. ATTIA, Y.A., Trans. I.M.M., 84, 829, C221(1975).
53. AGRAWAL, Y.K., Rev. in Anal. Chem., 5, 1-2, 3(1980).
54. CHATTERJEE, B., Coord. Chem. Rev., 26, 281(1981).
55. SHENDRIKAR, A.D., Talanta, 16, 51(1969).

56. AGRAWAL, Y.K. and TANDON, S.G., *Talanta*, 19, 700(1972).
57. SHUKLA, J.P. and TANDON, S.G., *Talanta*, 19, 711(1972).
58. SHPAK, E.A. et al in *Chem. Abs* 92, 87387e. *Zh. Anal. Khim.*, 34(9), 1849(1979).
59. STARY, J., "Critical evaluation of equilibrium constants involving 8-hydroxyquinoline and its metal chelates", *International Union of Pure and Applied Chemistry, Chem. Data Series*, 240, Oxford, Pergamon, (1979).
60. ANDERSEN, D.M.W. and KARAMELLA, K.A., *J. Chem. Soc. C. Org.*, 8, 762(1966).
61. FEIGL, F., *Mickrochemic*, 1, 74(1923).
62. HOSKING, J.W. and RICE, N.M., *Hydrometallurgy*, 3, 217(1978).
63. FRITZ, J.S., BEUERMAN, D.R. and RICHARD, J.J., *Talanta*, 18, 1095(1971).
64. SUTER, H.A. and WEST, P.W., *Anal. Chim. Acta*, 13, 501(1955).
65. CHAKRAVORTY, A., *Co-ord. Chem. Rev.*, 13, 32(1974).
66. BOBTELESKY, M. and JUNGREIS, E., *Anal. Chim. Acta*, 13, 449(1955).
67. JARSKI, M.A. and LINGAFELTER, E.C., *Acta Cryst.*, 17, 1109(1964).
68. BURGER, K. and EGYED, I., *J. Inorg.Nucl. Chem.*, 27, 2361(1965).
69. ASHURST, K.G. and HARRIES, A.J., *NIM Tech. Mem. No 14125*, Randburg, South Africa(1979).
70. CLARKE, K., COWAN, R.A., GRAY, G.W. and OSBORNE, E.H., *J. Chem. Soc.*, 245(1963).
71. GRANVILLE, A., FINKELSTEIN, N.P. and ALLISON, S.A., *Trans. I.M.M.*, 81, C1(1972).
72. SCHNEIDER, V.L., HOLMAN, R.L. and BURR, G.O., *J.Phys. Coll. Chem.*, 53, 1016(1949).

73. RAMASWAMI, K.K., JOSE, C.I. and SEN, Q.N., Indian J. Chem., 15, 6(1967)
74. WELCHER, F.J. and BOSCHMANN, E., "Organic Reagents for Copper", R.E. Kreiger Pub. Co., New York(1979).
75. ASHBROOK, A.W., Co-ord. Chem Rev., 16, 285(1975).
76. FANNING, J.C. and JONASSEN, H.B., J.Inorg. Nucl. Chem., 25, 29(1963).
77. HOY, R.C. and MORRIS, R.H., Acta Cryst., 22, 476 (1967).
78. PALENIK, G.J., Acta Cryst., 17, 687(1964).
79. FANNING, J.C. and JONASSEN, H.B., J. Inorg. Nucl. Chem. 25, 29(1963).
80. WALTON, A., "The Formation and properties of Precipitates," Interscience, New York(1967).
81. PACKTER, A. and CHAUHAN, P., Kristal and Technik, 8 12, 1357(1973).
82. PACKTER, A., CHAUHAN, P. and SAUNDERS, D.F., Kristal and Technik, 4 (1), 45(1969).
83. WALKER, R.J., Chem. Ed., 57 (11), 189(1980).
84. LEE, A.F., J. of South African Inst. Mining Metall., 70, 95(1969).
85. HARRIS, P., Proc. Conf. on Recent Advances in Minerals Science and Technology, Sandton, South Africa, March 1984, in press.
86. GAUDIN, A.M., "Flotation," 2nd ed., McGraw, New York(1957).
87. OGLE, I.C.G. and POLING, G.W., Can. Metall. Quat. 14, 1, 37(1975).